Experimental Techniques

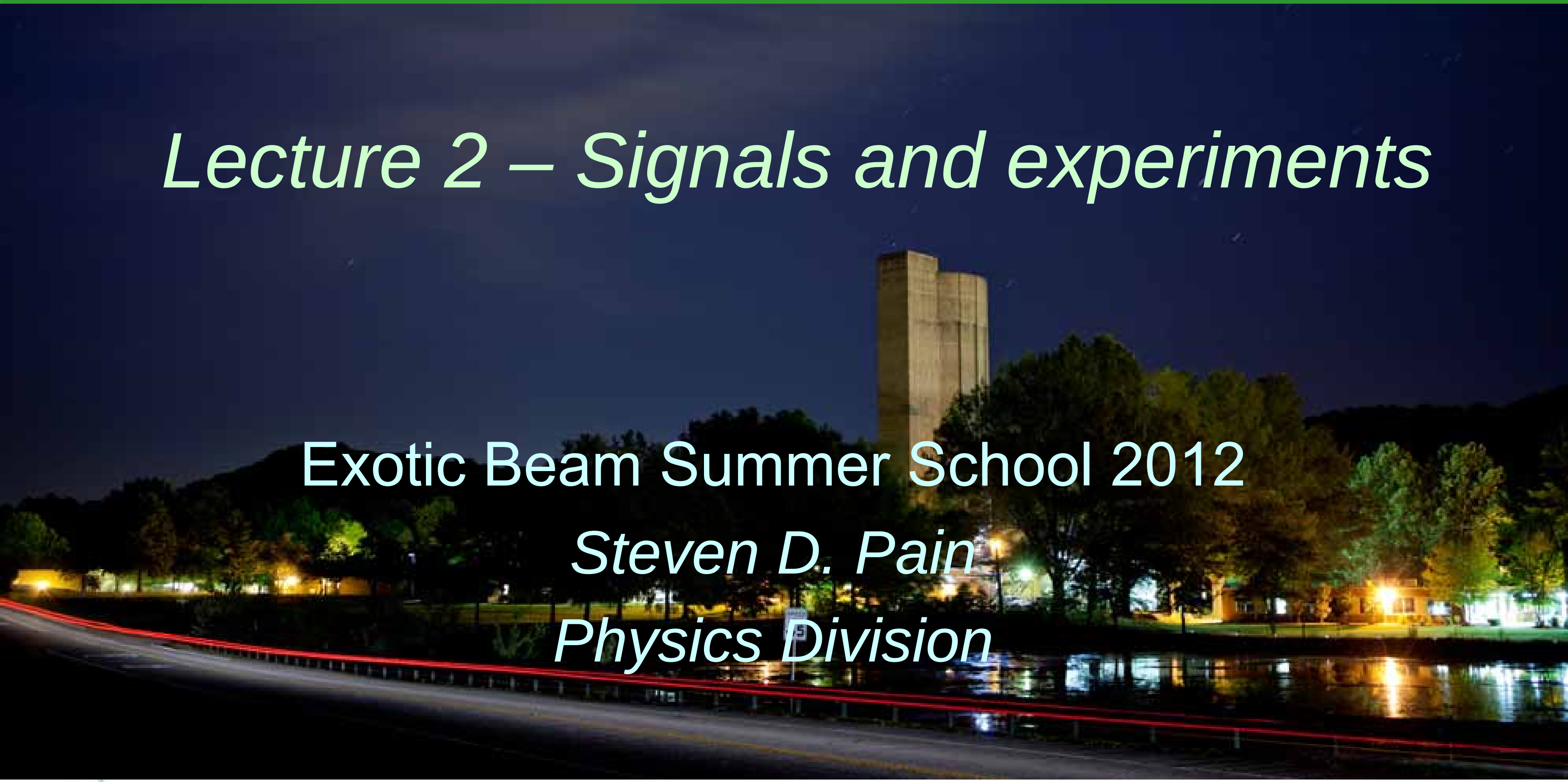

Lecture 2 – Signals and experiments

Exotic Beam Summer School 2012

Steven D. Pain

Physics Division

OAK RIDGE NATIONAL LABORATORY

Managed by UT-Battelle for the Department of Energy

Analogue signal processing

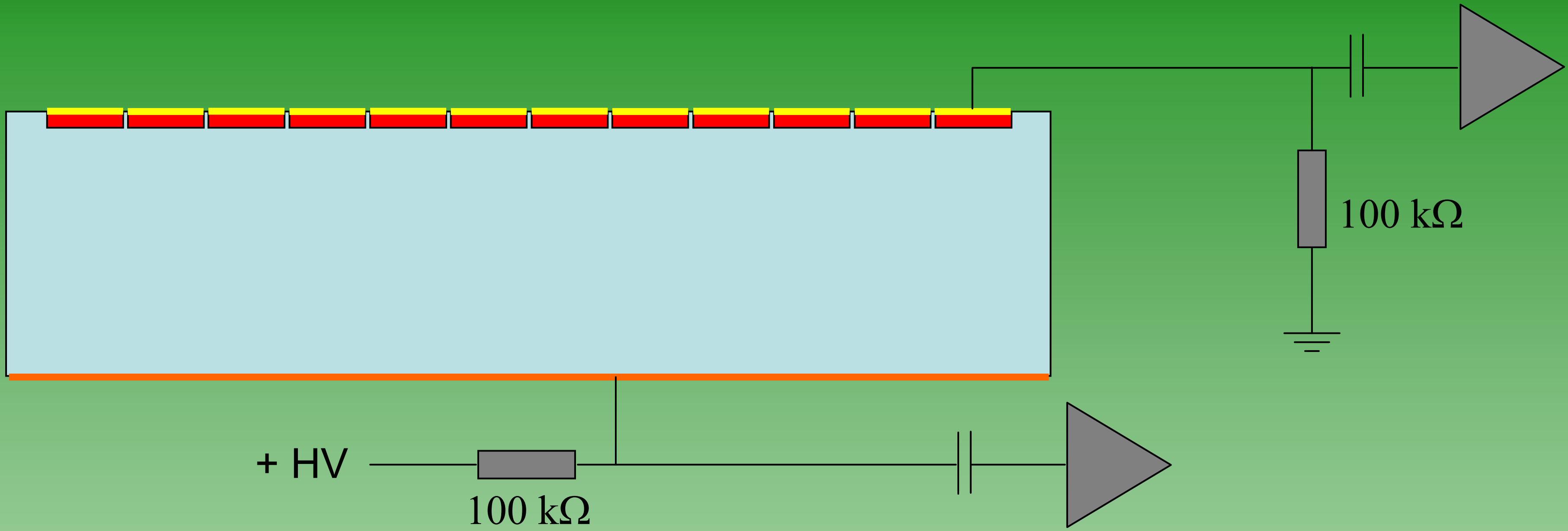

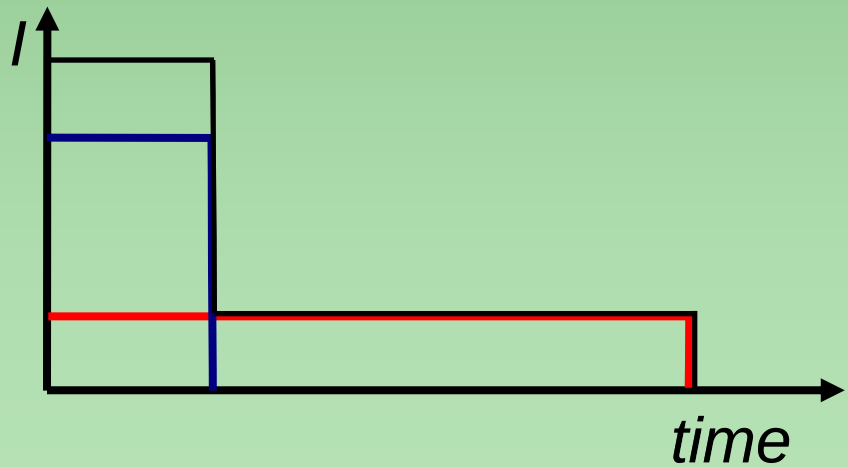

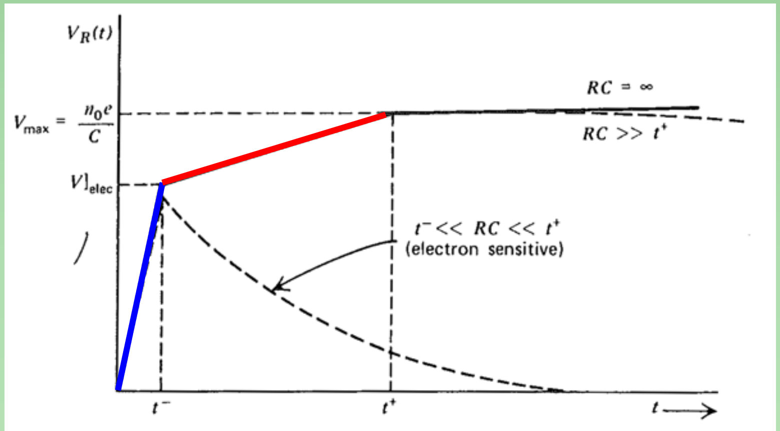

Analogue signal processing

Voltage sensitive preamplifier

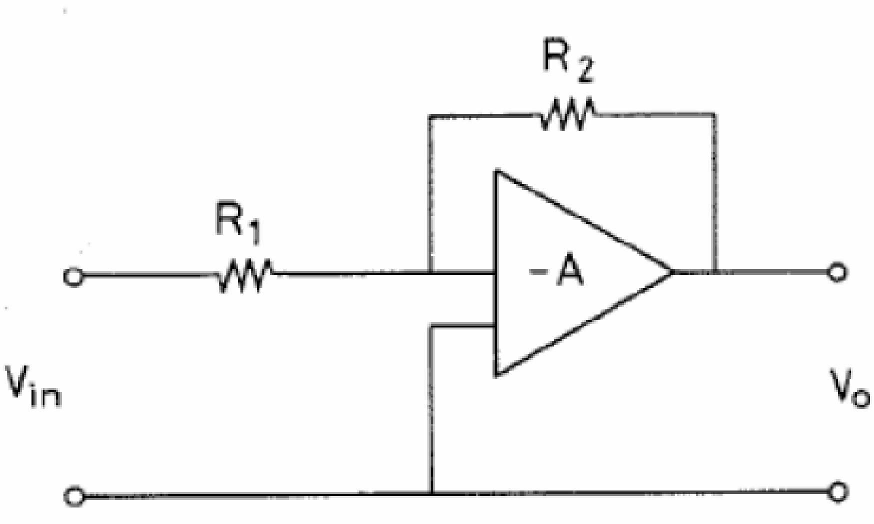

$$V_0 = \frac{Q}{C_{tot}}$$

Gain dependent on the detector capacitance (can vary)

Charge sensitive preamplifier

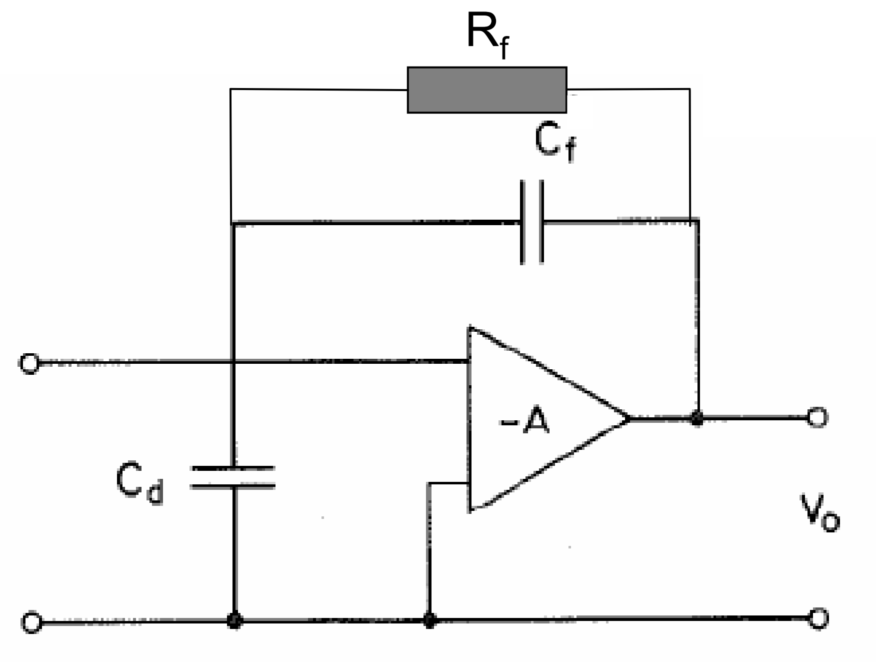

$$V_0 = -\frac{Q}{C_f}$$

Output is proportional to charge integrated on C_f, if signal is fast compared to R_fC_f

Noise is proportional to C_d

Analogue signal processing

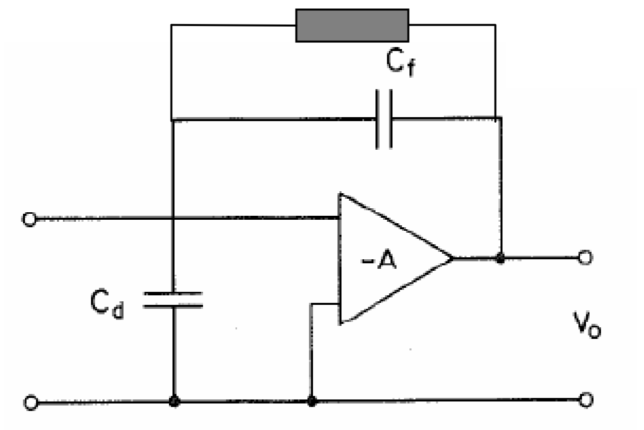

Charge sensitive preamplifier

Fast rise-time – pulse height proportional to input signal

Slow rise-time – rise and decay convolved (non-linear signals, worse resolution) – *ballistic deficit*

Position dependent RC

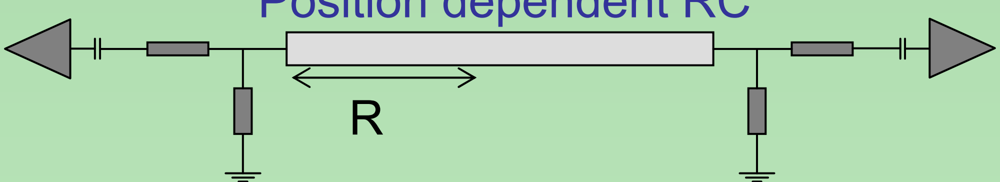

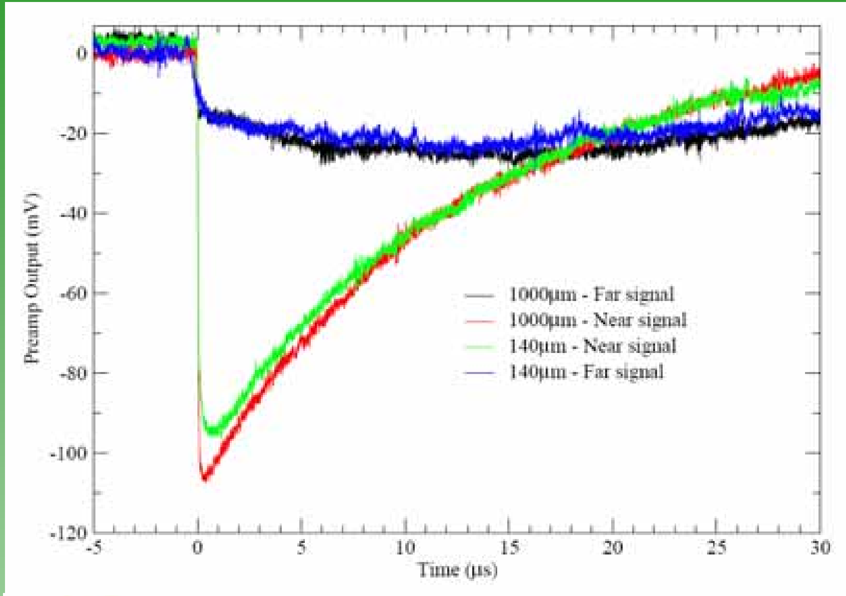

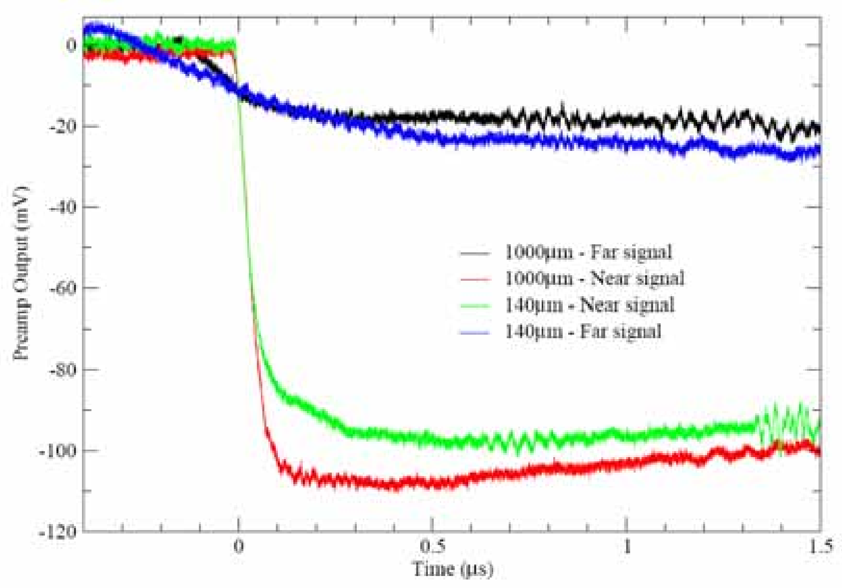

Signal processing

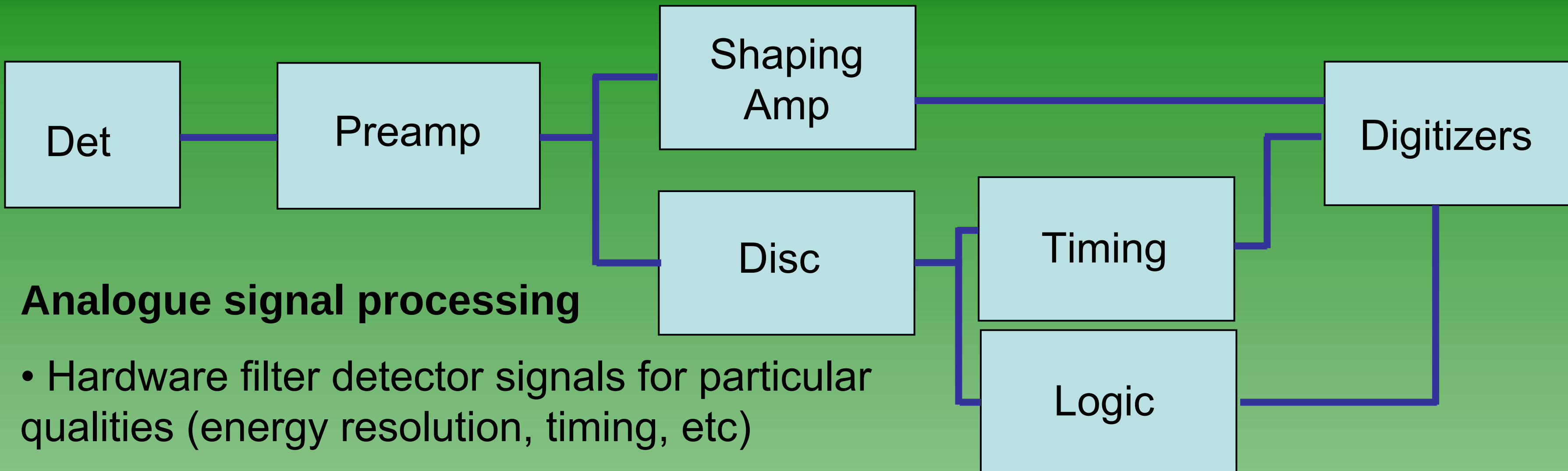

Analogue signal processing

• Hardware filter detector signals for particular qualities (energy resolution, timing, etc)

• Excellent resolution, but some information is discarded

• Separate optimized processing required for different parameters (energy, time, etc)

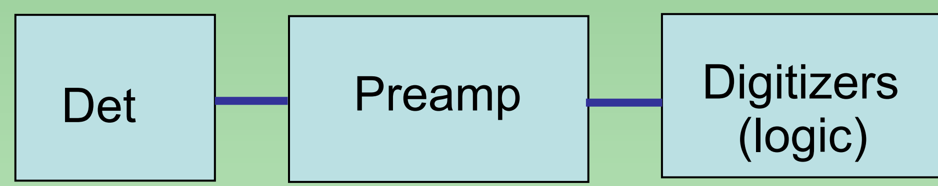

Digital signal processing

• Process (and sometimes store) a digital approximation of the trace from a detector/preamp

• All information encoded in the preamp trace can be processed (software)

• Single data stream can be multiplied and each stream processed independently

Leading-edge discriminators

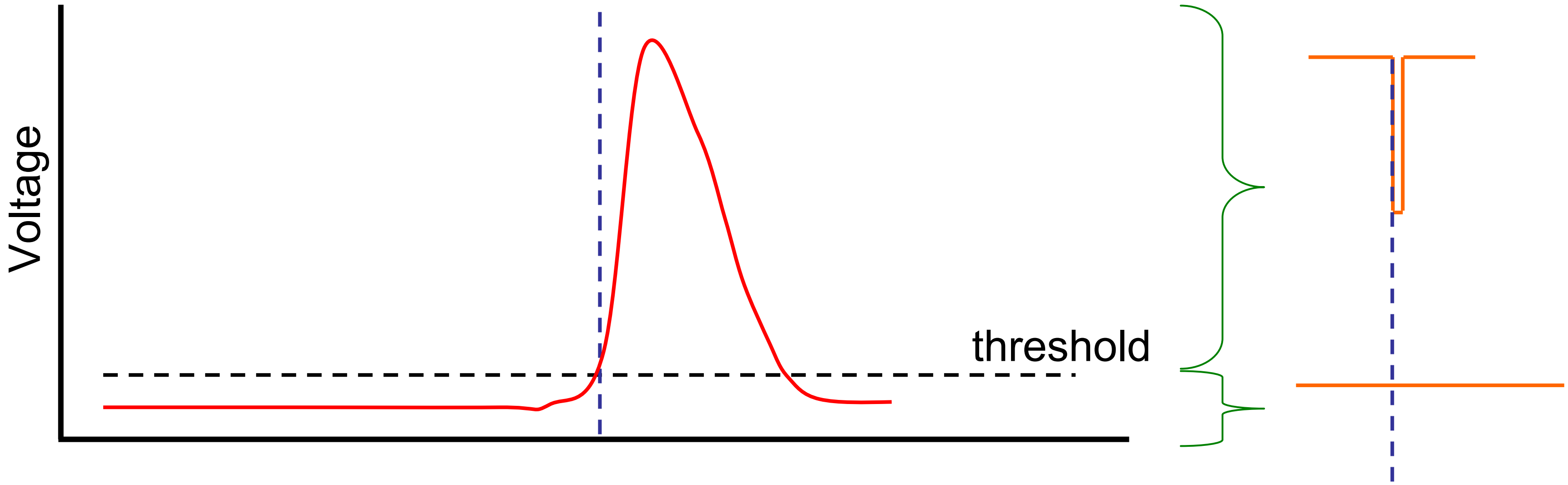

Leading-edge discriminators

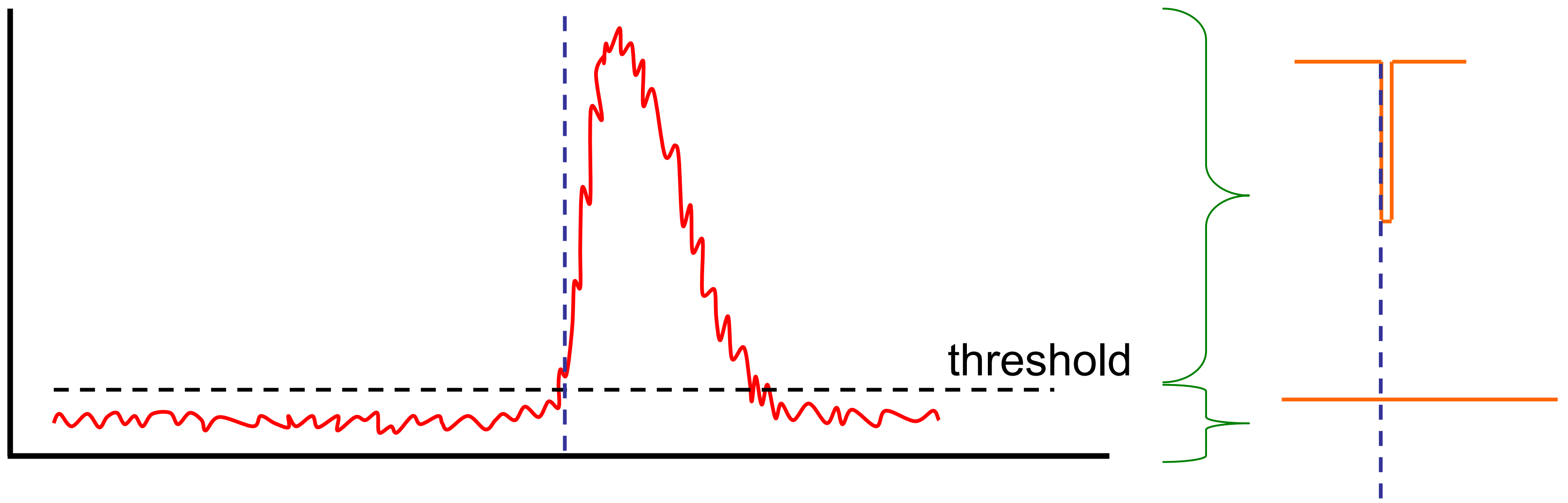

Leading-edge discriminators

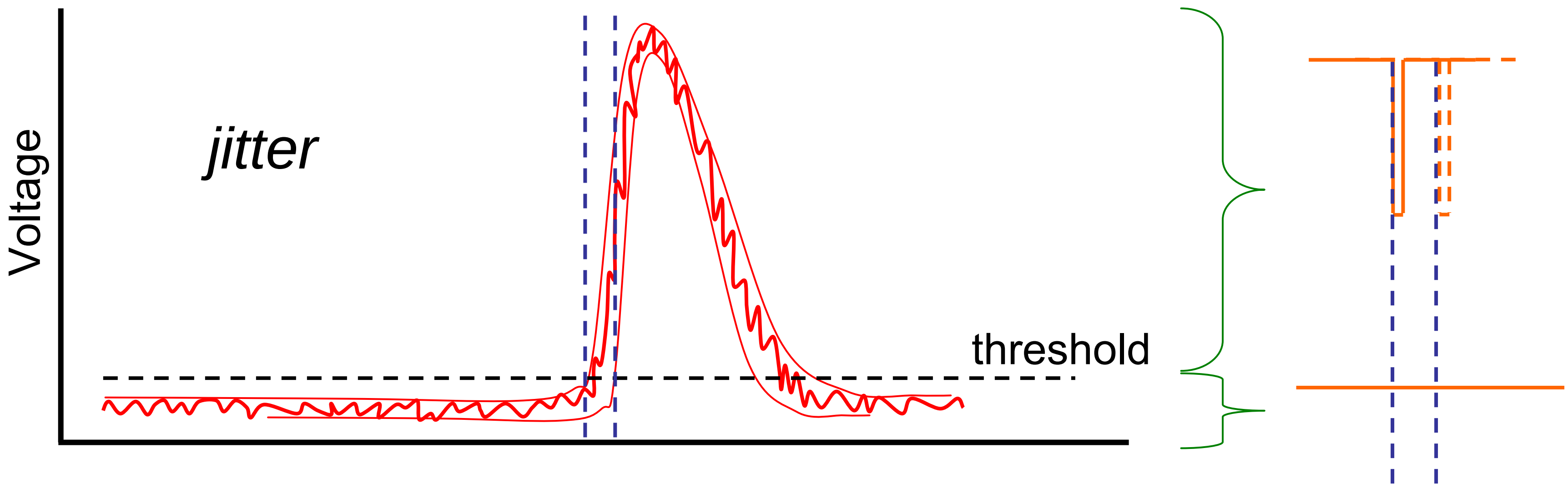

Leading-edge discriminators

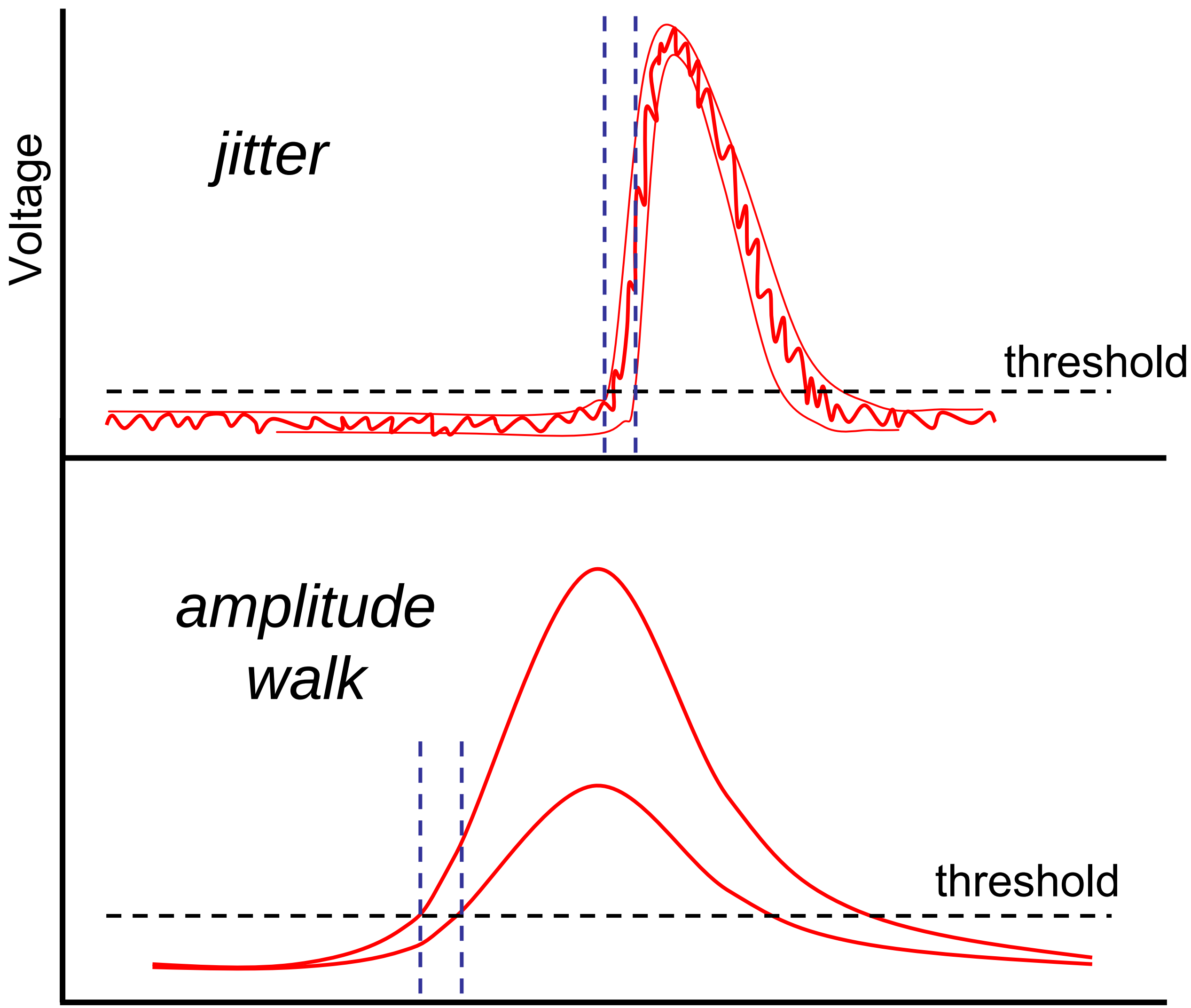

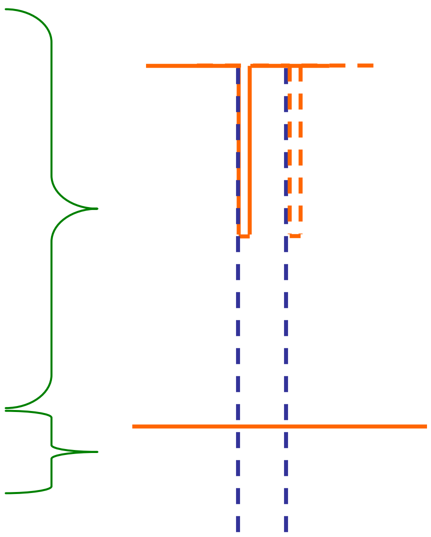

Good for trigger decisions

Bad for timing

Constant-fraction discriminators

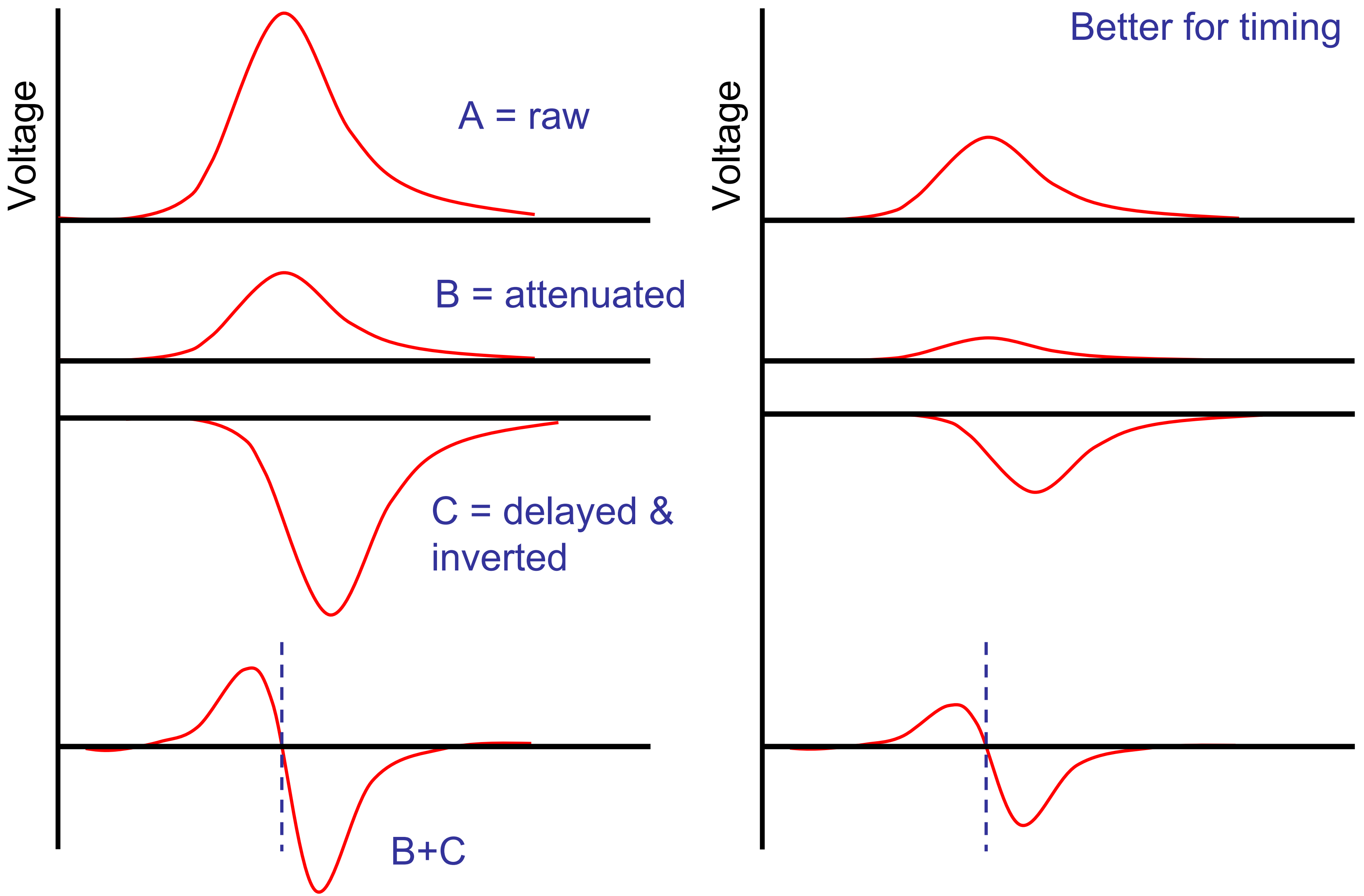

Signal processing

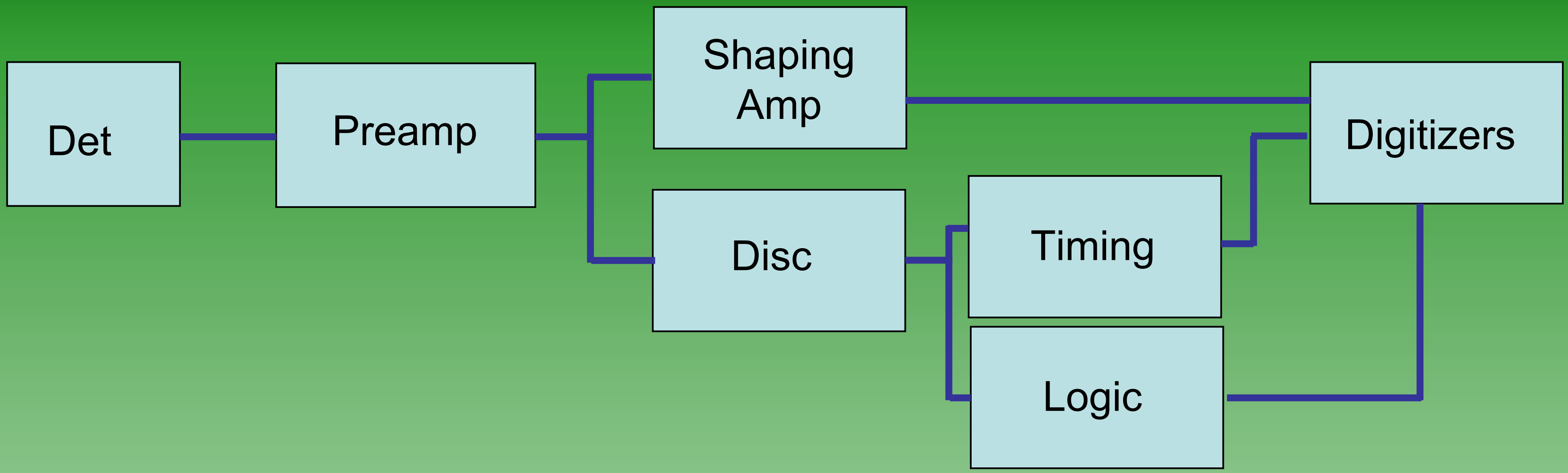

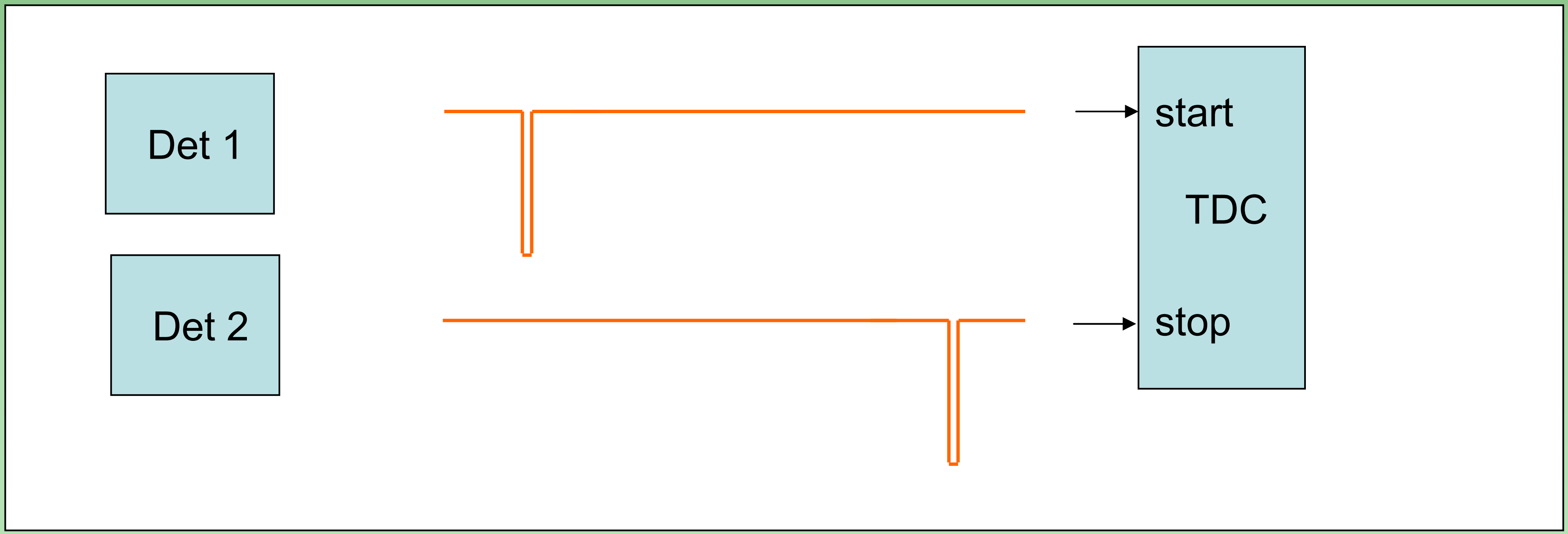

Analogue signal processing

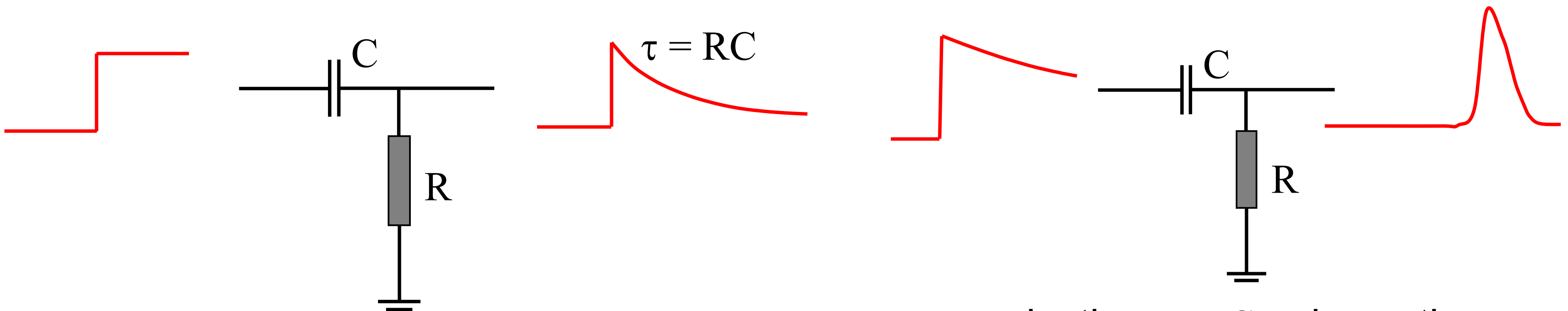

risetime < RC < decay time

High pass filter

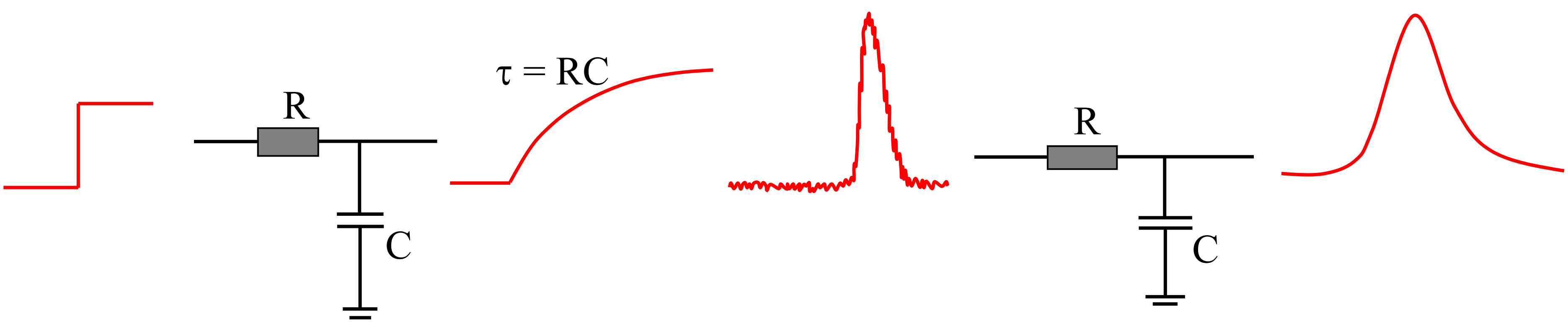

signal length < RC

Low pass filter

Shaping amplifiers

Shape pulses to:

- *Improve signal to noise*
- *Reduce pileup effects*

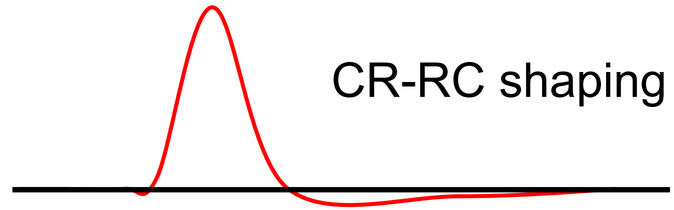

CR-RC shaping

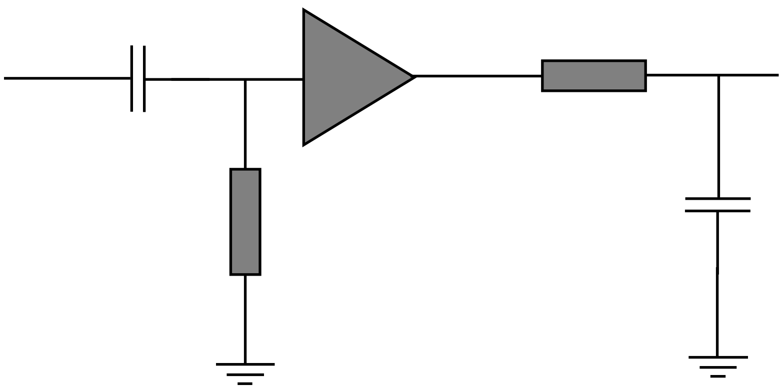

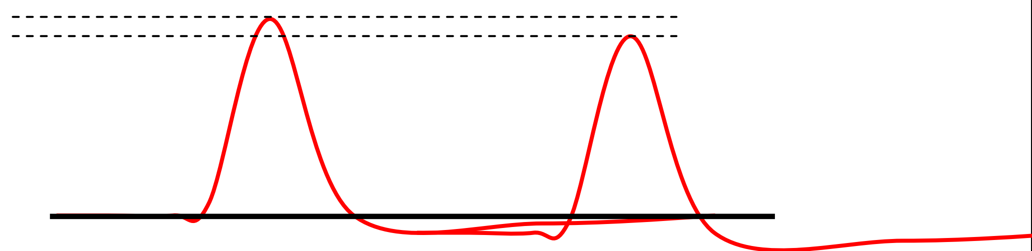

Undershoot leading to
degraded energy resolution

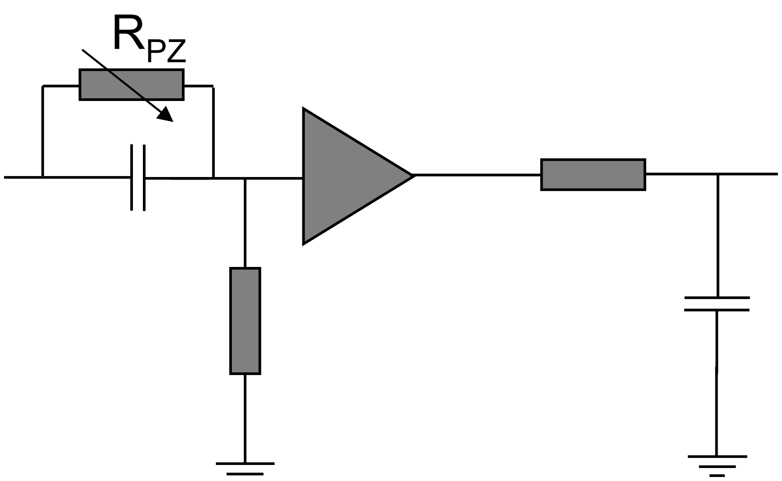

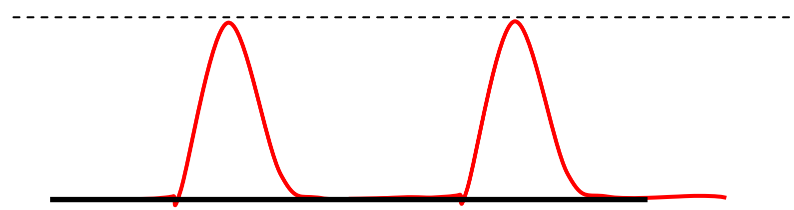

Pole zero variable resistor used to tune undershoot

Shaping amplifiers

Shape pulses to:

- *Improve signal to noise*
- *Reduce pileup effects*
- *Keep signal height information*
- *Lose information (eg trace shape)*

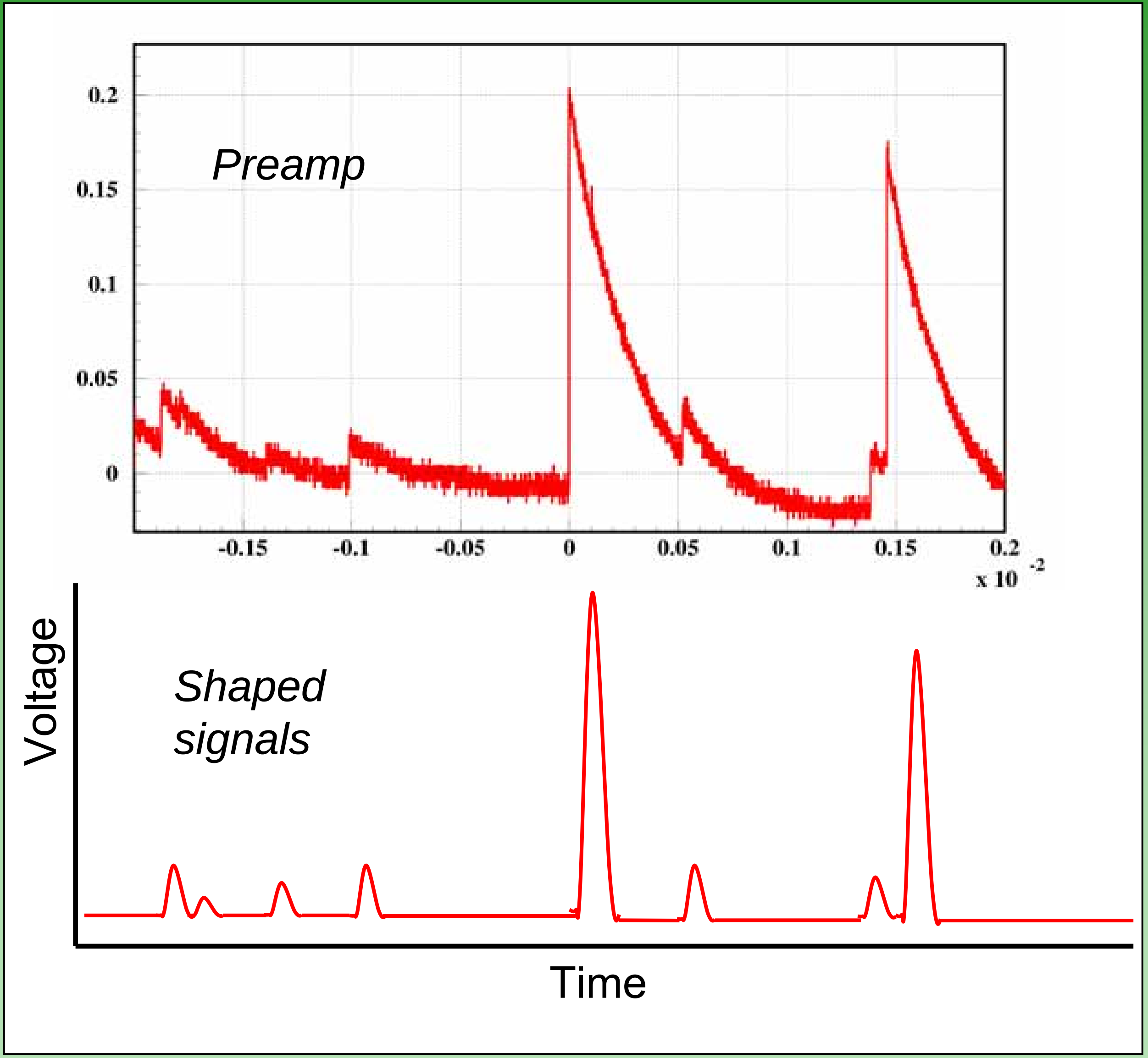

Shaping amplifiers – ballistic deficit

A = Shaping time too short

B = Shaping time better matched

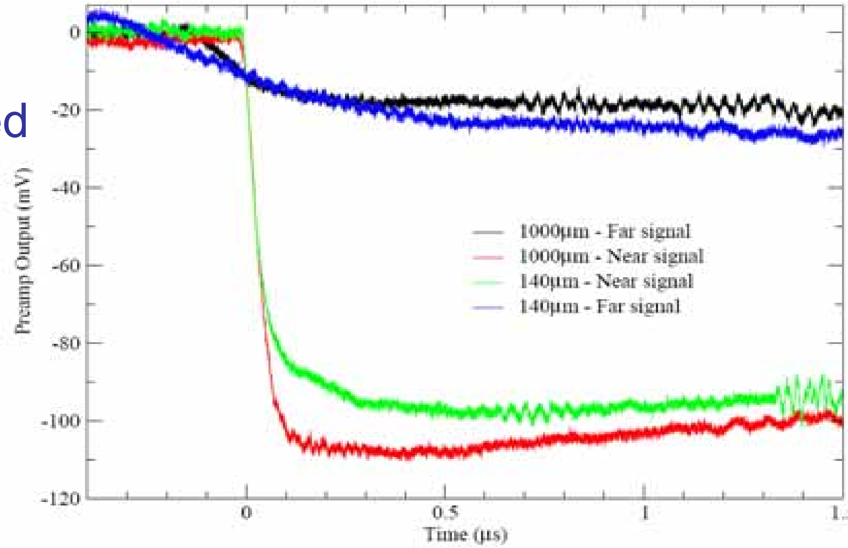

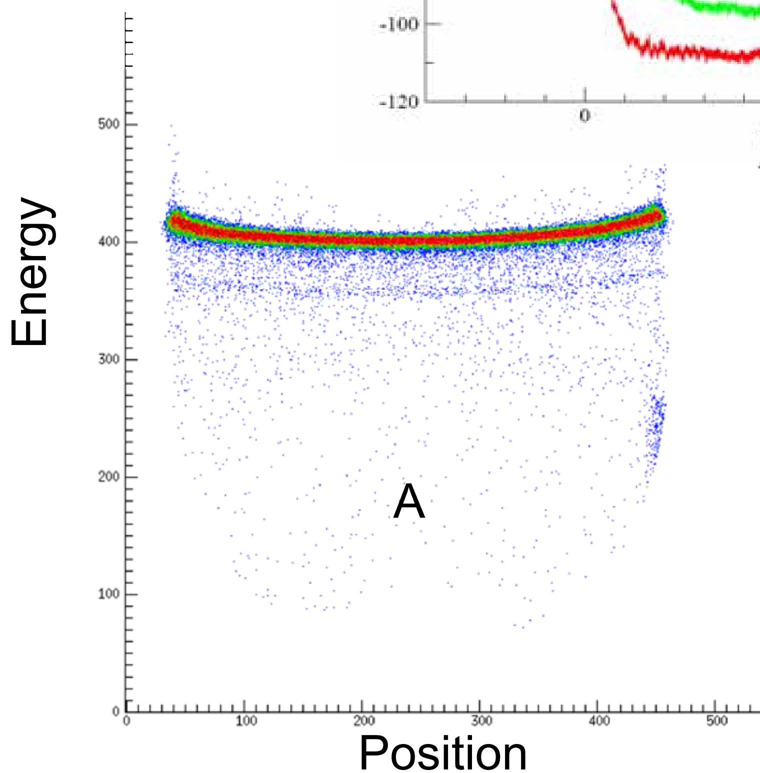

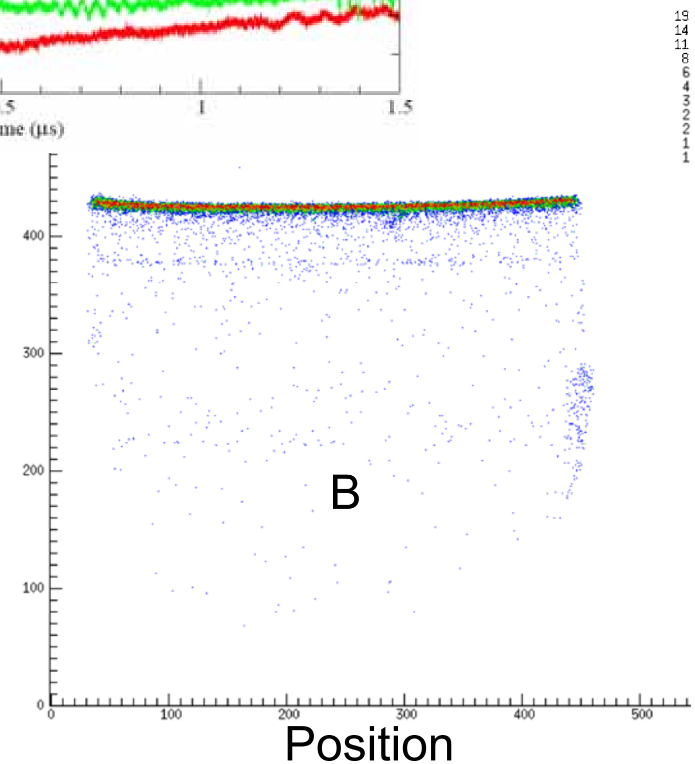

signal processing

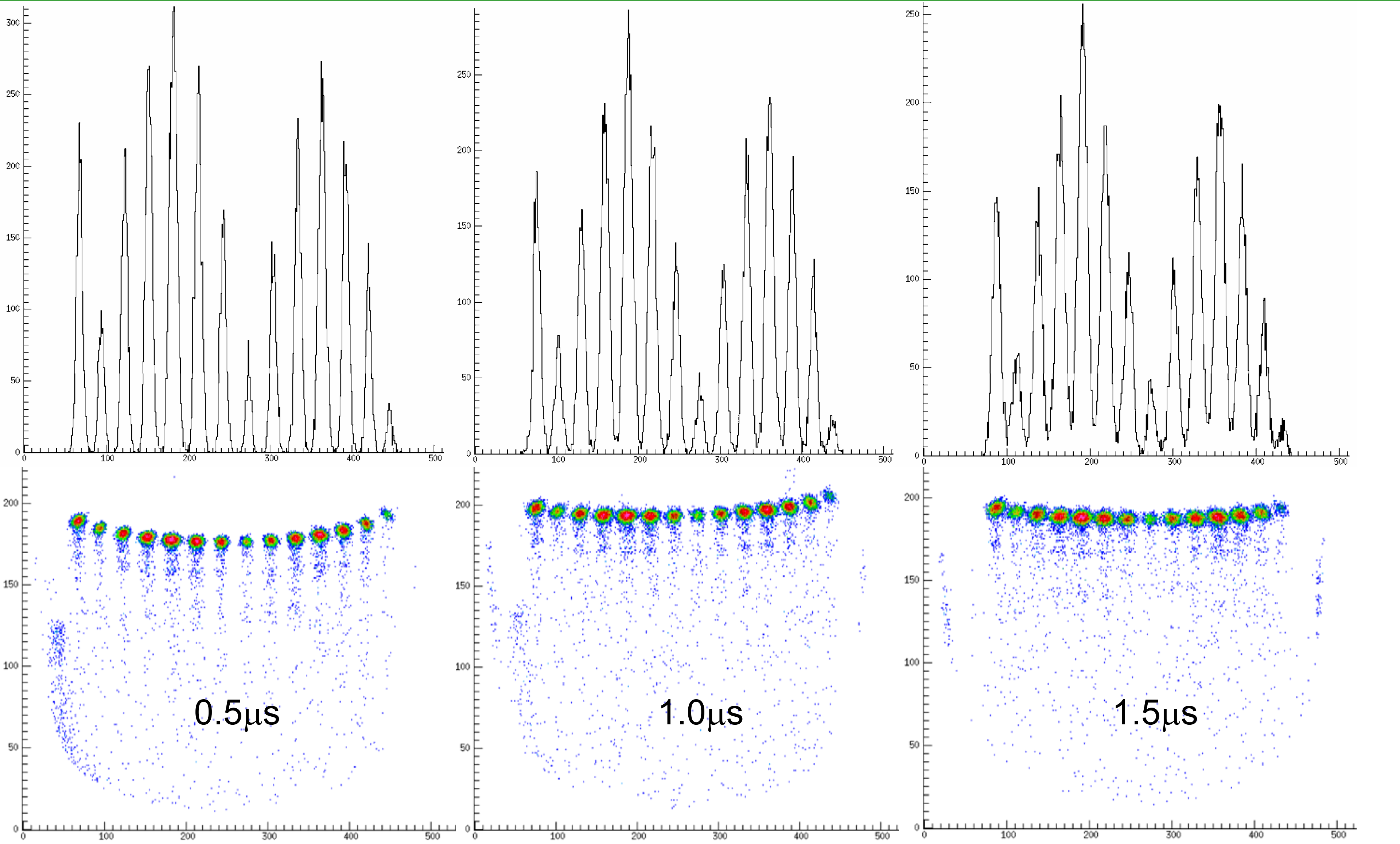

signal processing

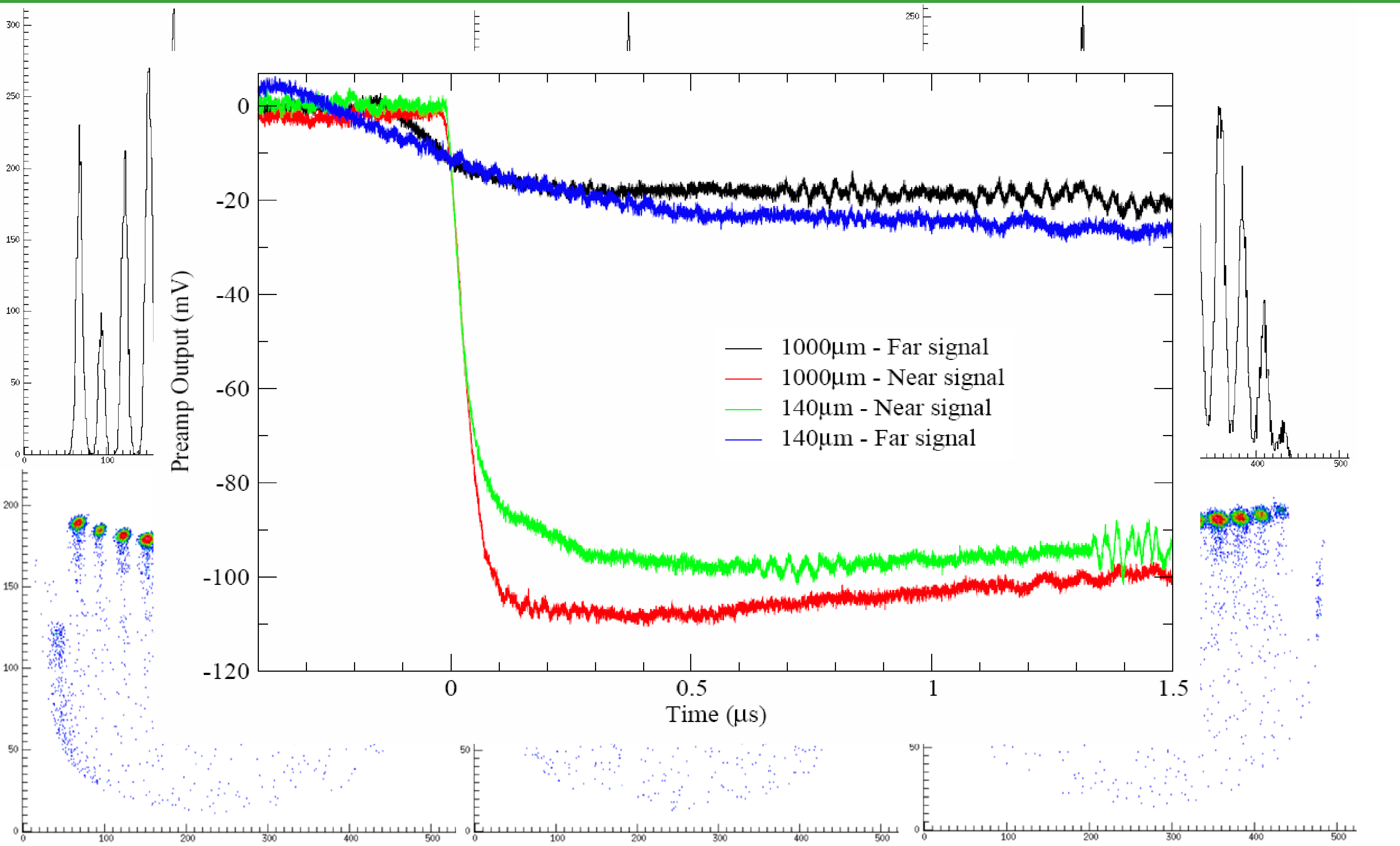

Shaping amplifiers

Shape pulses to:

- *Improve signal to noise*
- *Reduce pileup effects*

Keep signal height information

Lose shape information

Genuine second pulses missed

→ *Digital!*

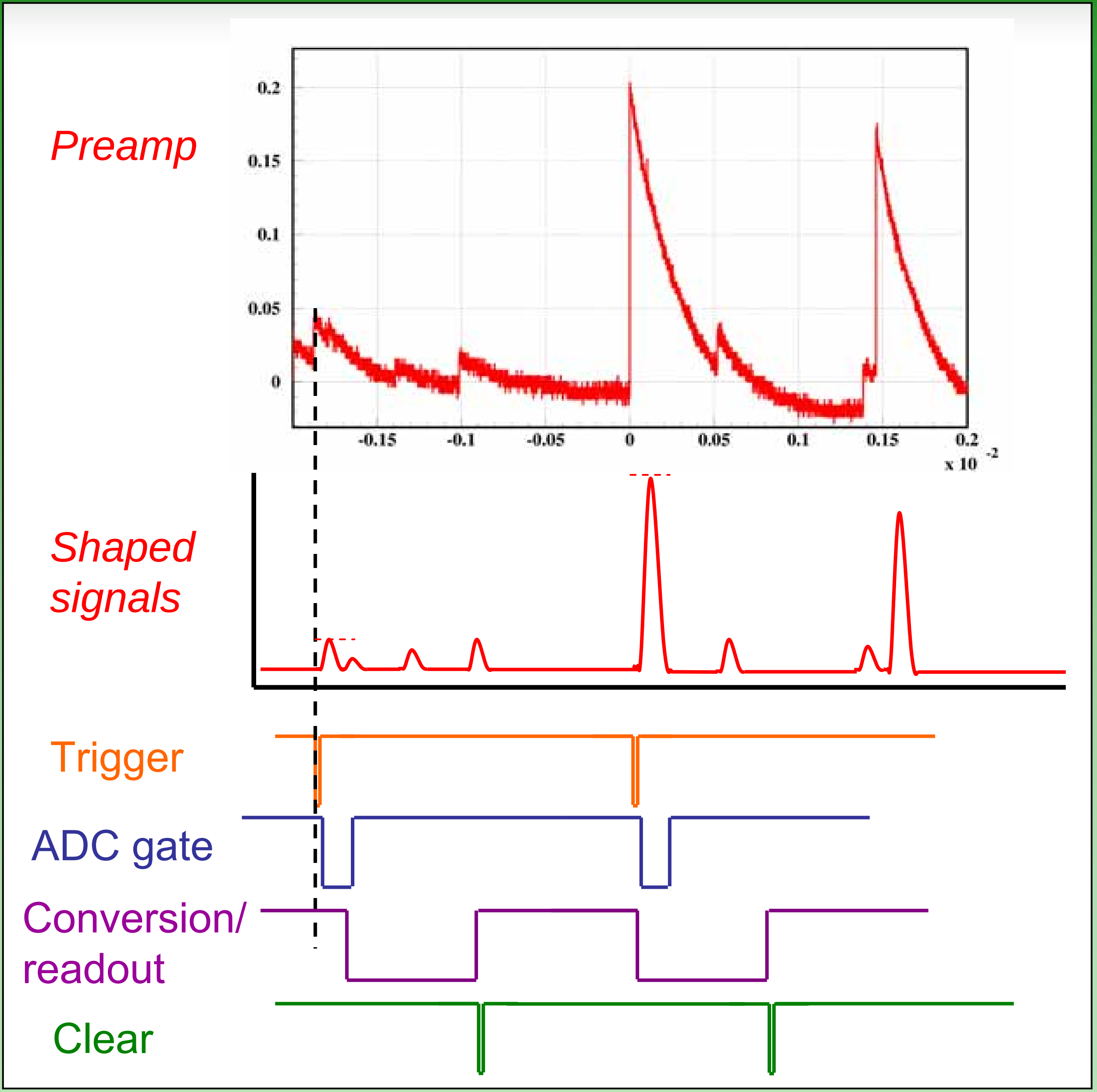

Signal processing

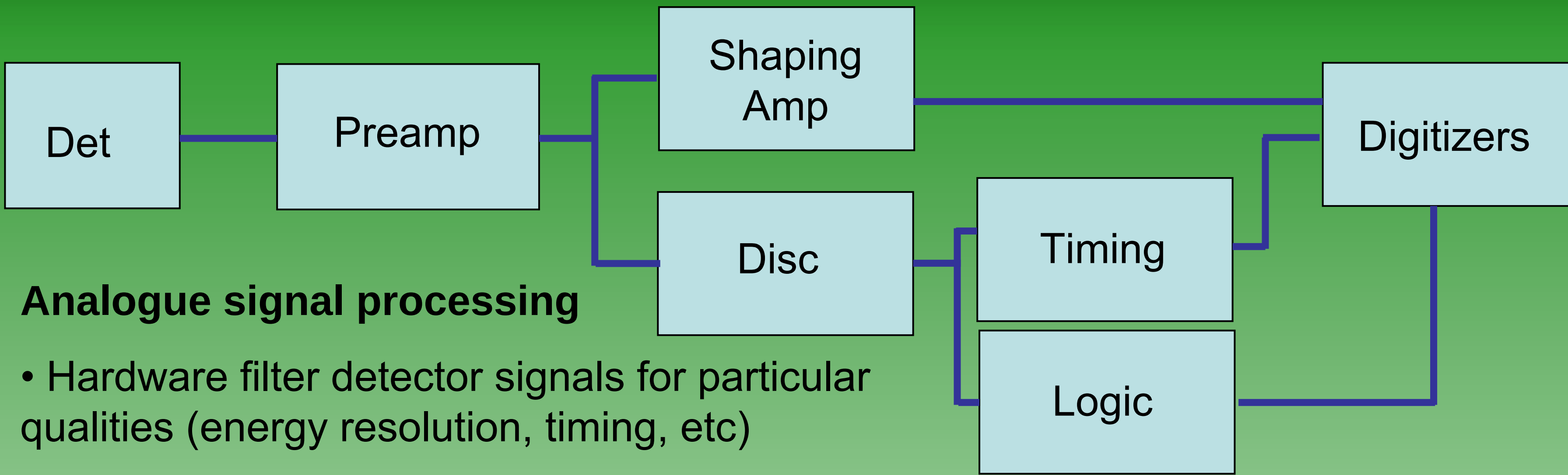

Analogue signal processing

- Hardware filter detector signals for particular qualities (energy resolution, timing, etc)
- Excellent resolution, but some information is discarded
- Separate optimized processing required for different parameters (energy, time, etc)

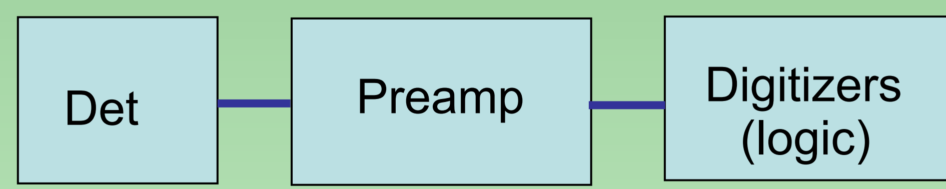

Digital signal processing

- Process (and sometimes store) a digital approximation of the trace from a detector/preamp
- All information encoded in the preamp trace can be processed (software)

Digital Signal Processing

- Digital information can be stored, retrieved and duplicated without losses
- Duplicated data streams processed independently (eg one optimized for energy, another for time)
- Correlations between separate data streams can be made on arbitrary time scale (time-stamping)
- Full traces can be recorded, and processed offline
- Information on signal shape (eg rise-time) and closely-timed events (eg implantation-decay) is maintained
- Data sampling rate MHz – GHz (depending on signal properties)

Thanks to Robert Grzywacz, University of Tennessee

Digital Signal Processing

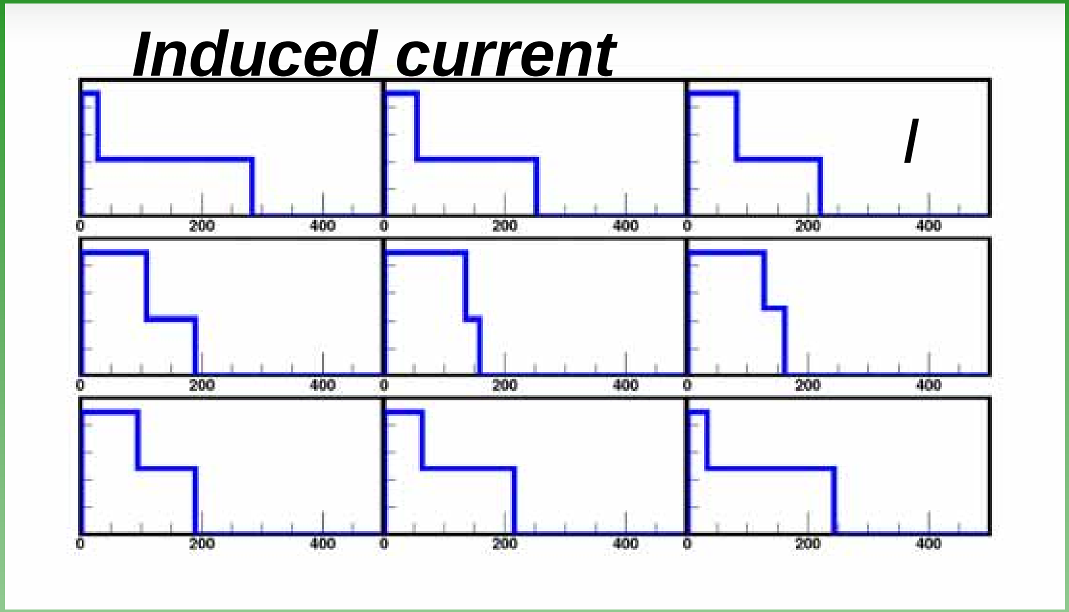

Large volume detector (eg Ge, gas detectors) has a pulse shape dependence on interaction position

Movement of the charge inside the detector induces image charges

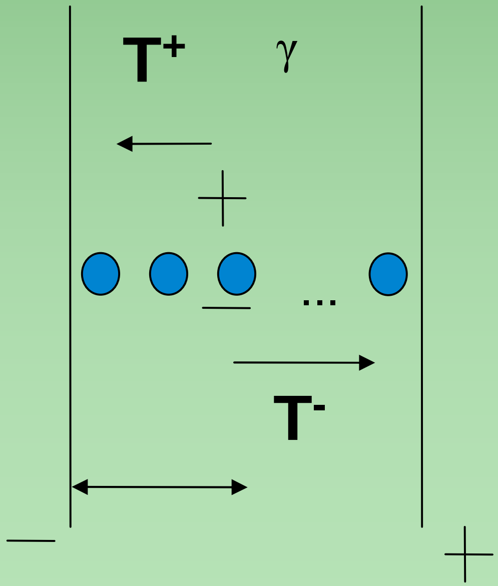

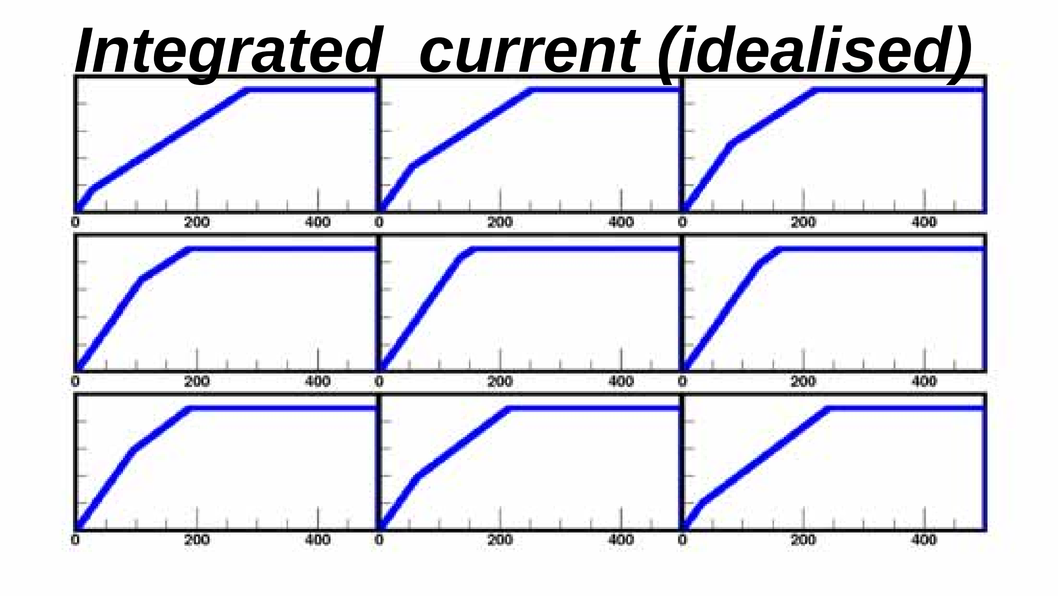

Digital Signal Processing

Integrated current (preamplifier)

$$I = \frac{dq}{dt}$$

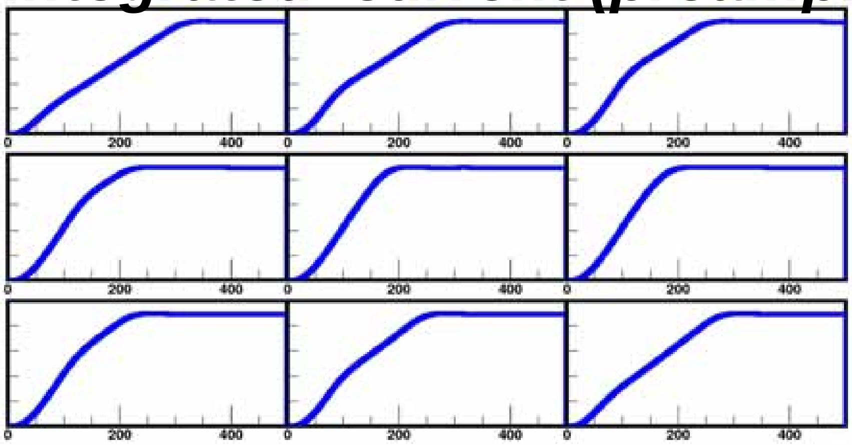

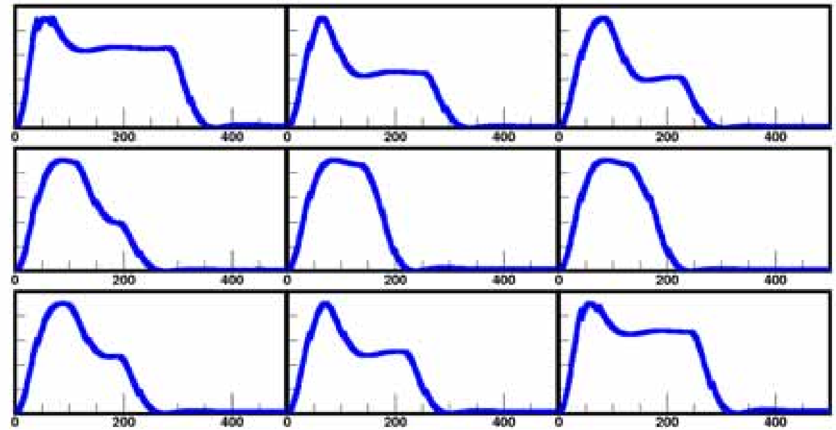

Integrated current (digitized)

$$I = \frac{\Delta q}{\Delta t}$$

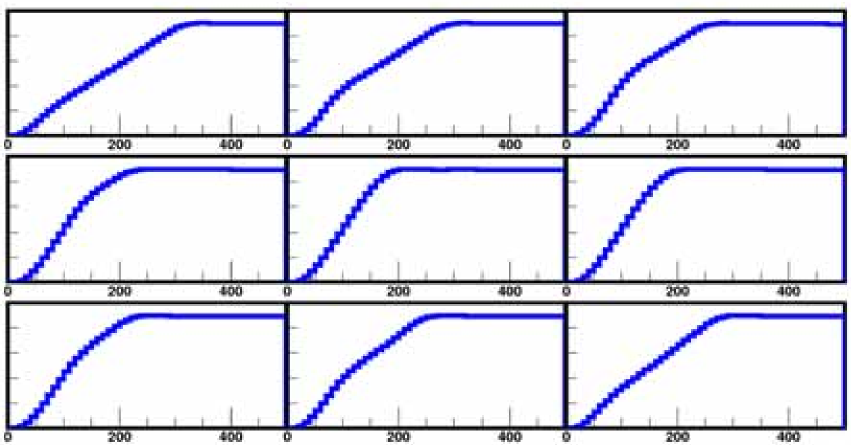

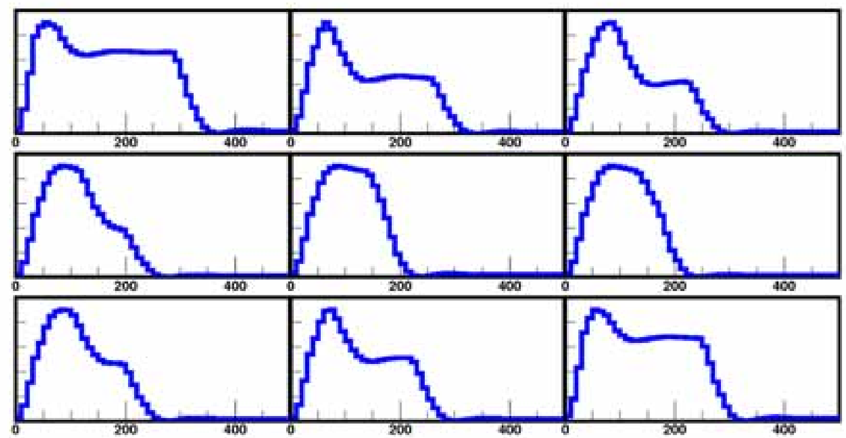

Digital Signal Processing

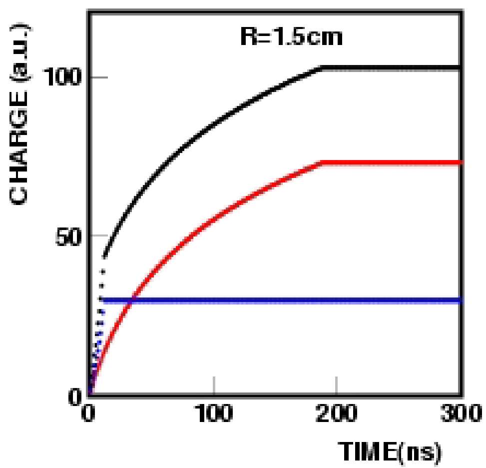

Gamma ray tracking

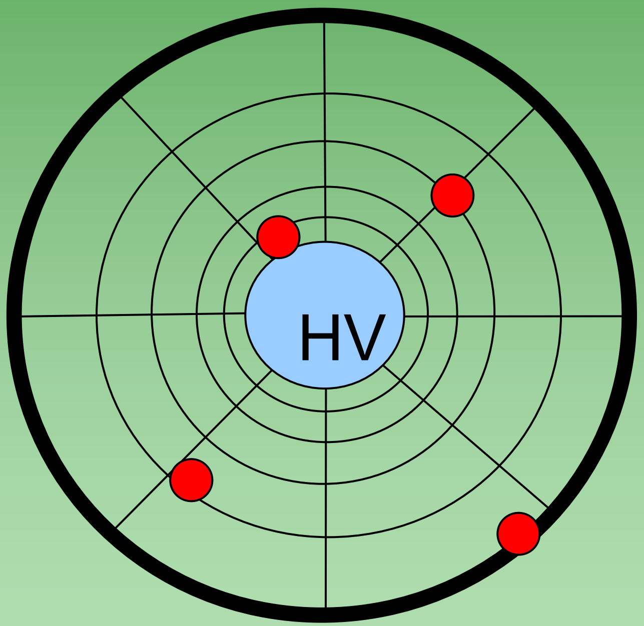

“cylindrical field”

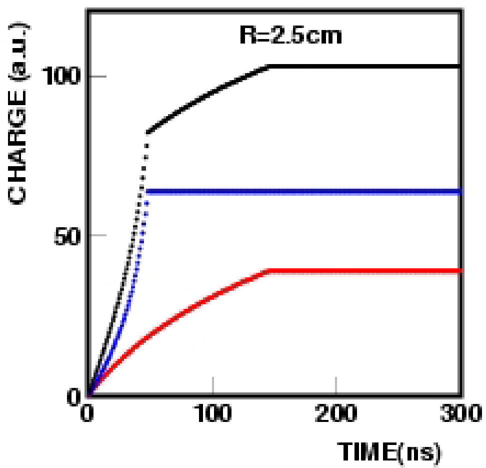

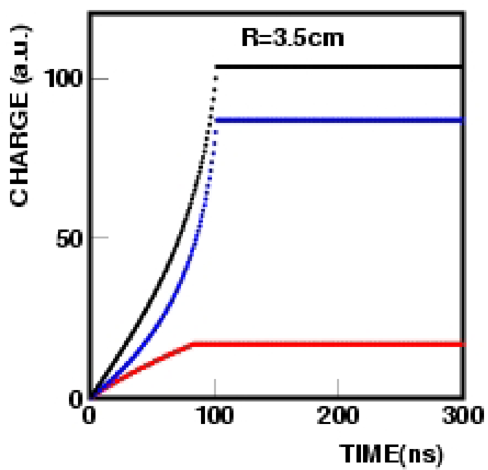

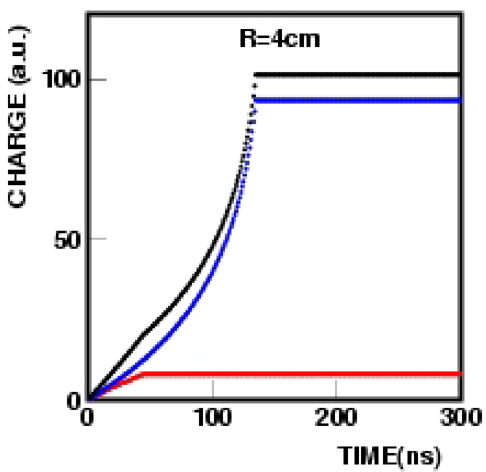

Digital Signal Processing

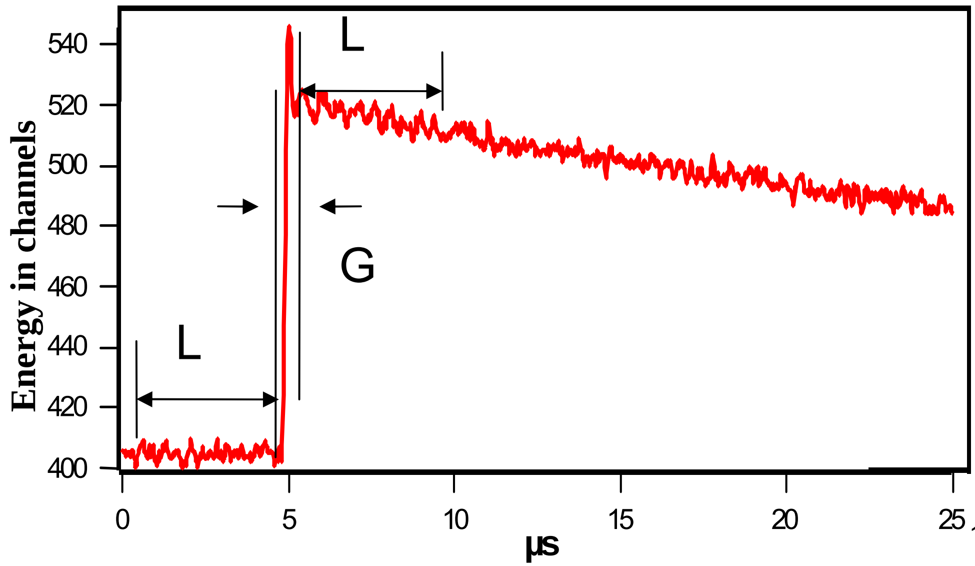

Detector pulse

Trapezoidal Filter

A digital equivalent to shaping

Sensitive to fast changes in signal

$$V = V_{L2}^{\ av} - V_{L1}^{\ av}$$

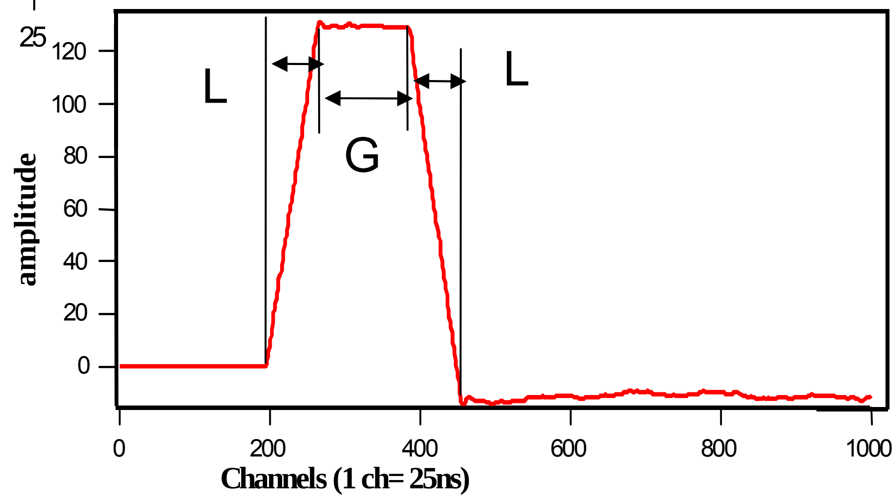

Transformed pulse

Match G to rise-time of the signal

L performs some shaping (low-pass)

Can run signal through multiple filters, optimized for different things

Digital Signal Processing – double events

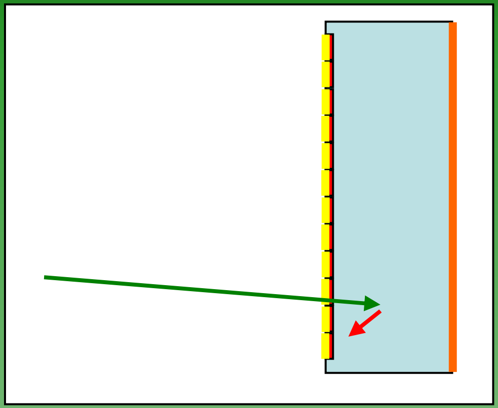

- Detect very short lived proton emitting nuclei at the final focus of the recoil separator
- Very rare event (mHz) in the presence of large implantation (kHz)

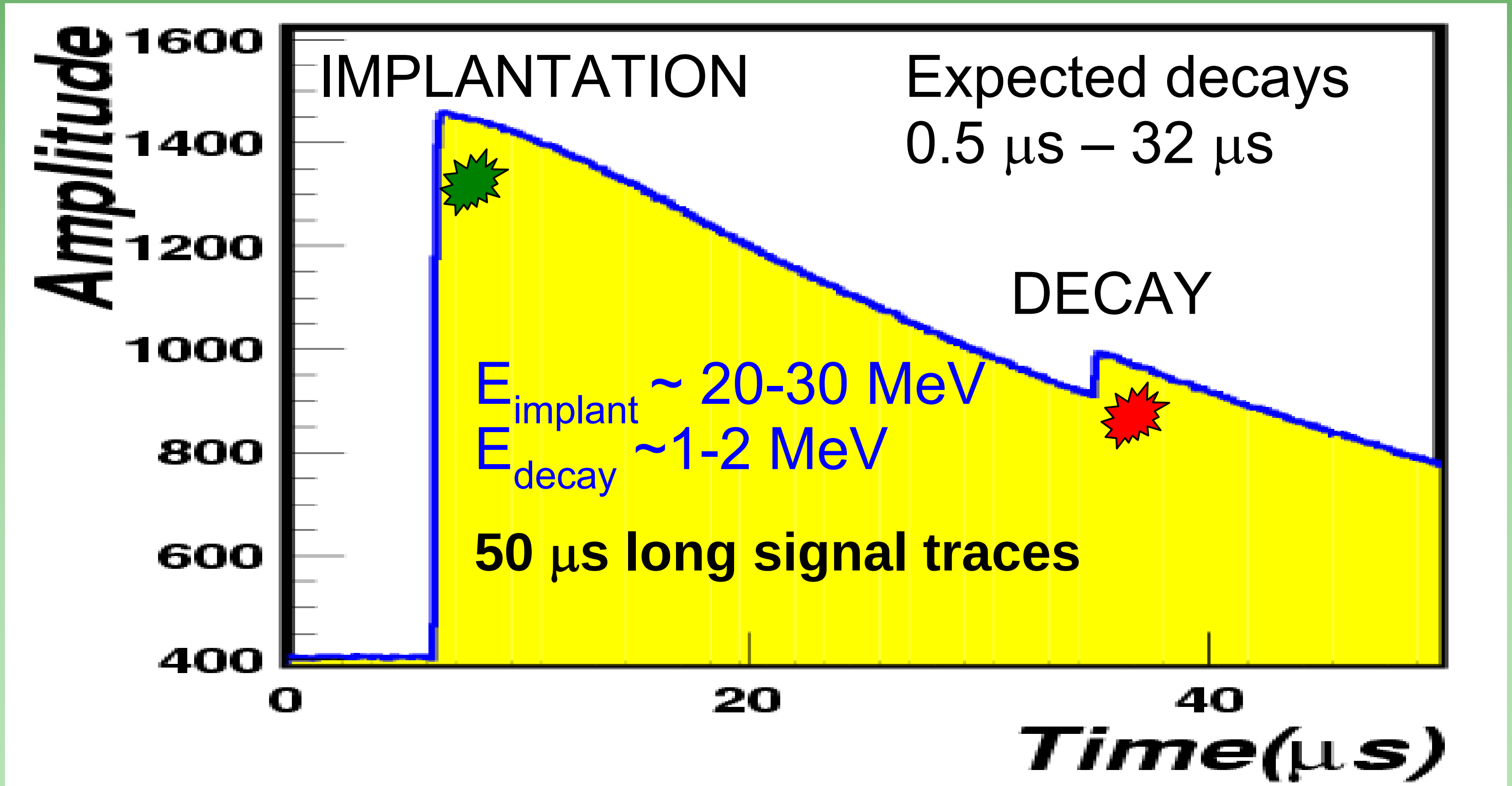

Digital Signal Processing

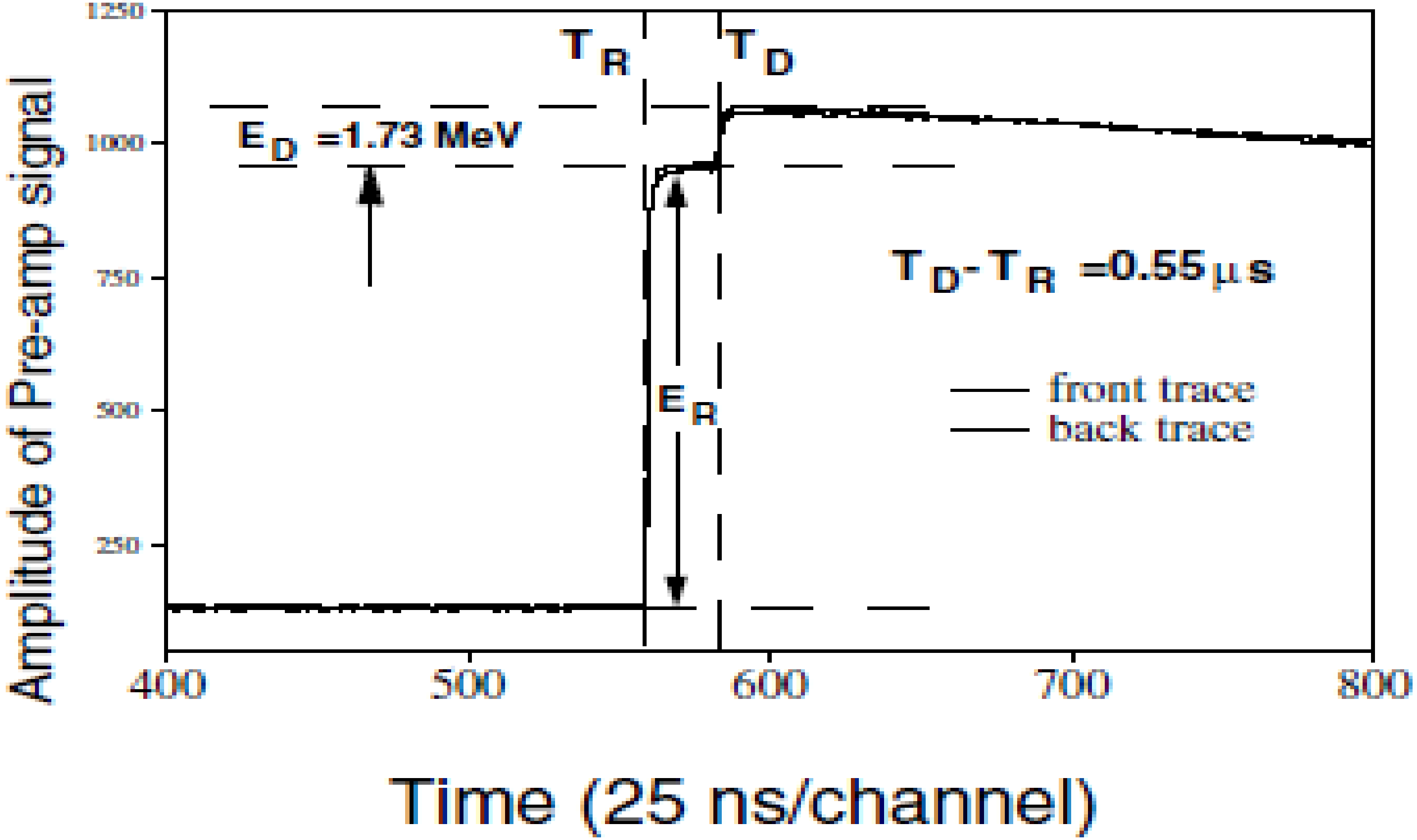

Experiments

Experiments

Direct measurement for nuclear astrophysics - $^{17}F(p,\gamma)^{18}Ne$ (K.A. Chipps, *et al.)*

- Counting

Requirements:

- Selectivity
- Efficiency
- Resolution

- Novae - the most common thermonuclear explosion (~0.2 GK)
  - Hydrogen from companion fuses with CNO nuclei in white dwarf
  - Mechanisms are not well understood (ejecta mass and composition)
- X-ray bursts
  - Hydrogen accretes onto a neutron star
  - Hotter environment initiates the (α,p) chain – heavier element synthesis

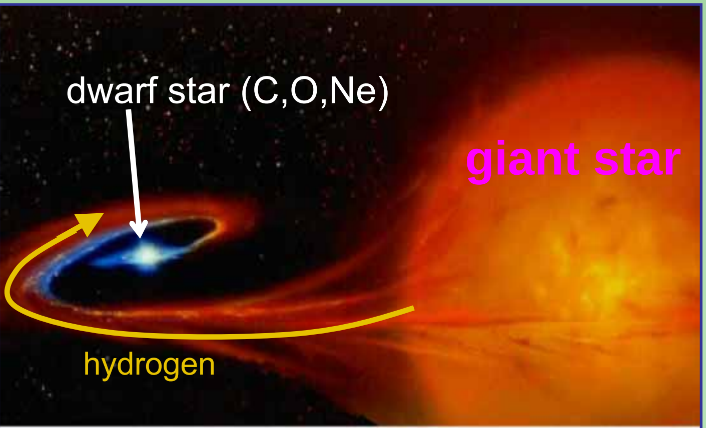

- $^{17}F(p,\gamma)^{18}Ne$ comparable to beta decay rate in novae
- The $^{17}F(p,\gamma)^{18}Ne$ rate is important for
  - Energy generation
  - ^{17}O production
  - ^{18}F production and gamma rays
  - $^{17}F(p,\gamma)^{18}Ne(e^{+}\nu_{e})^{18}F$

Binary systems

Mira system

420 light years away

6.5 billion miles apart (twice the distance between the sun and pluto)

UV image of 13 LY-long tail of Mira [GALEX]

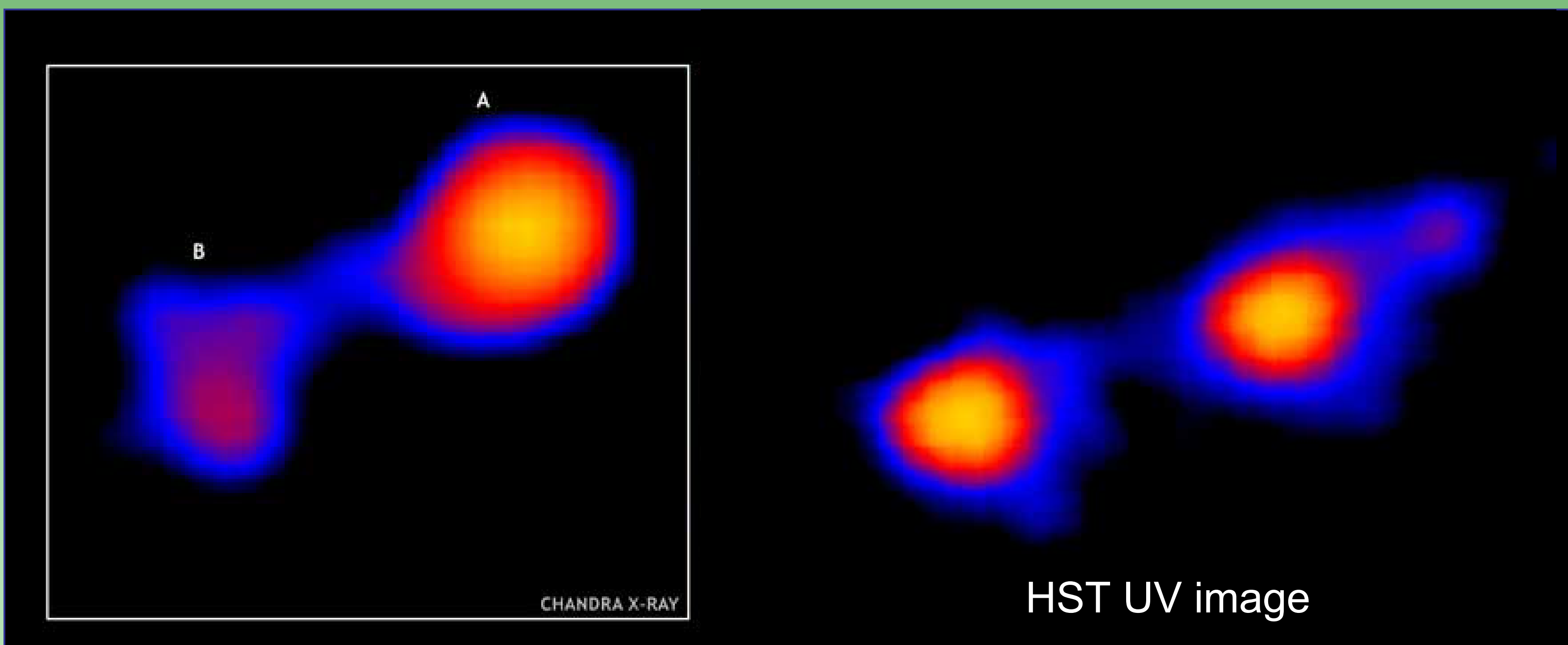

The $^{17}F(p,\gamma)^{18}Ne$ reaction rate – resonance location

A. Garcia *et al* , Phys. Rev. C 43 (1991) 2012

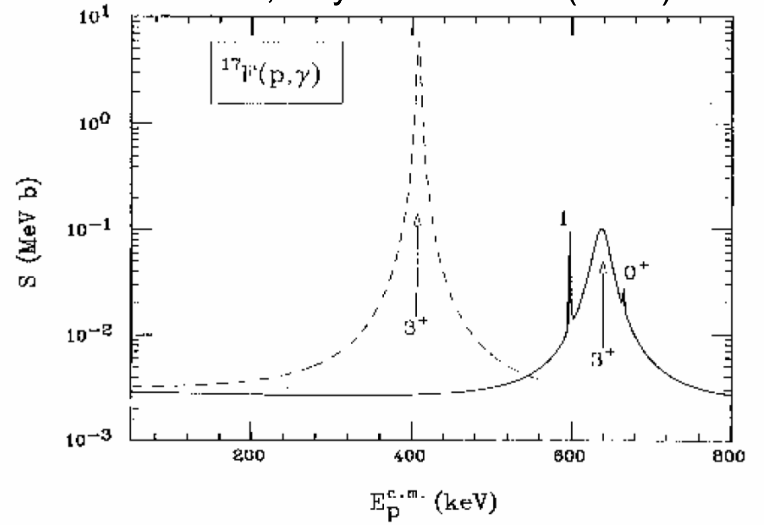

- Only two significant contributions to the rate:
  - 3^+ resonance
  - Direct capture

- The important 3^+ resonance location was unknown
- Various predictions for its location had significant impact on its contribution to reaction rate in novae

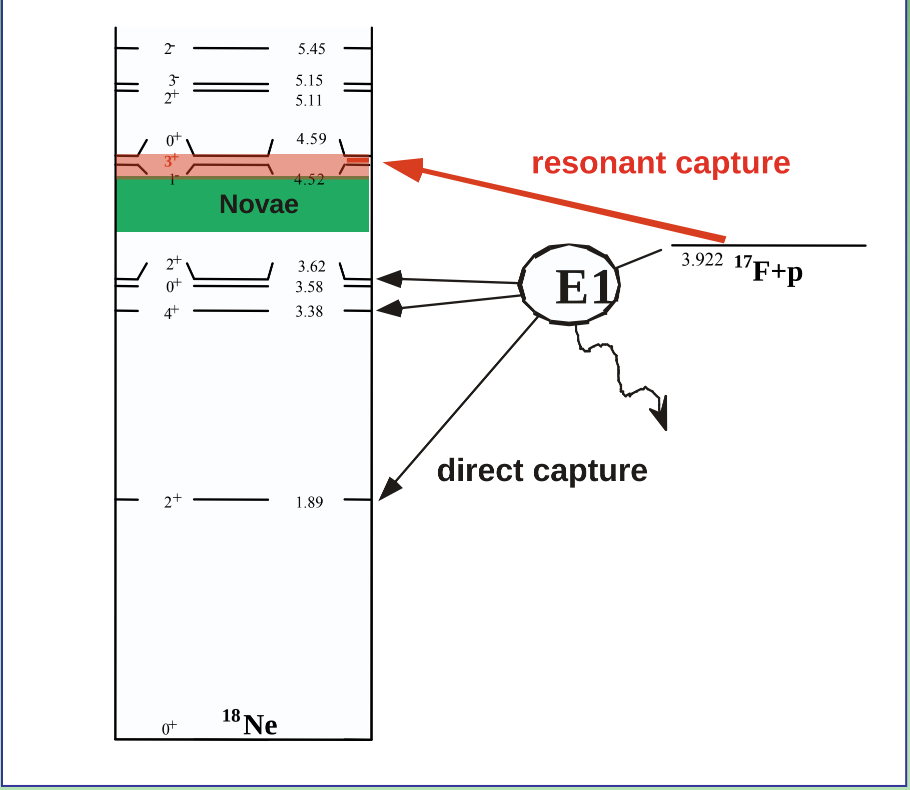

The $^{17}F(p,\gamma)^{18}Ne$ reaction rate – resonance location

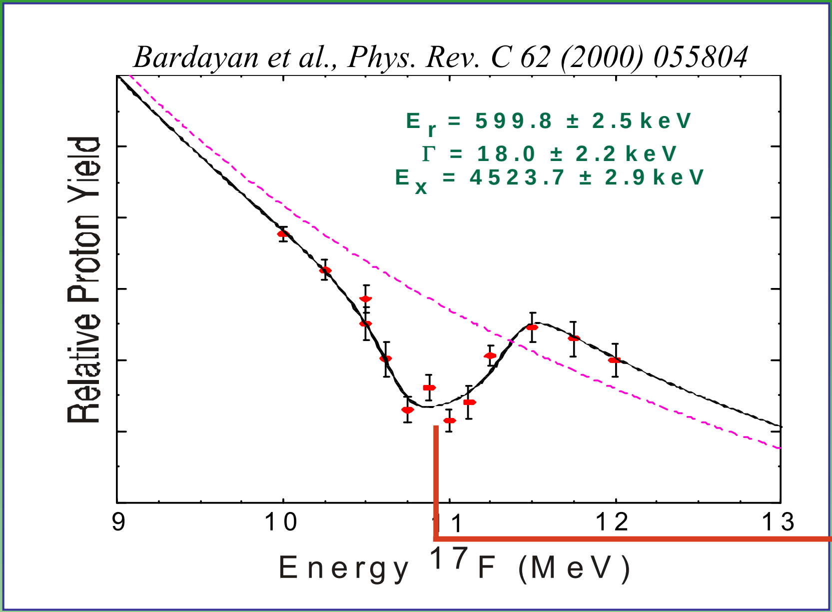

- Only two significant contributions to the rate:
  - 3^+ resonance
  - Direct capture

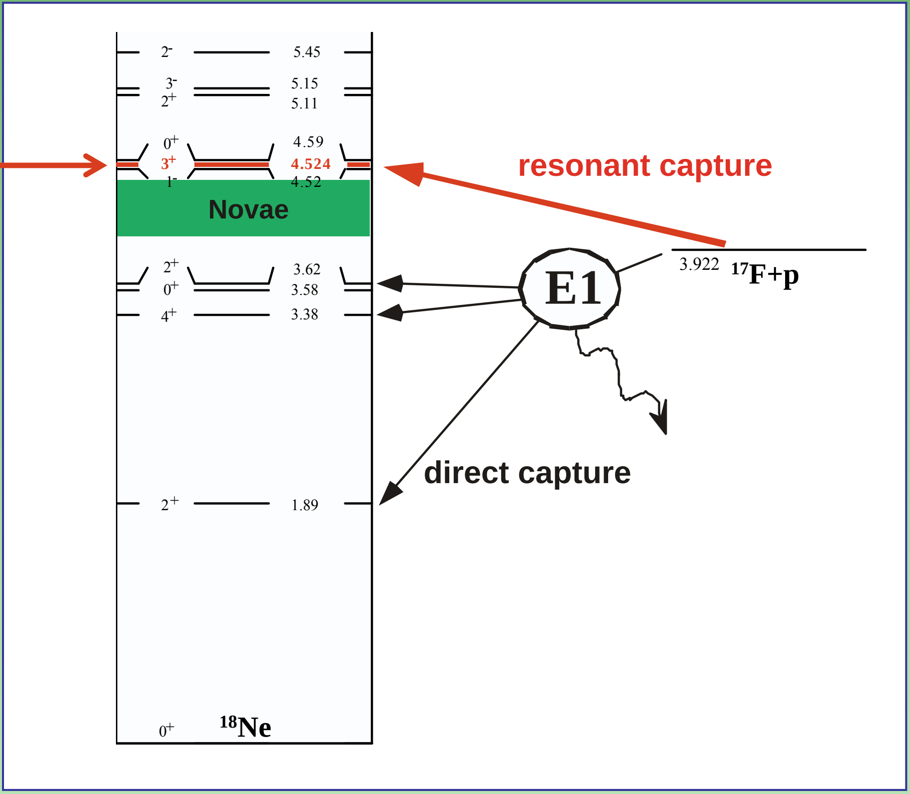

- The important 3^+ resonance is too high in energy to have a dominant contribution at nova temperatures
- The 3^+ resonance will dominate the reaction rate at higher temperatures, e.g. in X-ray bursts
- Resonance strength unknown

The $^{17}F(p,\gamma)^{18}Ne$ reaction rate – resonance strength

5×10^{6} pps ^{17}F
(50% purity)

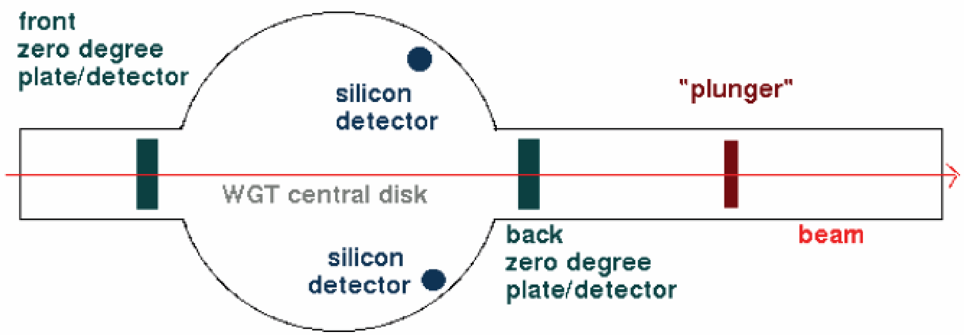

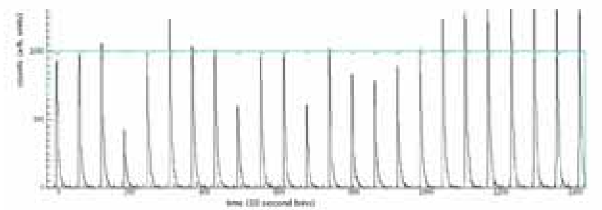

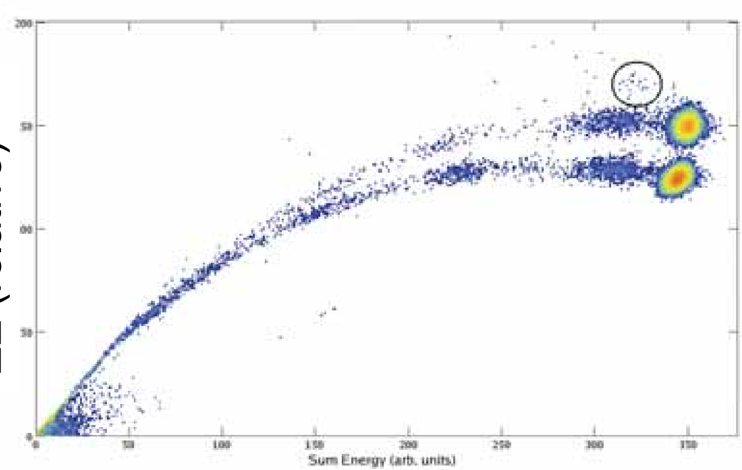

ΔE (relative)

Energy (MeV)

Ionization chamber

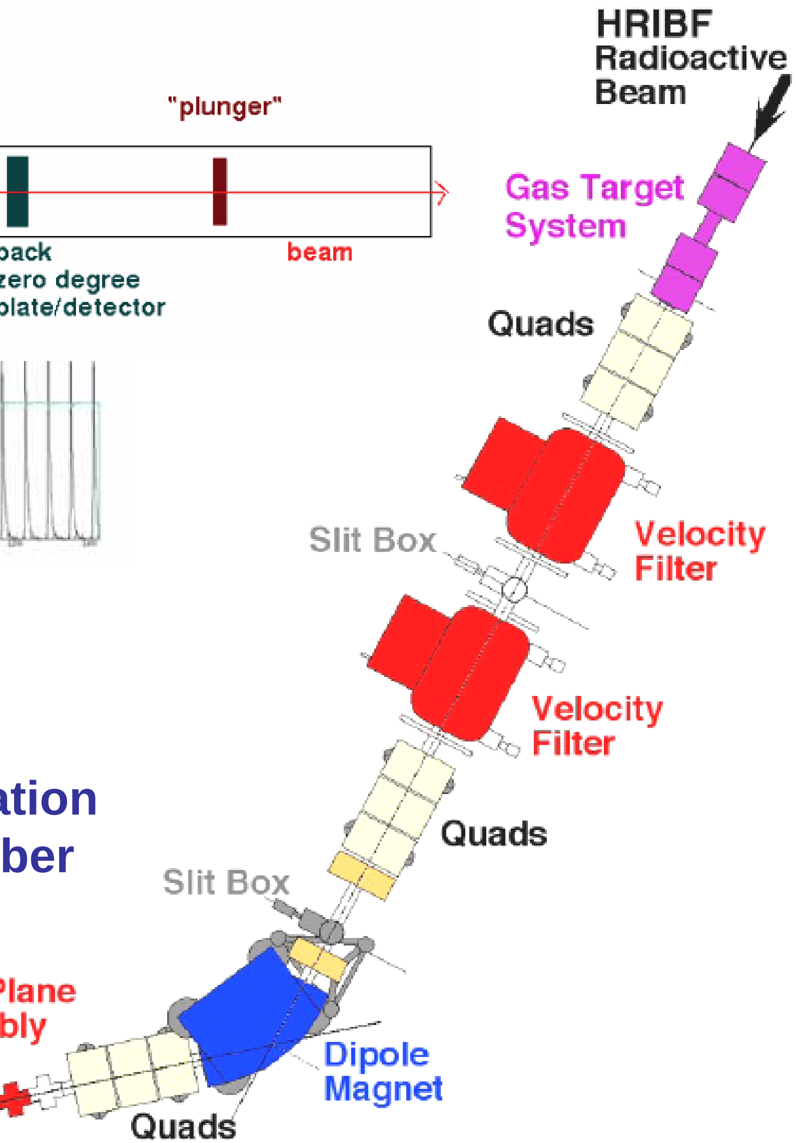

K.A. Chipps *et al.*, Phys. Rev. Lett. 102 (2009) 152502

The $^{17}F(p,\gamma)^{18}Ne$ reaction rate – resonance strength

5×10^{6} pps ^{17}F
(50% purity)

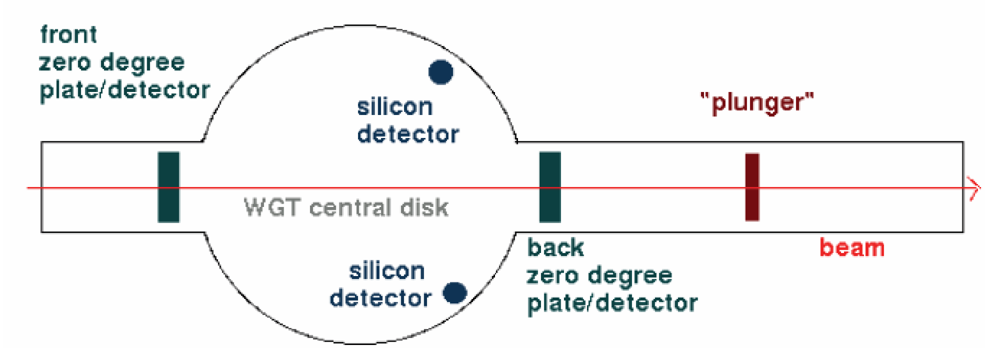

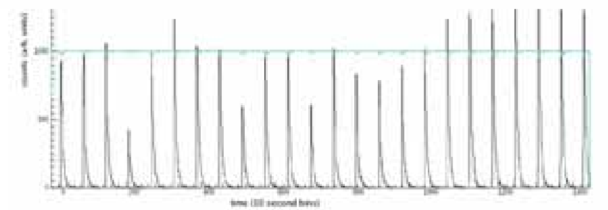

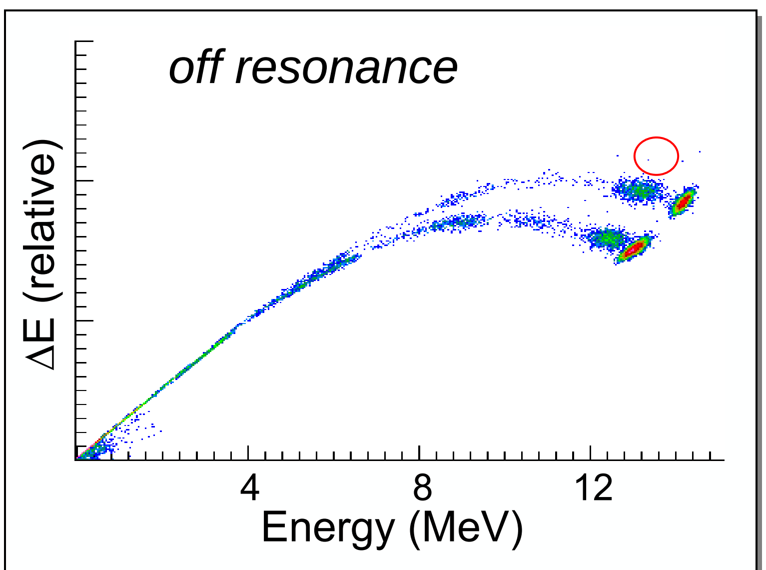

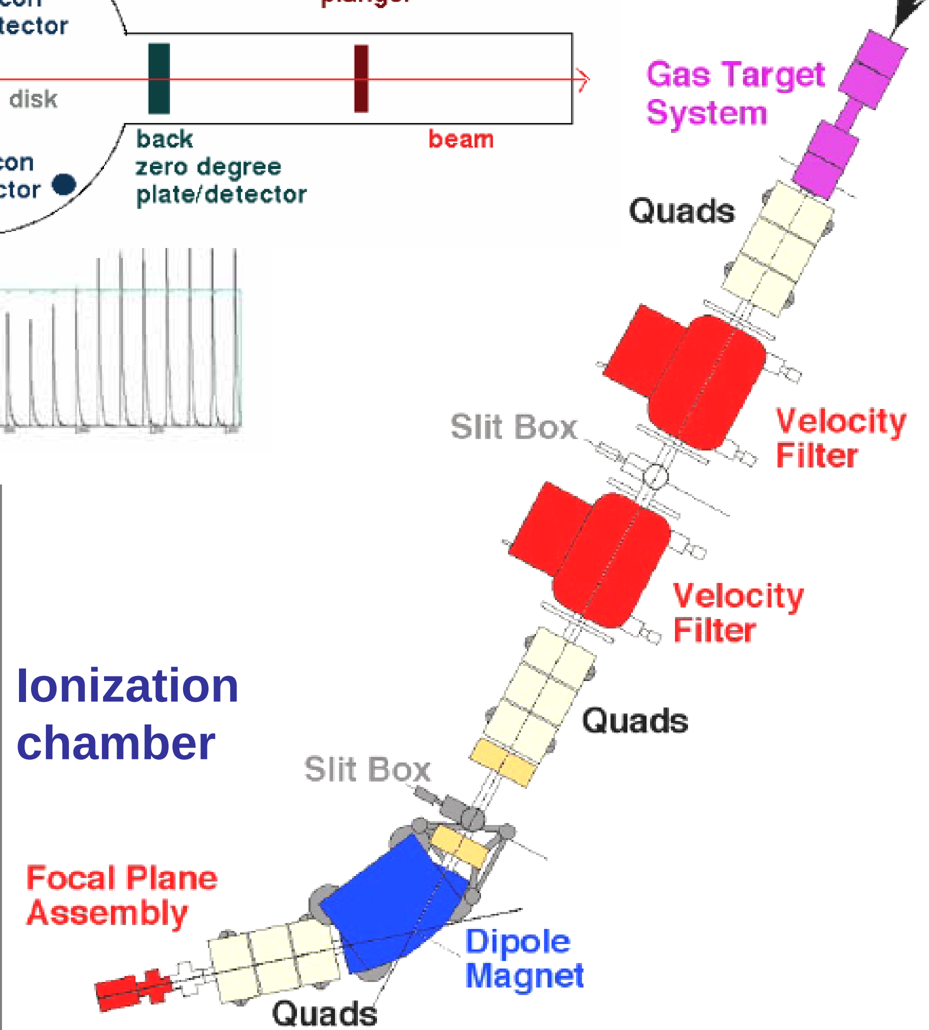

K.A. Chipps *et al.*, Phys. Rev. Lett. 102 (2009) 152502

The $^{17}F(p,\gamma)^{18}Ne$ reaction rate – resonance strength

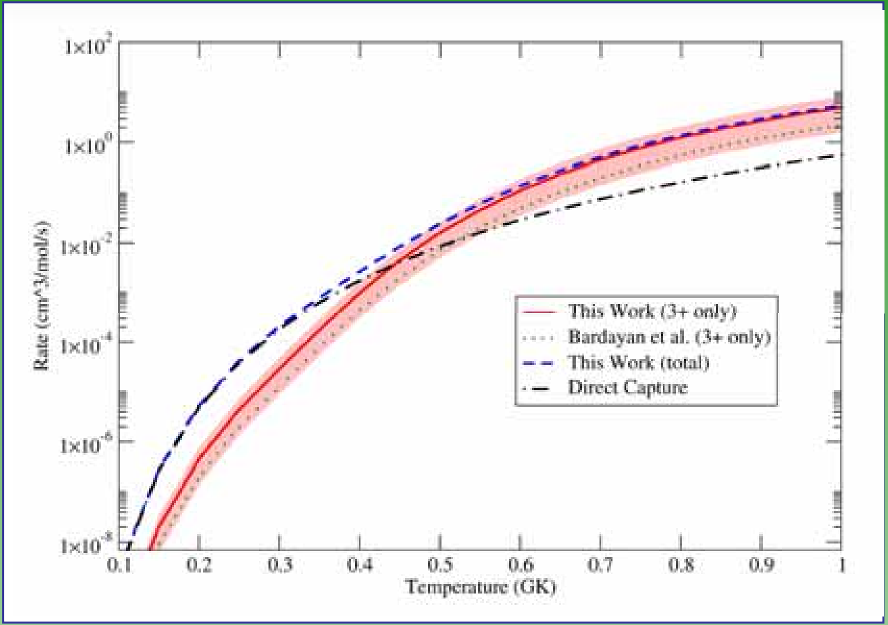

- $\omega\gamma$ = 33 ± 14 (stat) ± 17 (sys) meV
- Constrained resonant cross section to within factor of 2

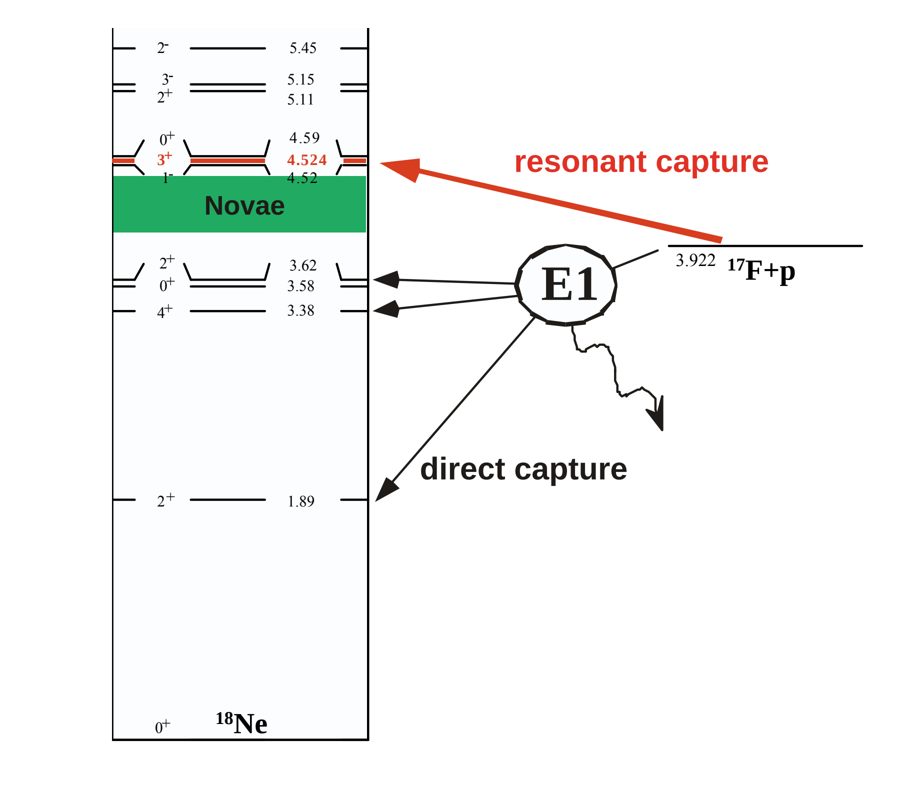

- The direct capture cross section dominates the $^{17}F(p,\gamma)^{18}Ne$ reaction rate in novae
- Direct measurement of $^{17}F(p,\gamma)^{18}Ne$ at nova temperatures requires ~ 10^{10} pps of ^{17}F/s, or *~40 years at current beam rates!*
- Indirect method required…

Direct capture rates from ANCs

- Direct capture occurs via an electromagnetic transition at large radii
- The cross section can be accurately calculated from the Asymptotic Normalization Coefficients (ANC's) with little model dependence
- The ANC's can be determined by measuring the cross section for peripheral proton transfer reactions
  - *Mukhamedzhanov et al., PRC56 (1997) 1302.*
  - *Gagliardi et al., PRC59 (1999) 1149.*
  - *Gagliardi et al., Eur. Phys. J. A13 (2002) 227.*

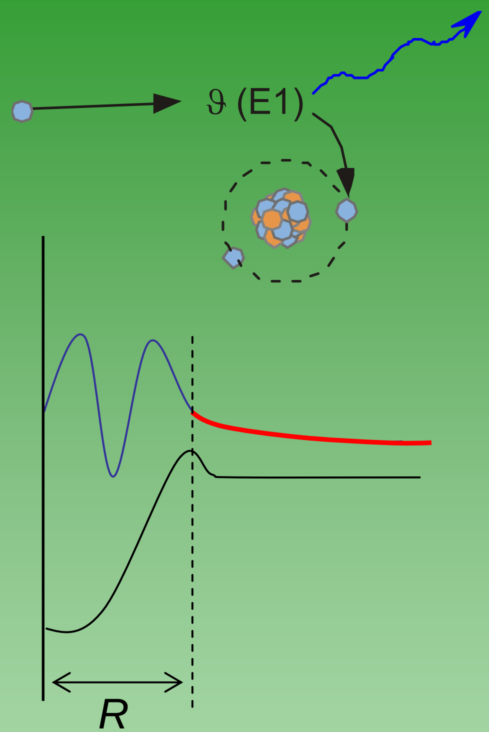

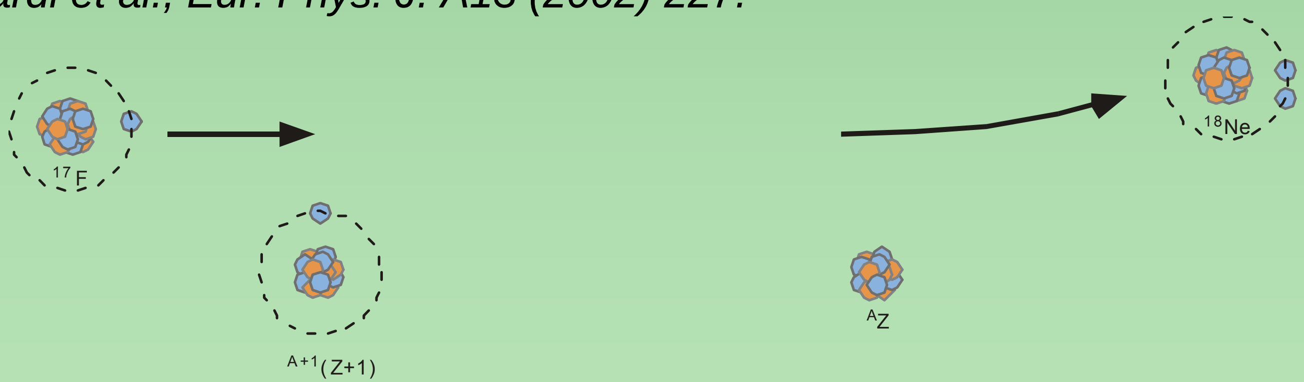

Transfer experiments in inverse kinematics

- Energies
- Angles
- Counting

Requirements:

- Resolution
- Efficiency
- Selectivity

- Traditionally performed in normal kinematics (light ion beam, heavy target nucleus) with magnetic spectrograph (excellent resolution)
- Short-lived exotic nuclei must be the beam
- Inverse kinematics on CD_2 targets
- Si array, or solenoid (HELIOS) device
- [Augmented with gammas]

(d,p) reactions

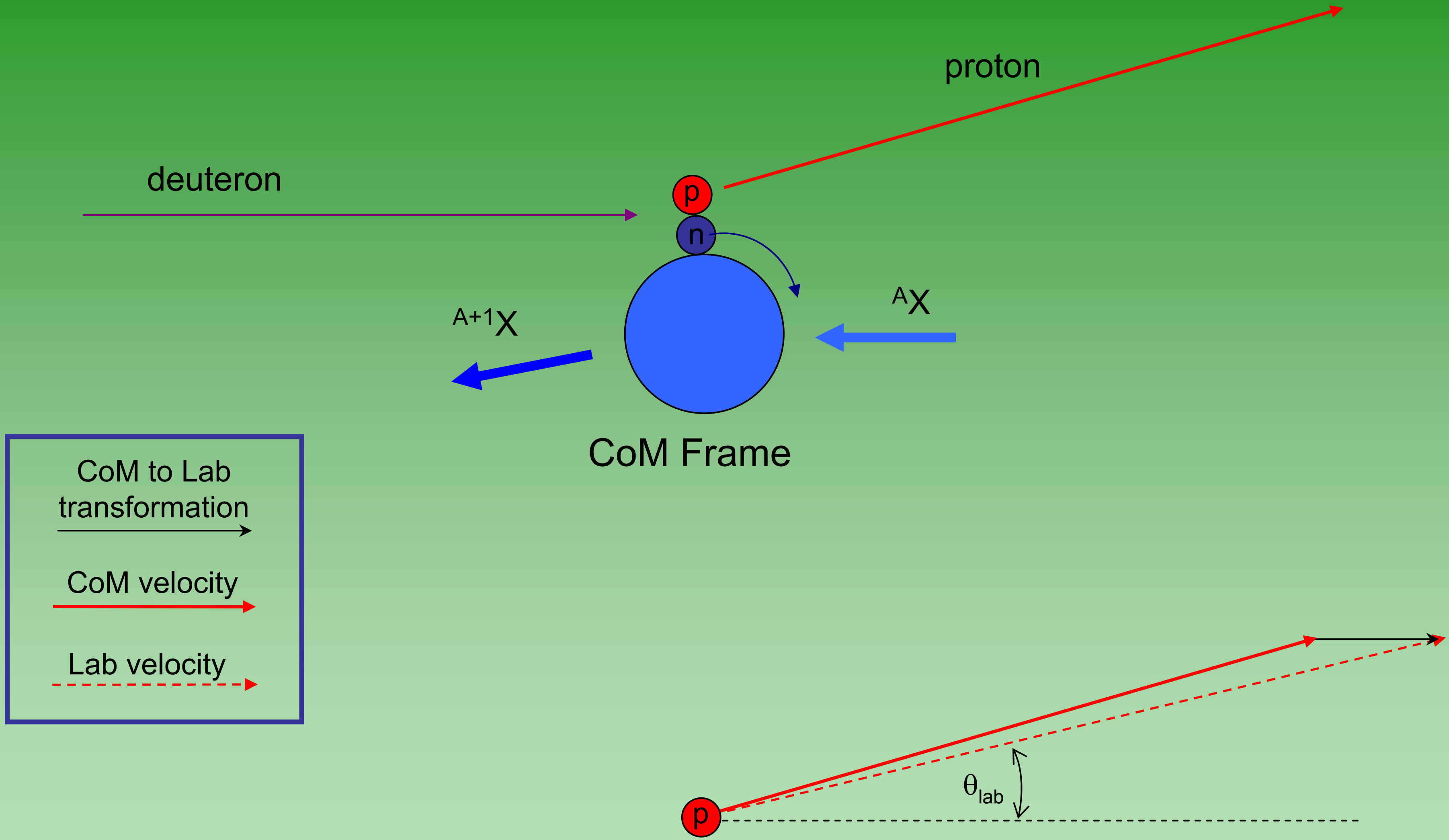

Normal Kinematics

(d,p) reactions

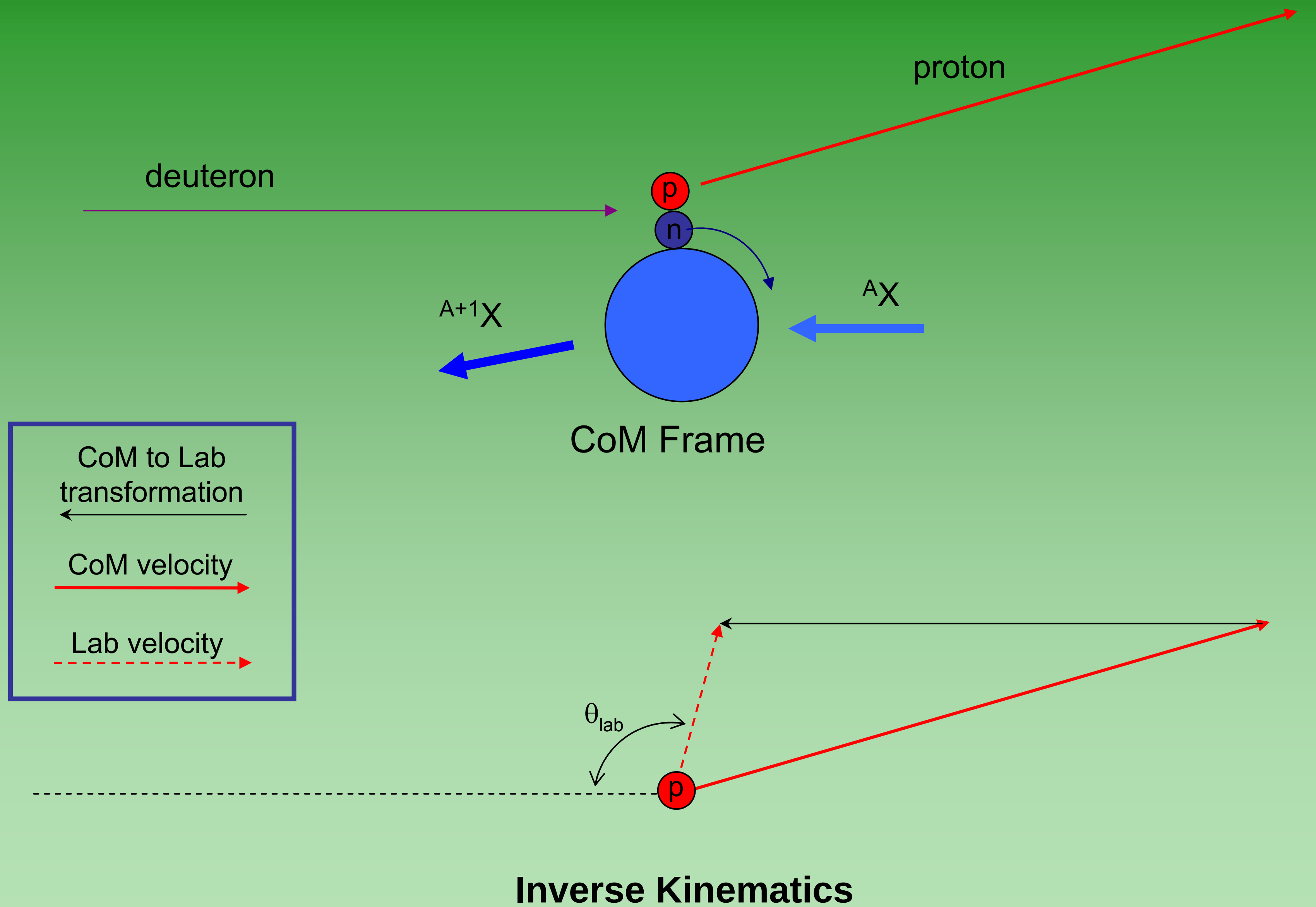

(d,p) reactions

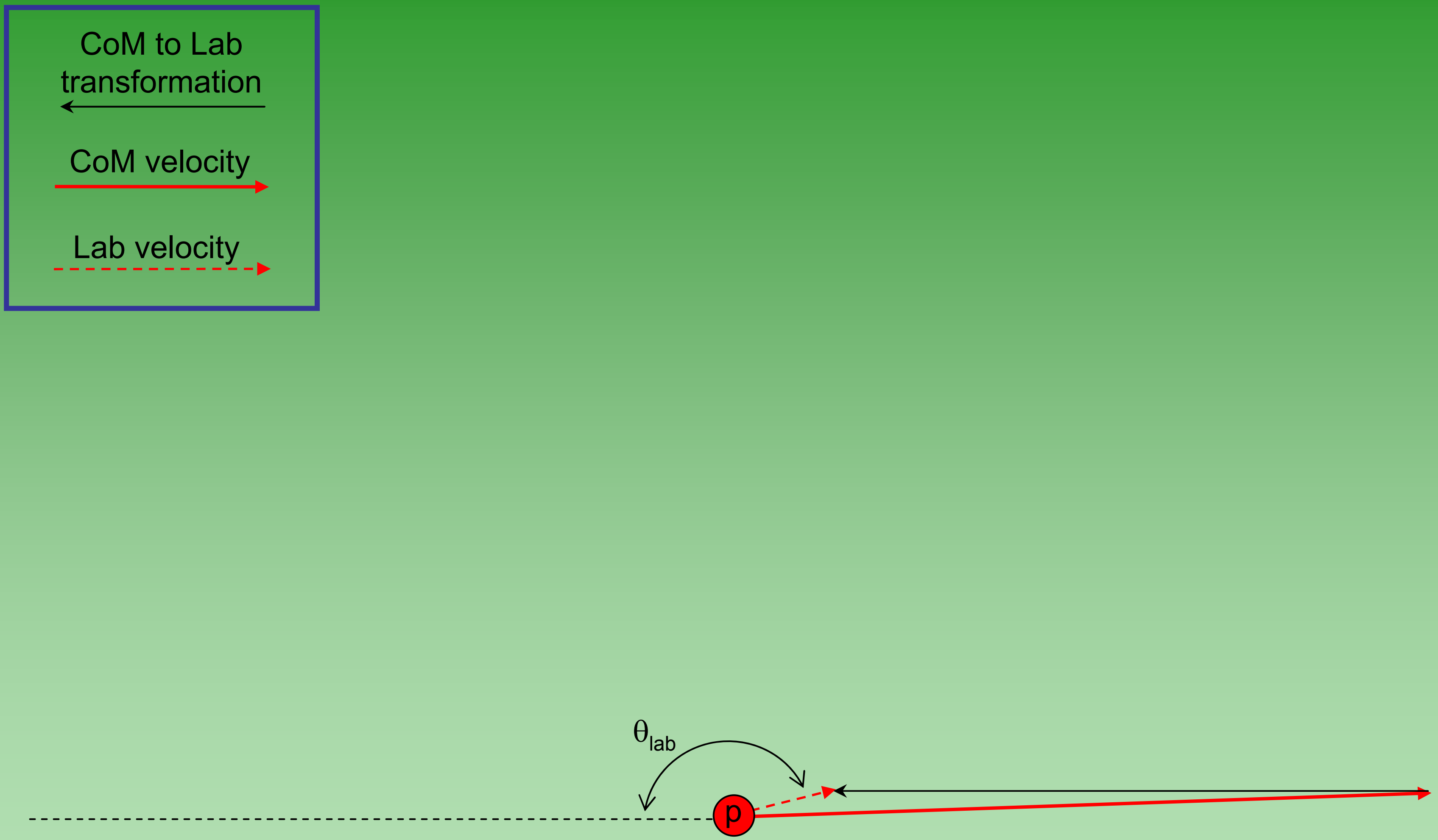

Inverse Kinematics

(d,p) reactions

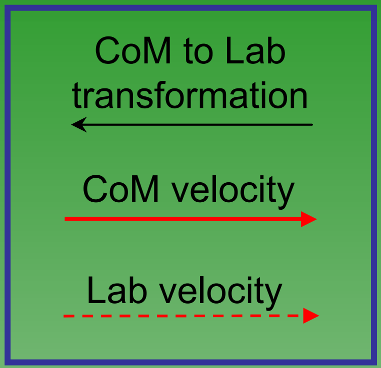

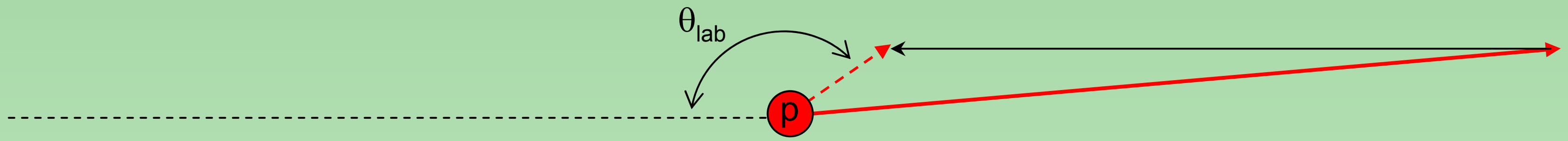

Inverse Kinematics

(d,p) reactions

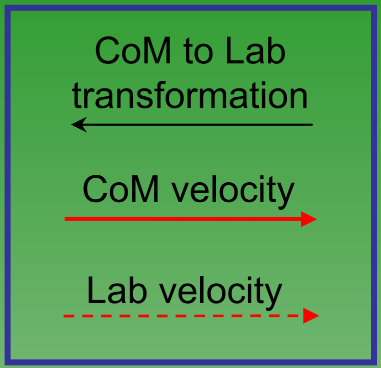

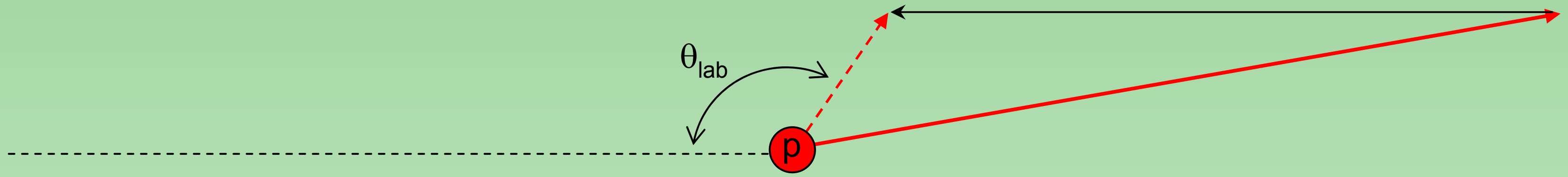

Inverse Kinematics

(d,p) reactions

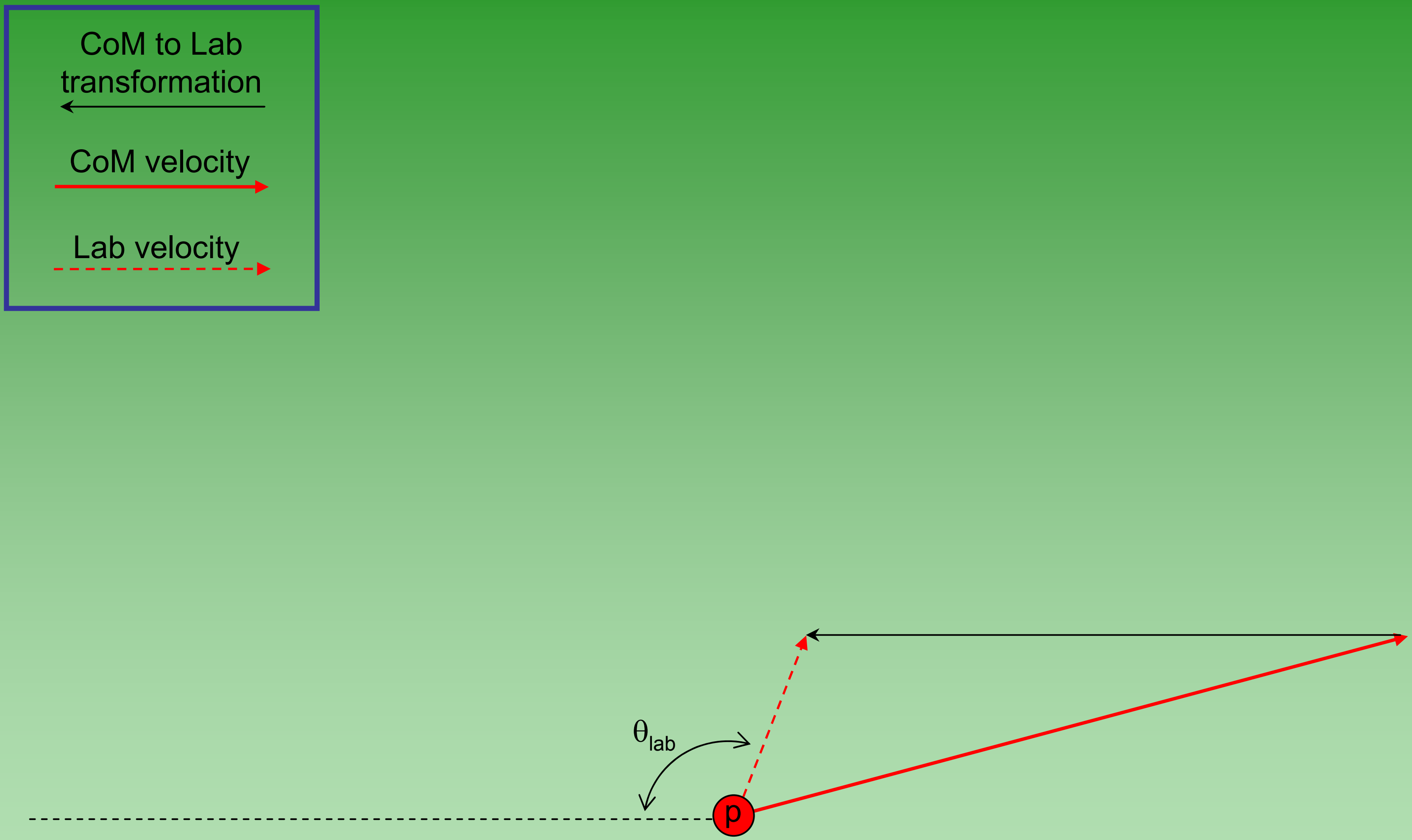

Inverse Kinematics

(d,p) reactions

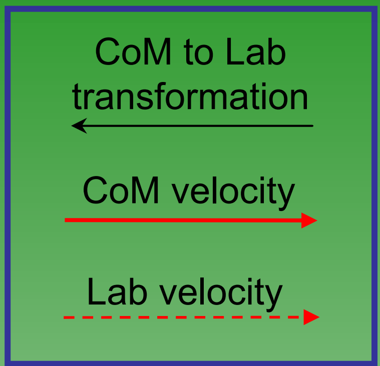

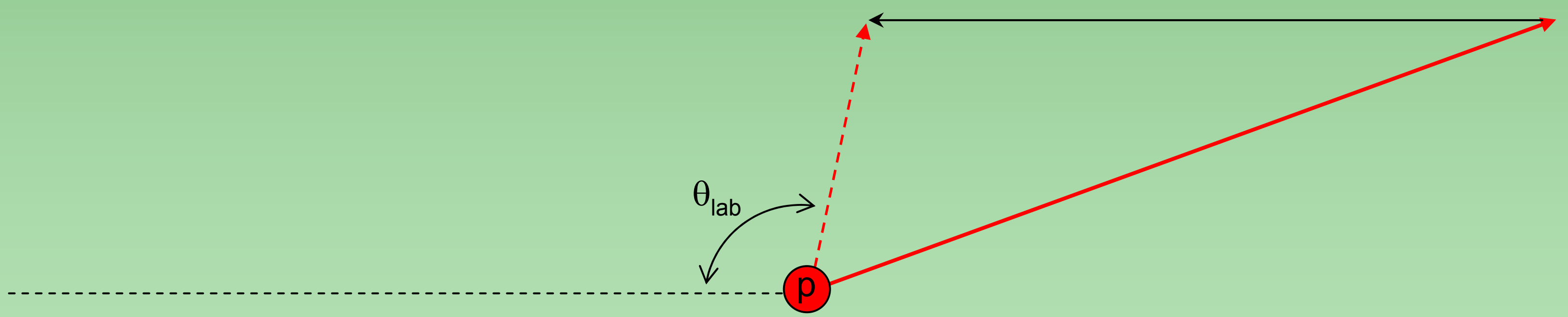

Inverse Kinematics

(d,p) reactions

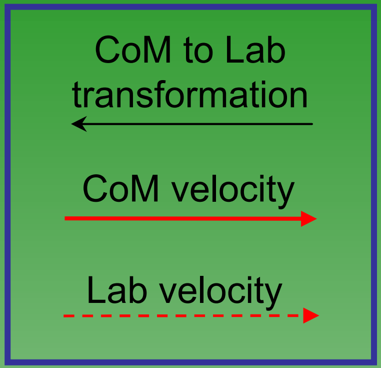

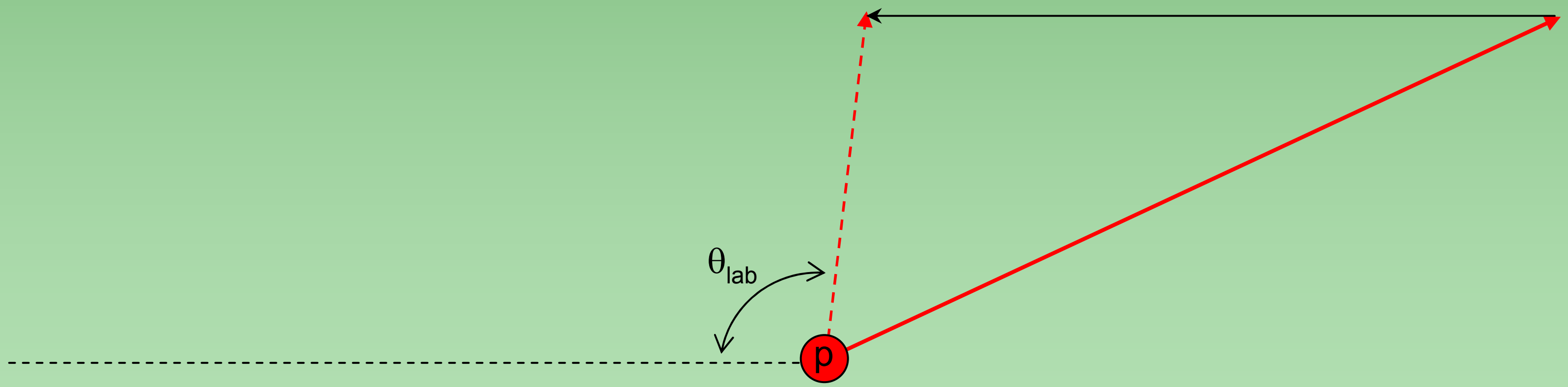

Inverse Kinematics

(d,p) reactions

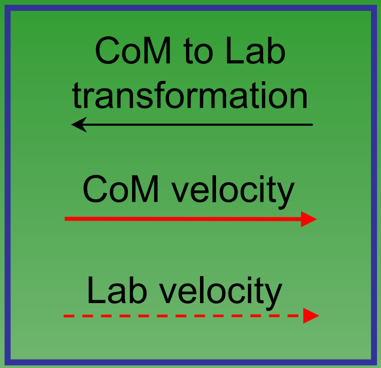

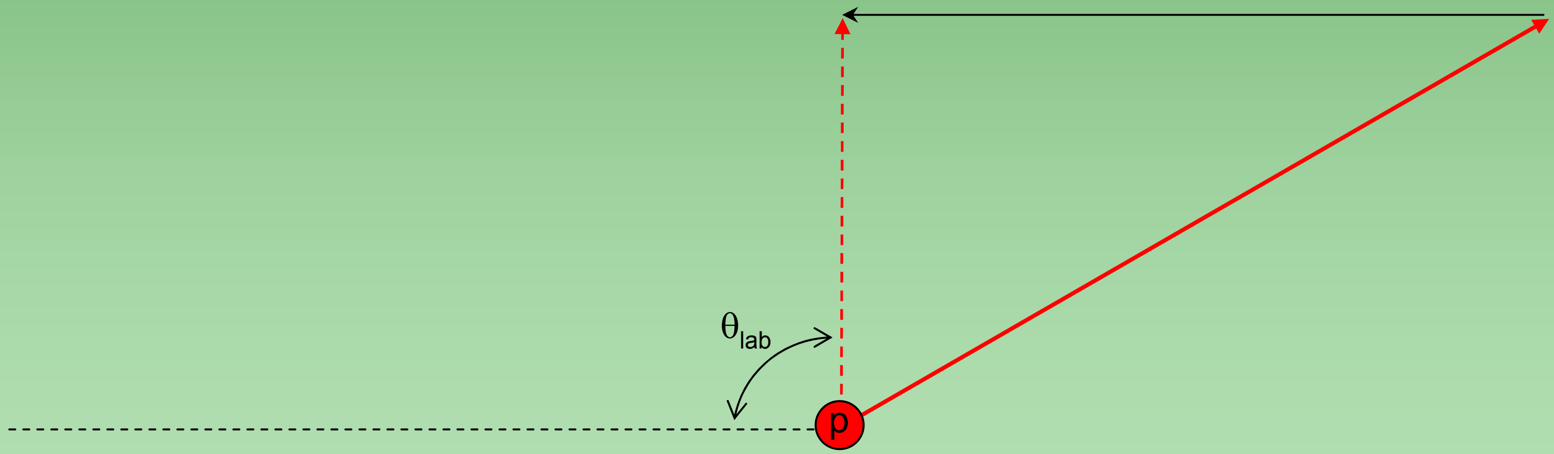

Inverse Kinematics

(d,p) reactions

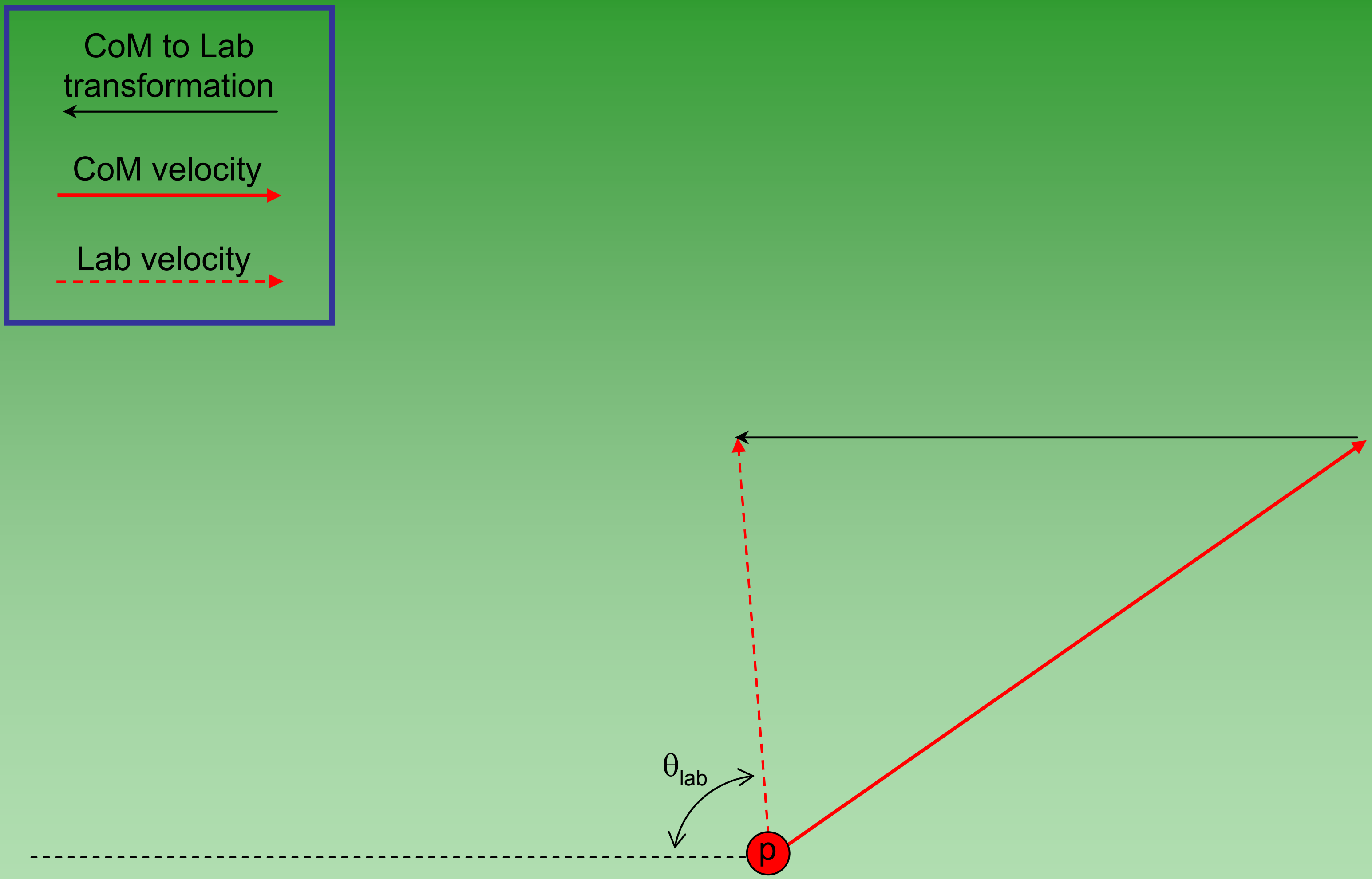

Inverse Kinematics

(d,p) reactions

CoM to Lab transformation

CoM velocity

Lab velocity

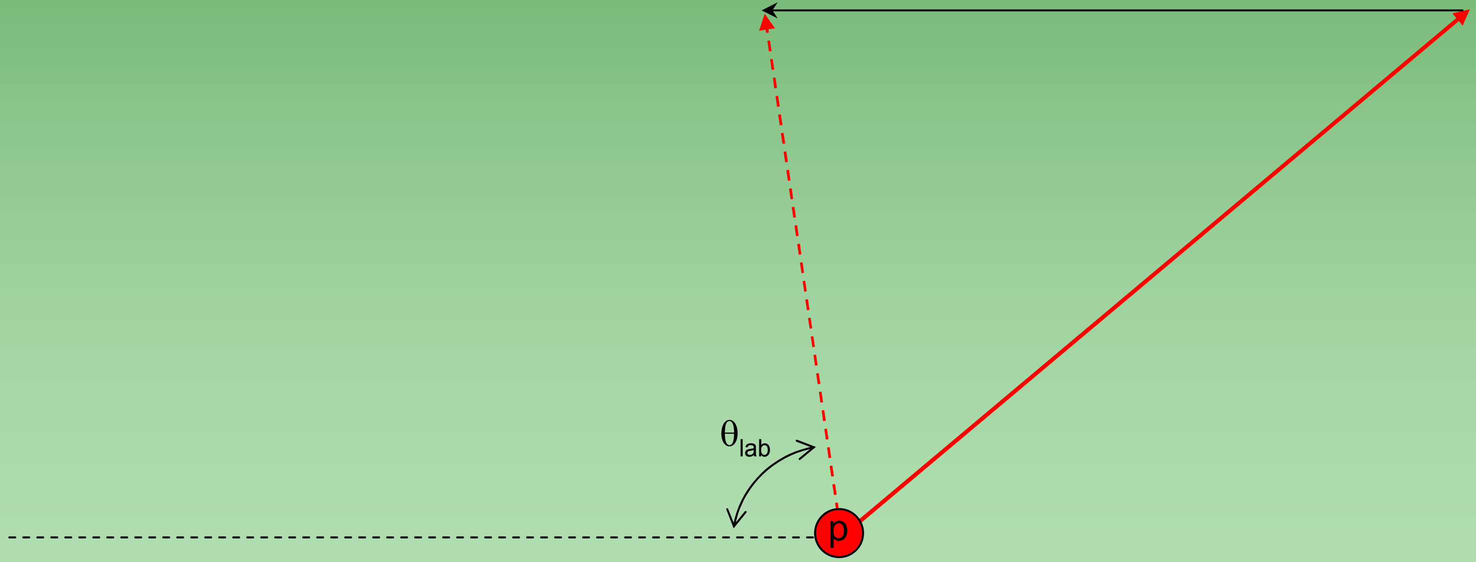

Inverse Kinematics

(d,p) reactions

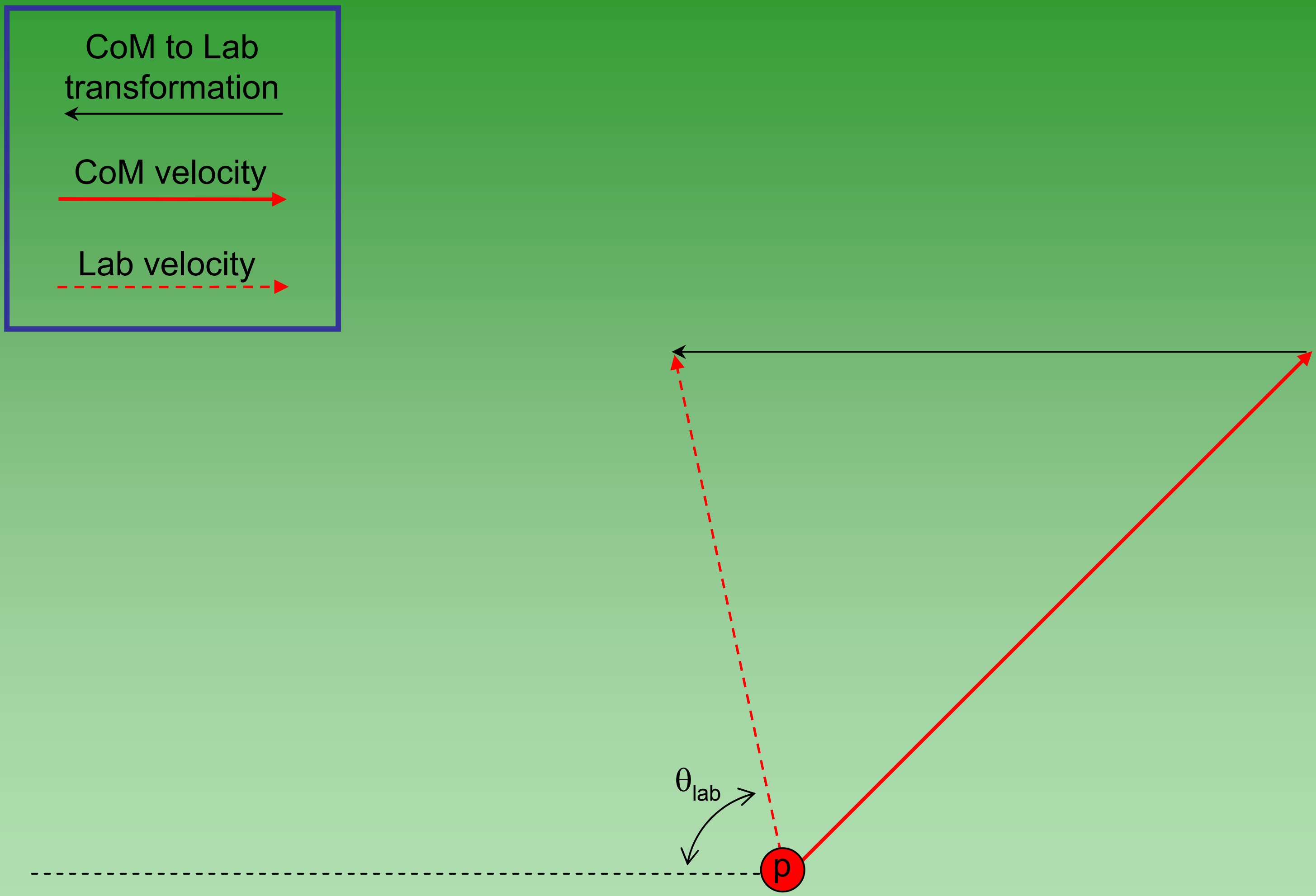

Inverse Kinematics

(d,p) reactions

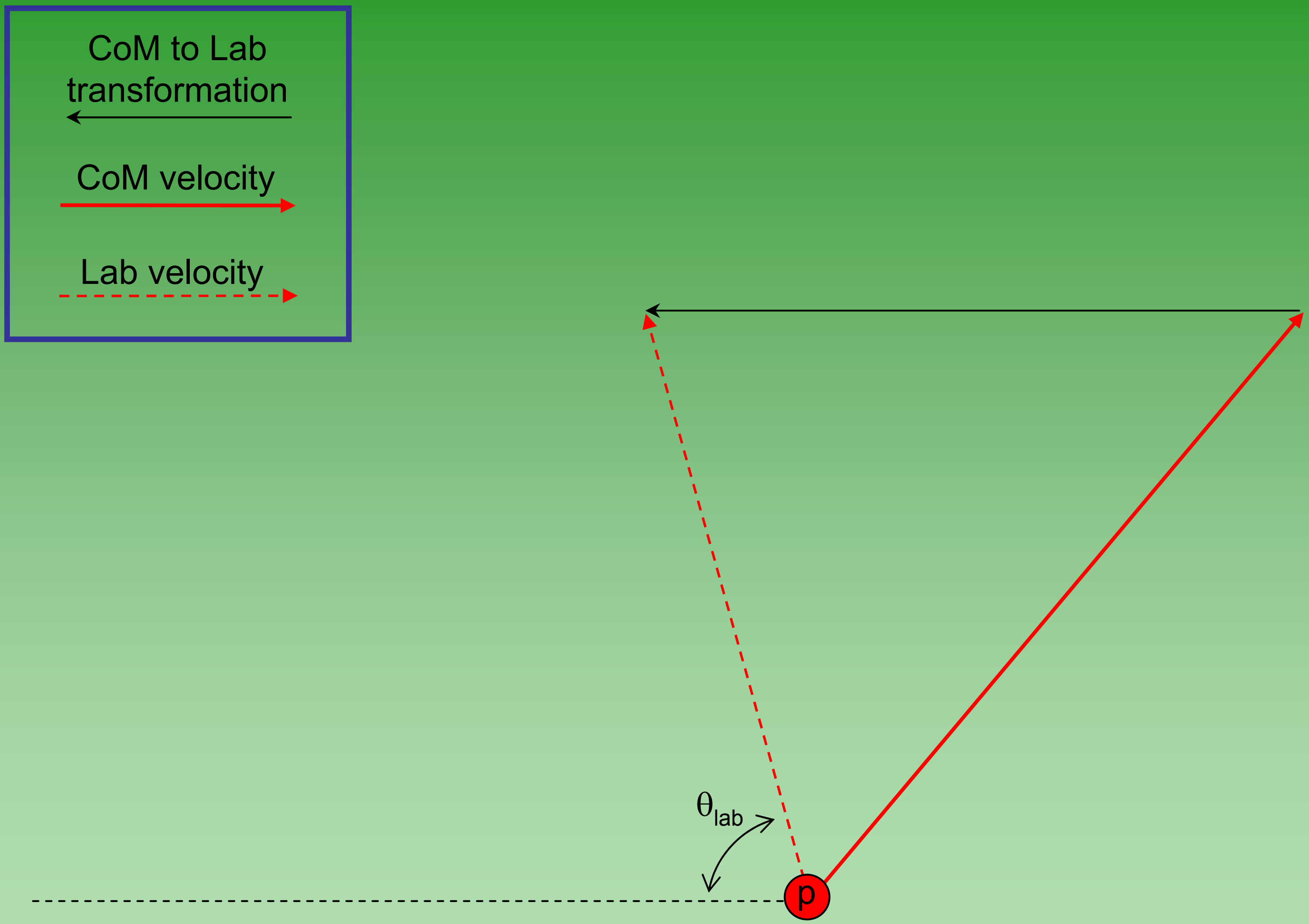

Inverse Kinematics

(d,p) reactions

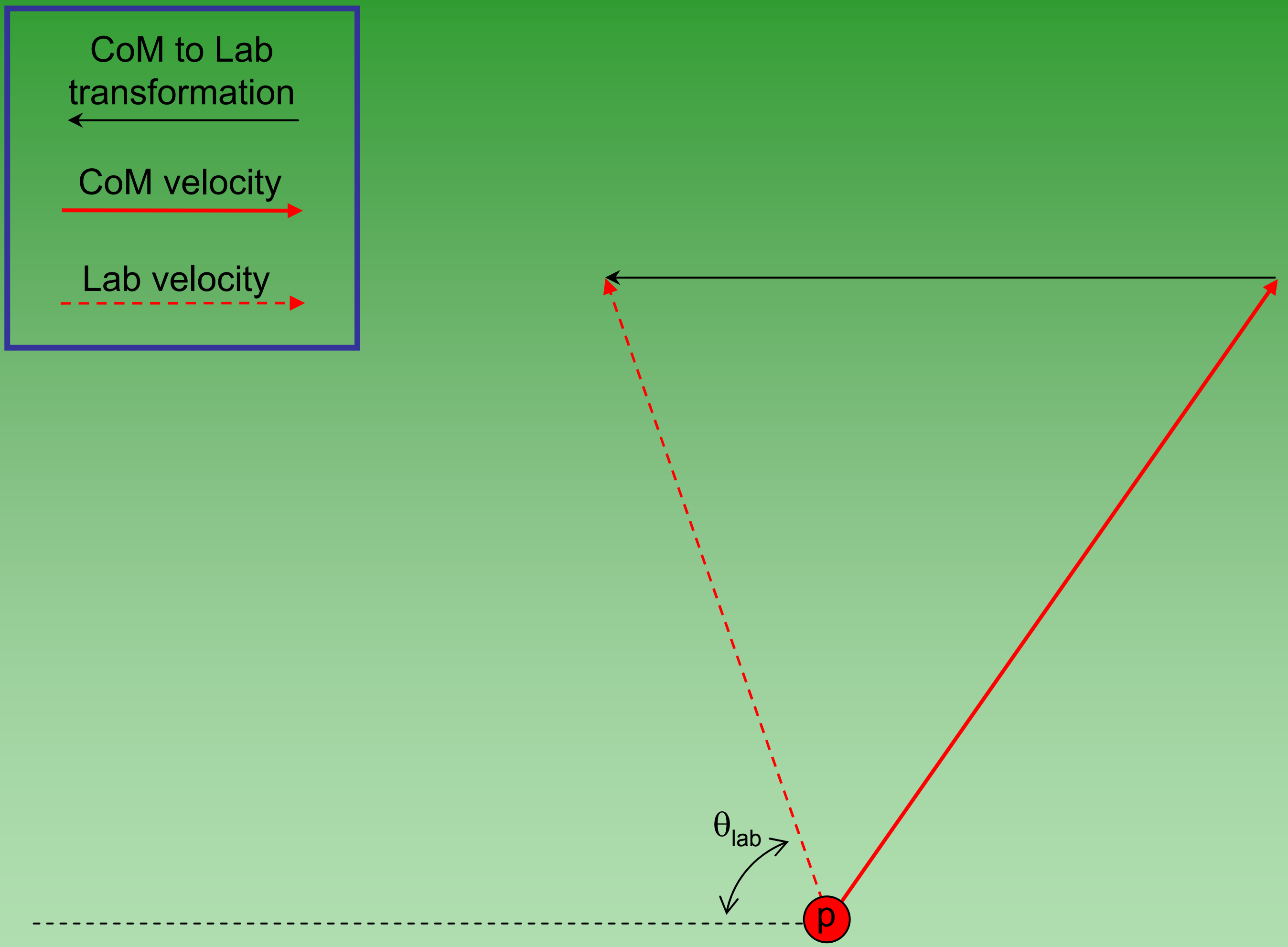

Inverse Kinematics

(d,p) reactions

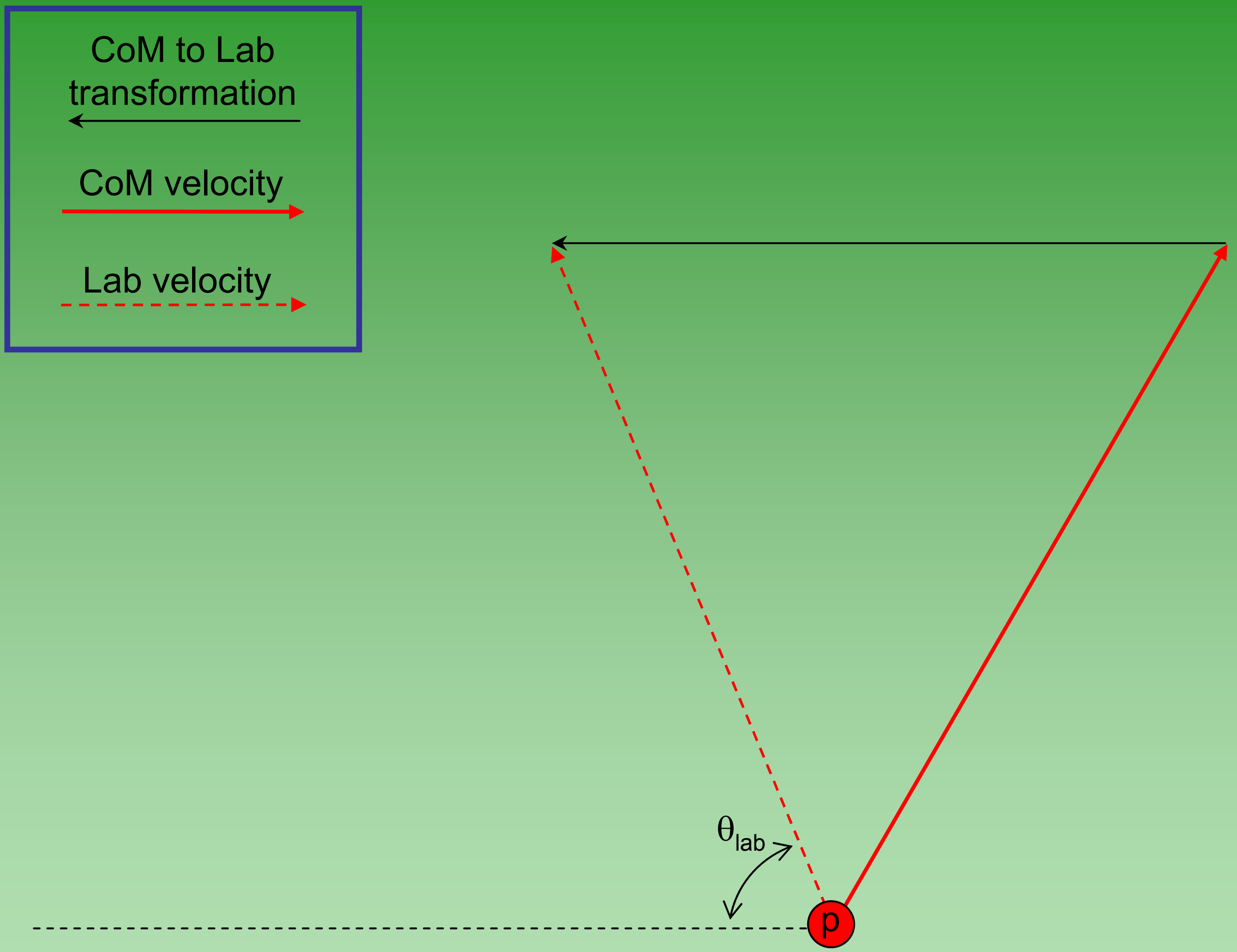

Inverse Kinematics

(d,p) reactions

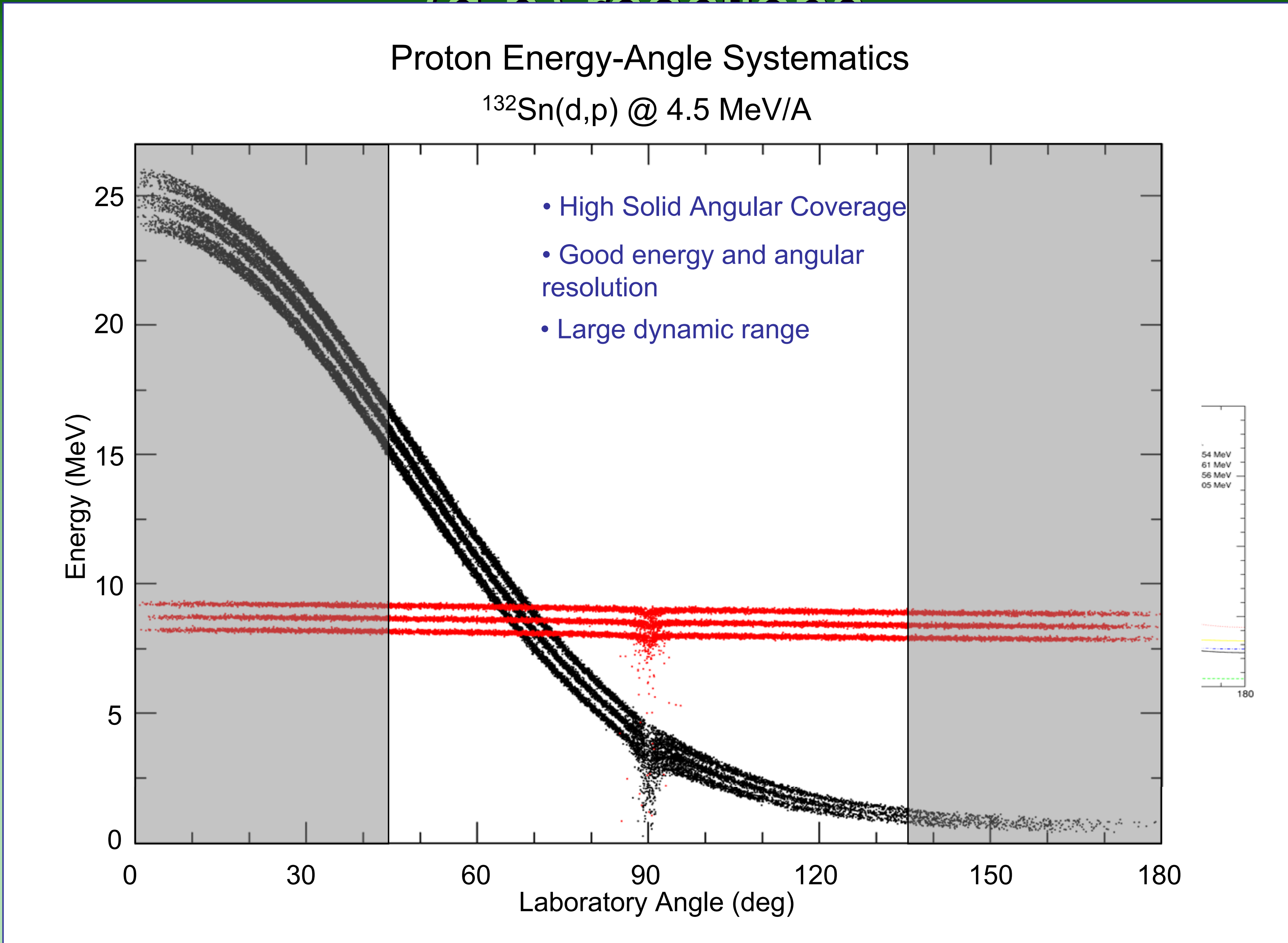

(d,p) reactions

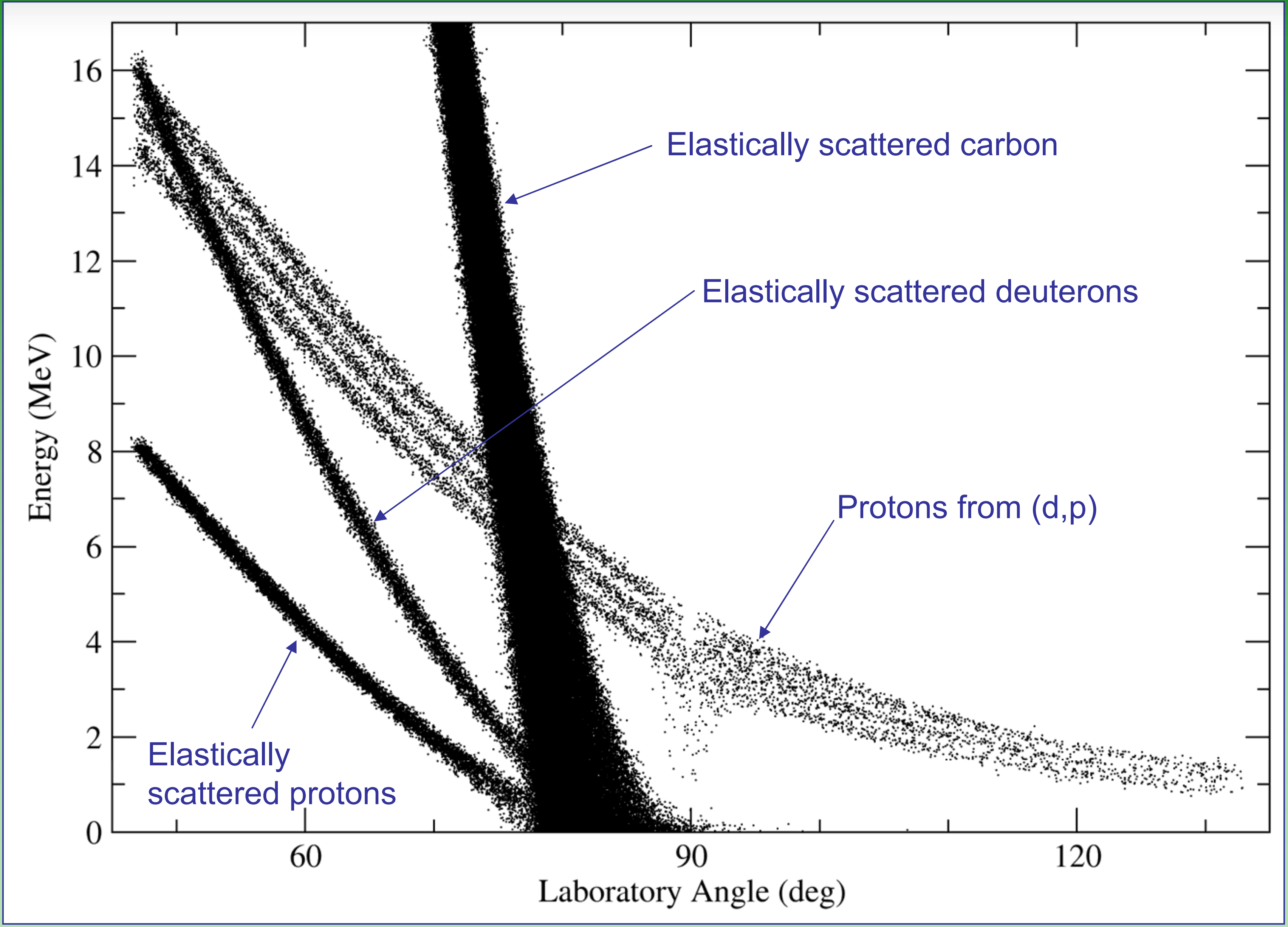

(d,p) reactions

- ORRUBA gives ~80% ϕ coverage over the range 47° →132°
- 2 rings
  - θ < 90°: 12 telescopes (1000μm R + 65μm NR)
  - θ > 90°: 12 detectors (500μm R)
- 324 channels total (288 front side, 36 back side)
- HI beam
- Deuterated plastic targets

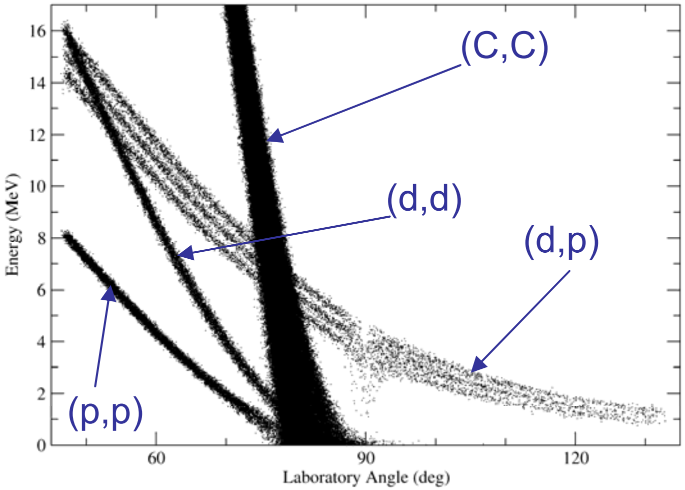

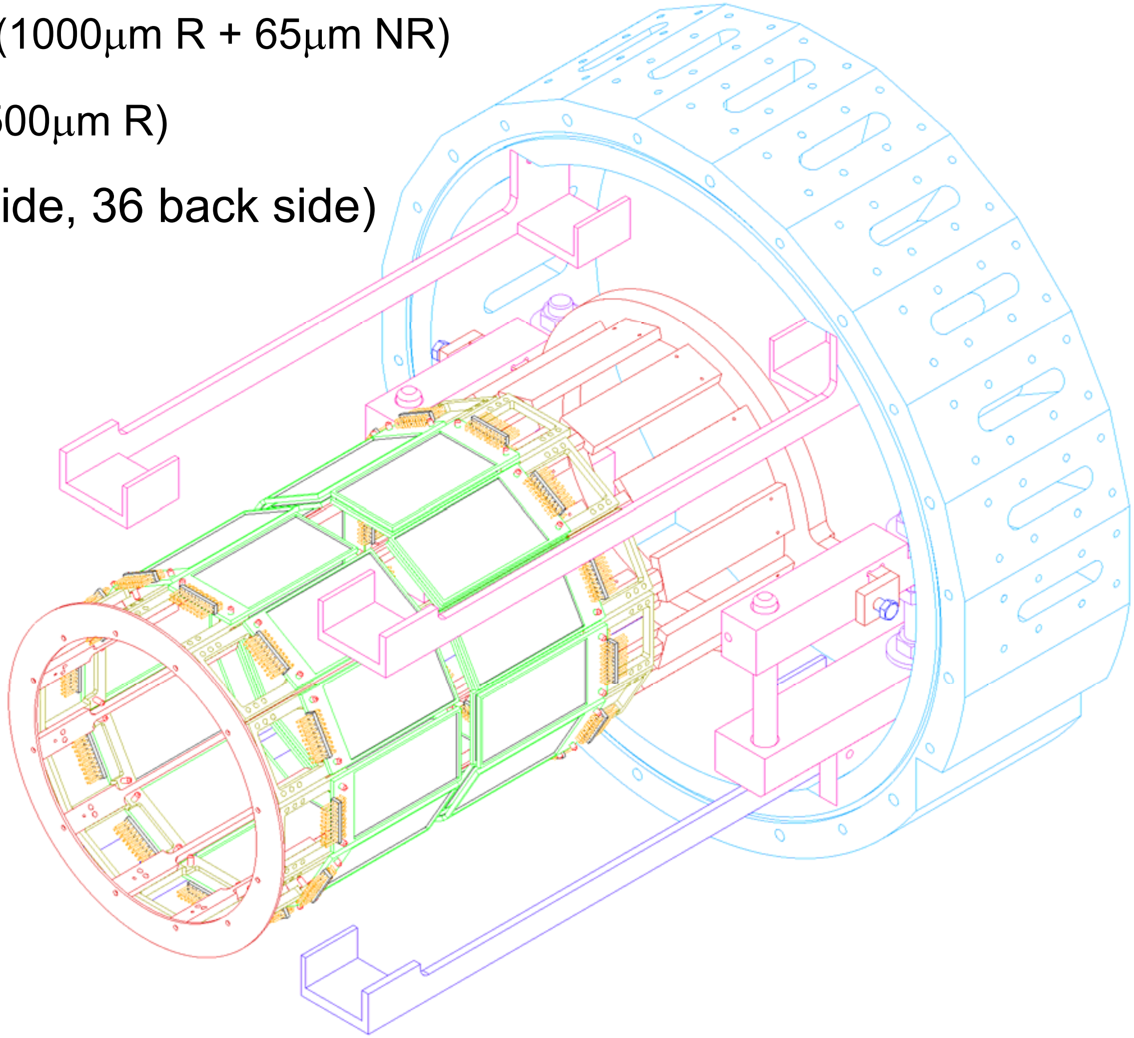

$^{132}Sn(d,p)^{133}Sn$

K.L. Jones, University of Tennessee

- Measure single-particle levels above N=82
- 50k pps ^{132}Sn average, at 630 MeV
- ~175 $\mu g/cm^2$ CD_2 target
- First transfer measurement on ^{132}Sn

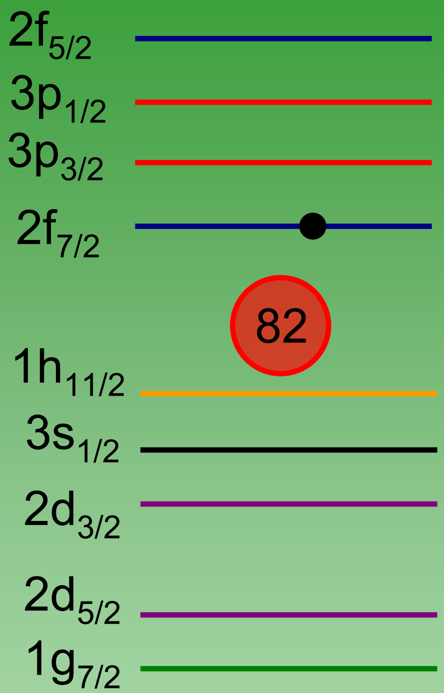

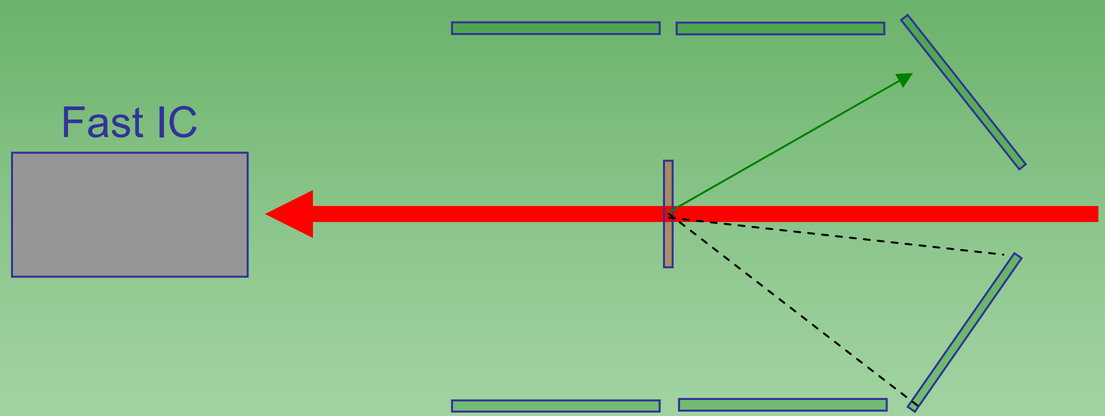

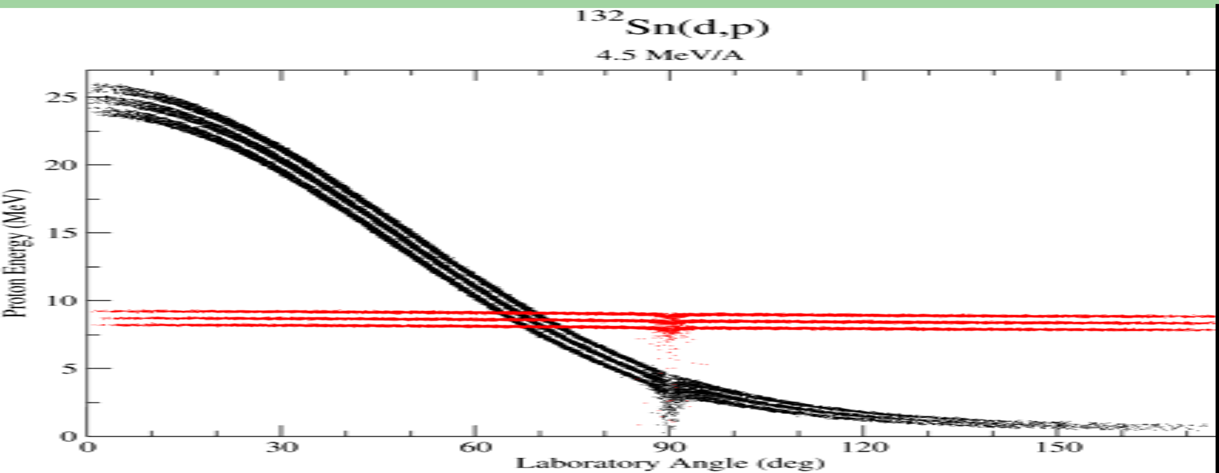

$^{132}Sn(d,p)^{133}Sn$

K.L. Jones *et al.*

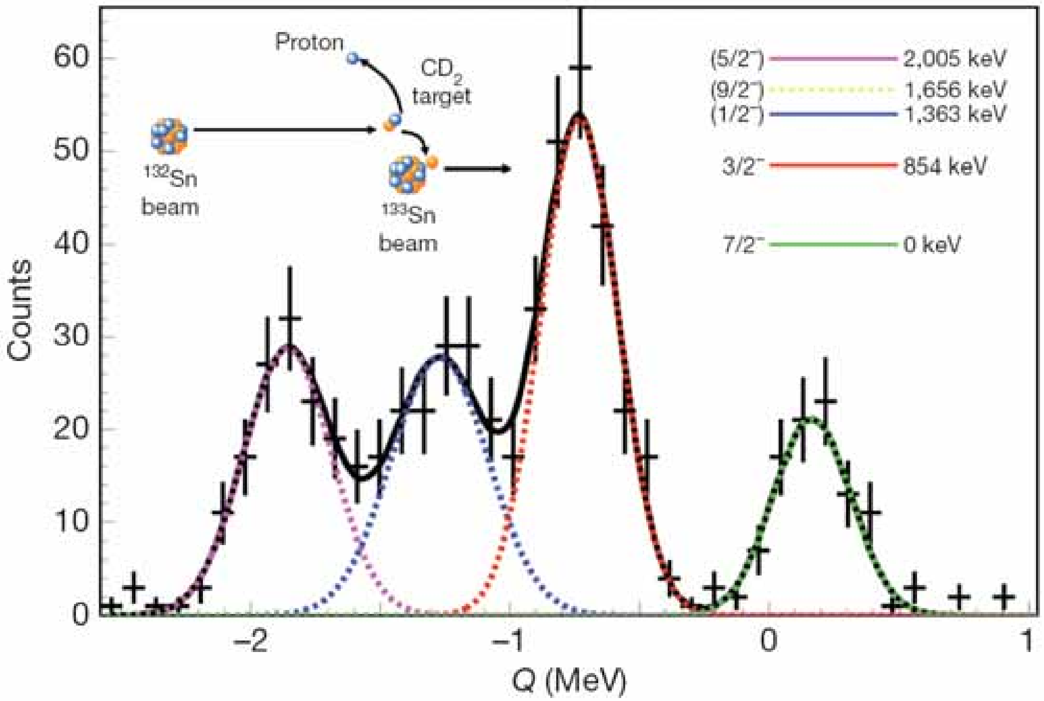

nature Vol 465|27 May 2010|doi:10.1038/nature09048

LETTERS

The magic nature of ^{132}Sn explored through the single-particle states of ^{133}Sn

K. L. Jones[1,2], A. S. Adekola[3], D. W. Bardayan[4], J. C. Blackmon[4], K. Y. Chae[1], K. A. Chipps[5], J. A. Cizewski[2], L. Erikson[5], C. Harlin[6], R. Hatarik[2], R. Kapler[1], R. L. Kozub[7], J. F. Liang[4], R. Livesay[5], Z. Ma[1], B. H. Moazen[1], C. D. Nesaraja[4], F. M. Nunes[8], S. D. Pain[2], N. P. Patterson[6], D. Shapira[4], J. F. Shriner Jr[7], M. S. Smith[4], T. P. Swan[2,6] & J. S. Thomas[6]

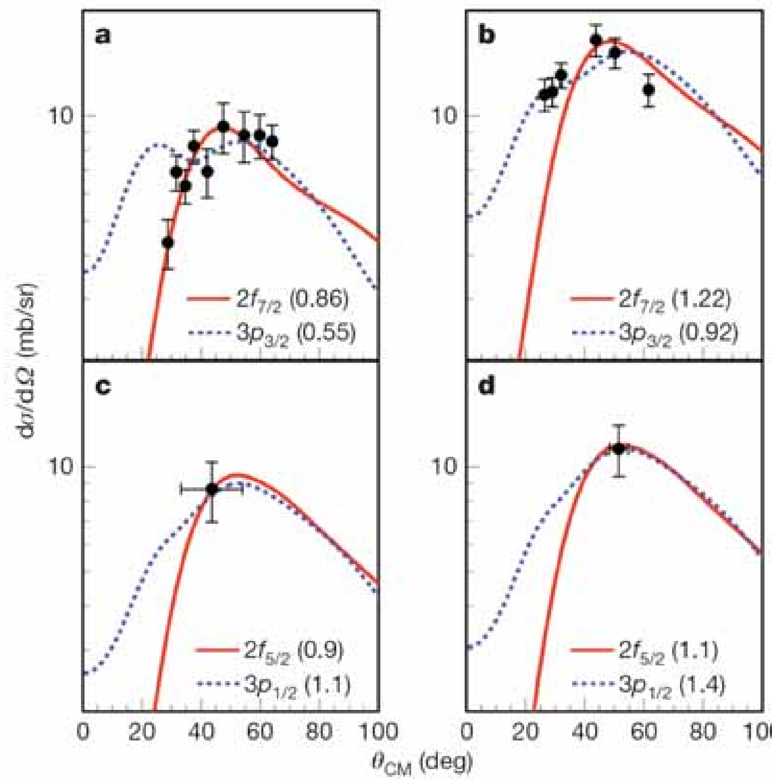

Table 1 | Properties of the four single-particle states populated by the $^{132}Sn(d,p)^{133}Sn$ reaction

E_x (keV)	J^{π}	Configuration	S	C^2 (fm^{-1})
0	$7/2^-$	$^{132}Sn_{gs} \otimes \nu_{f7/2}$	0.86 ± 0.16	0.64 ± 0.10
854	$3/2^-$	$^{132}Sn_{gs} \otimes \nu_{p3/2}$	0.92 ± 0.18	5.61 ± 0.86
$1,363 \pm 31$	$(1/2^-)$	$^{132}Sn_{gs} \otimes \nu_{p1/2}$	1.1 ± 0.3	2.63 ± 0.43
2,005	$(5/2^-)$	$^{132}Sn_{gs} \otimes \nu_{f5/2}$	1.1 ± 0.2	$(9 \pm 2) \times 10^{-4}$

The spectroscopic factors (S) were extracted from the data by using the Strömich optical potentials, a radius parameter $r = 1.25$ and diffuseness $a = 0.65$. The asymptotic normalization coefficient (ANC) is quoted as C^2. All errors are expressed as standard deviations. Excitation energies were taken from the ENSDF database (http://www.nndc.bnl.gov/ensdf/) and the present work.

$^{132}Sn(d,t)^{131}Sn$

- Last experiment to run at the HRIBF!
- 12k pps ^{132}Sn average, at 560 MeV
- ~150 $\mu g/cm^2$ CD_2 target
- First (d,t) measurement on a heavy fission fragment in inverse kinematics

Riccardo Orlandi, CSIC Madrid

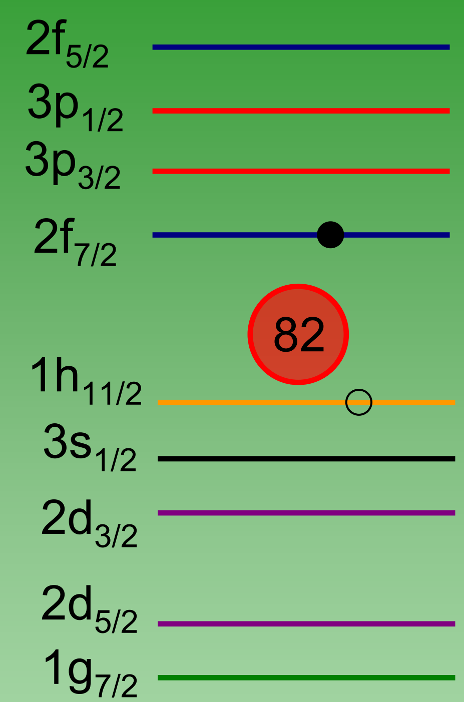

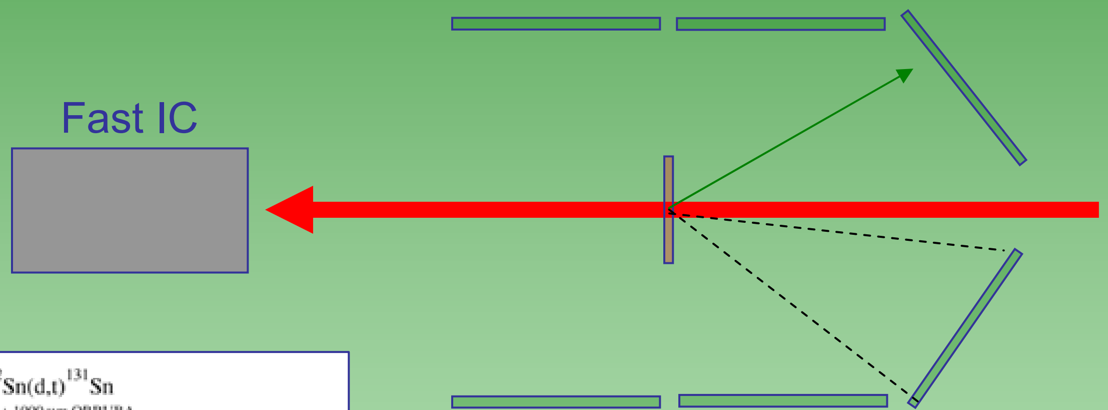

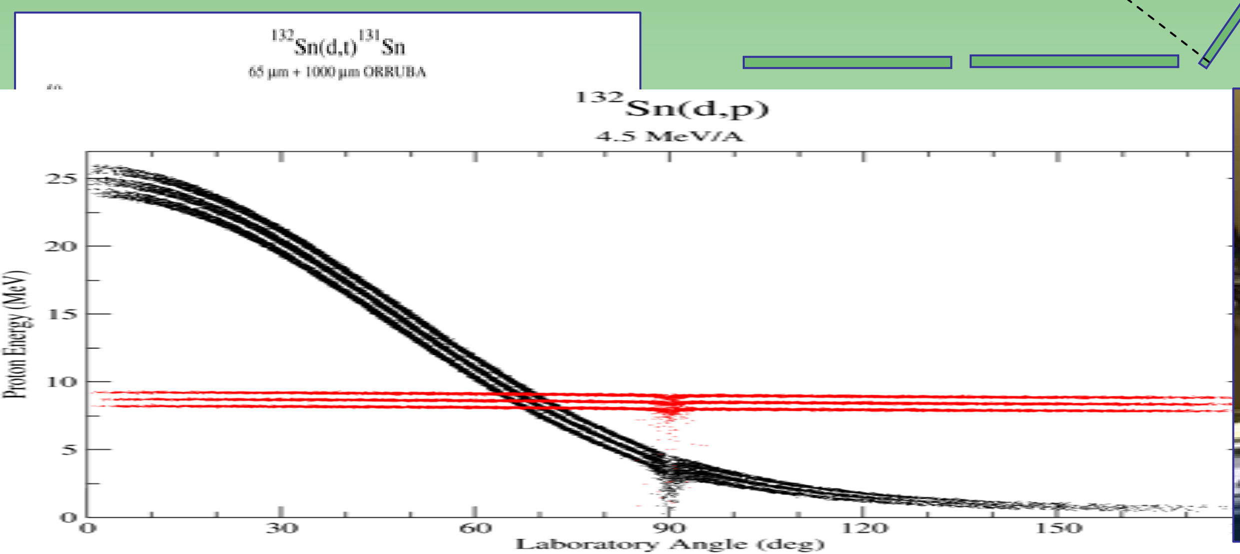

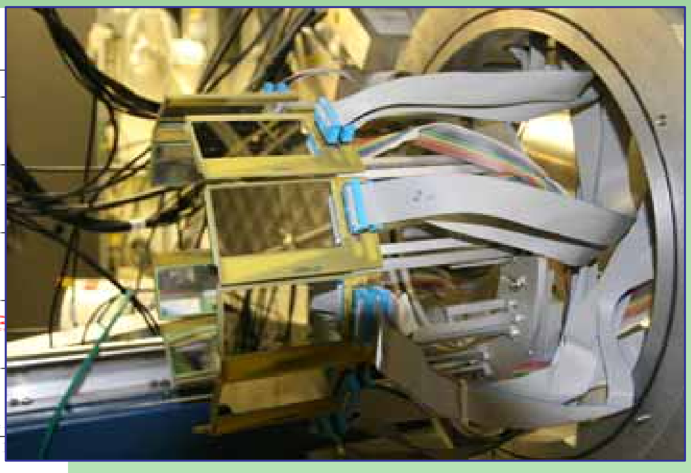

$^{132}Sn(d,t)^{131}Sn$

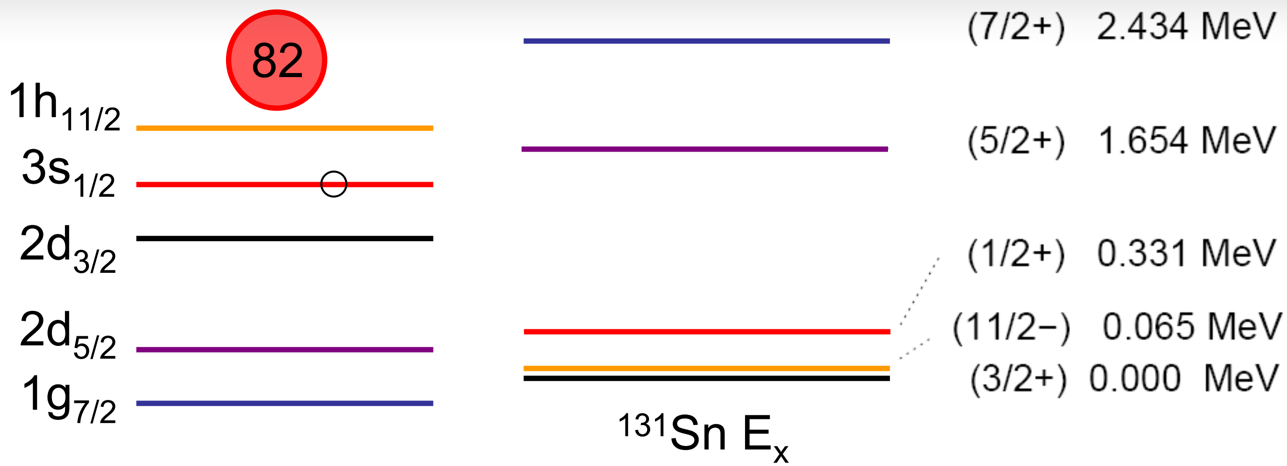

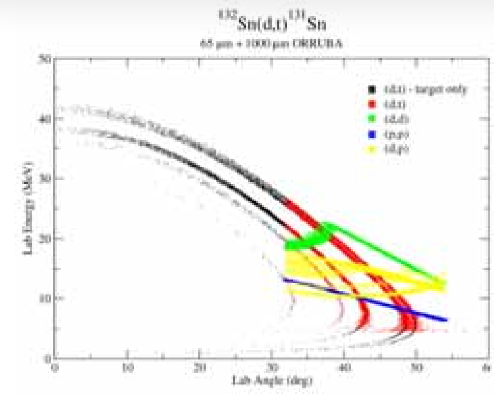

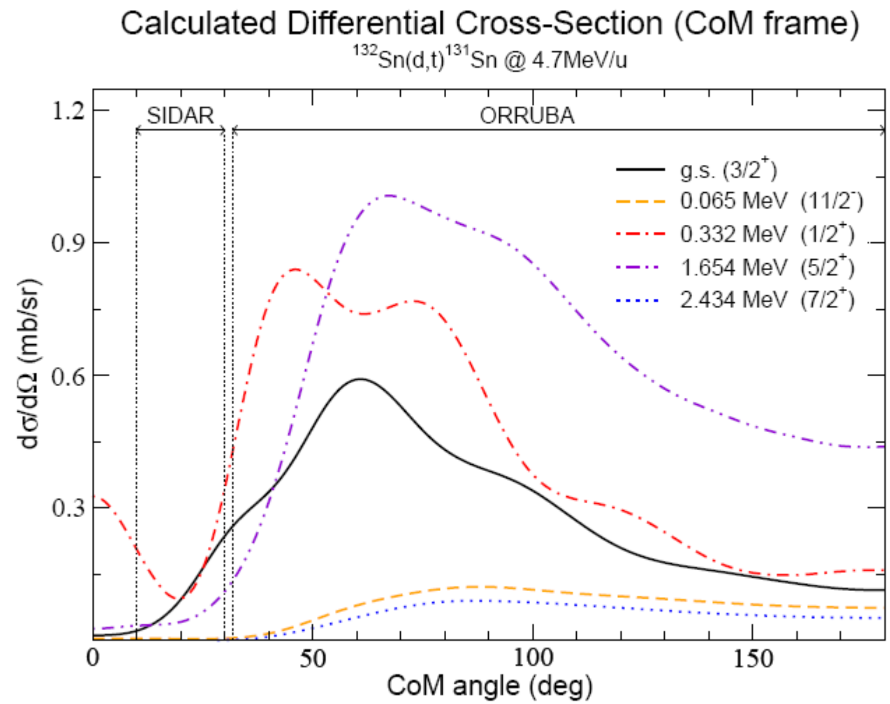

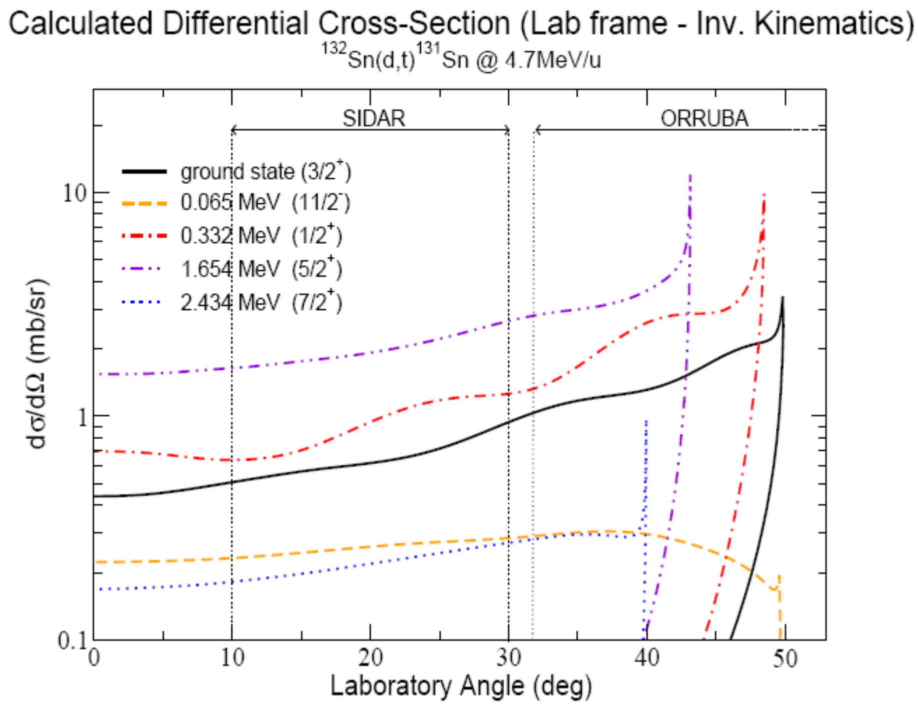

$^{132}Sn(d,t)^{131}Sn$

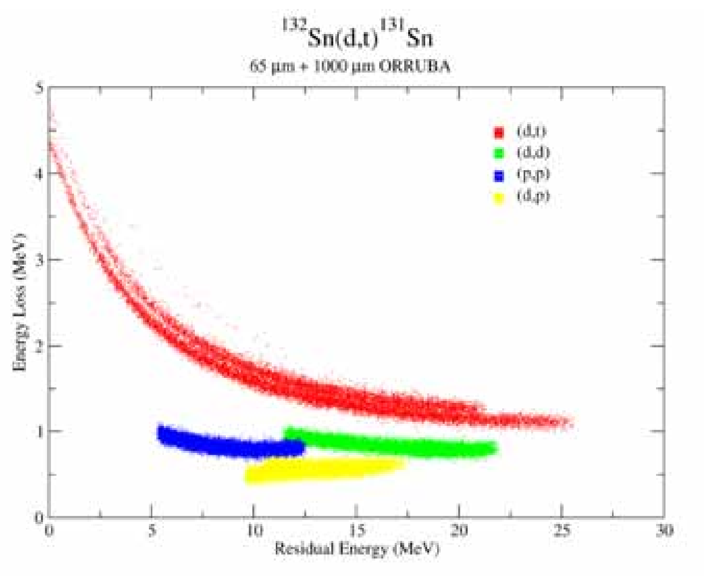

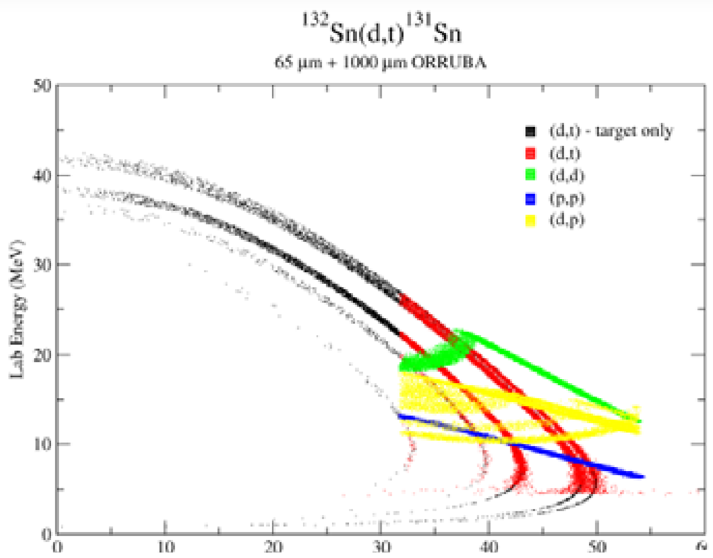

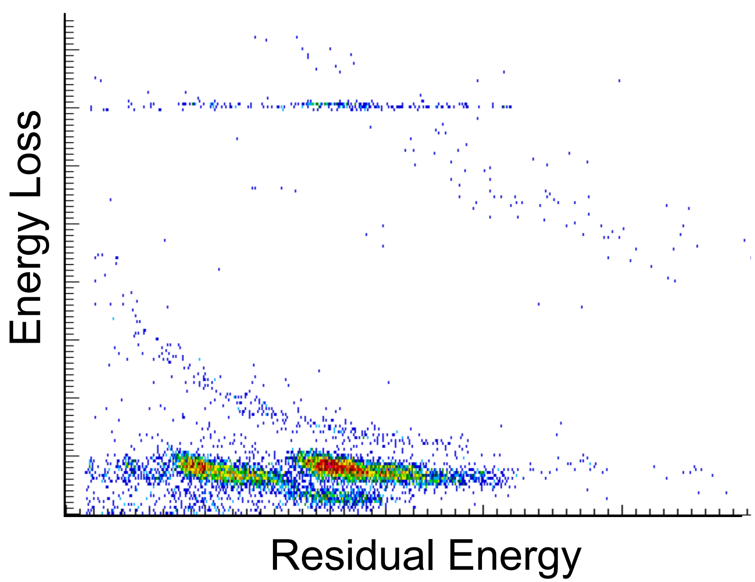

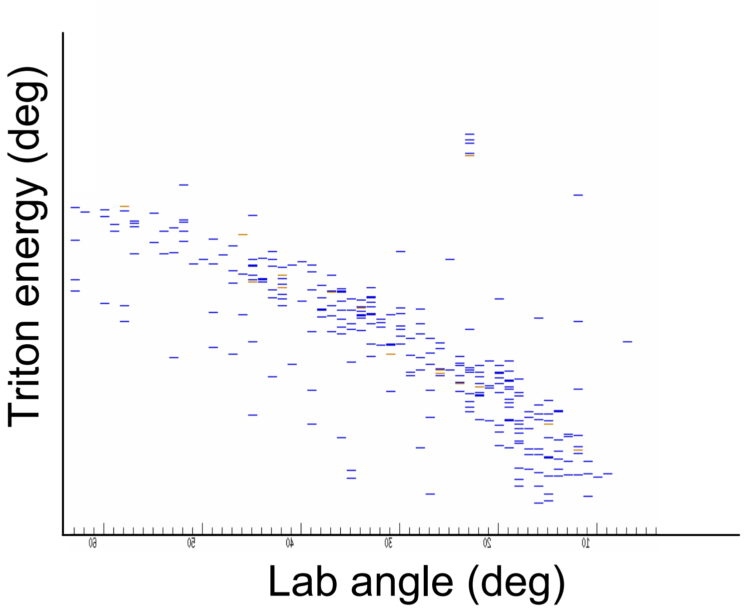

$^{132}Sn(d,t)^{131}Sn$

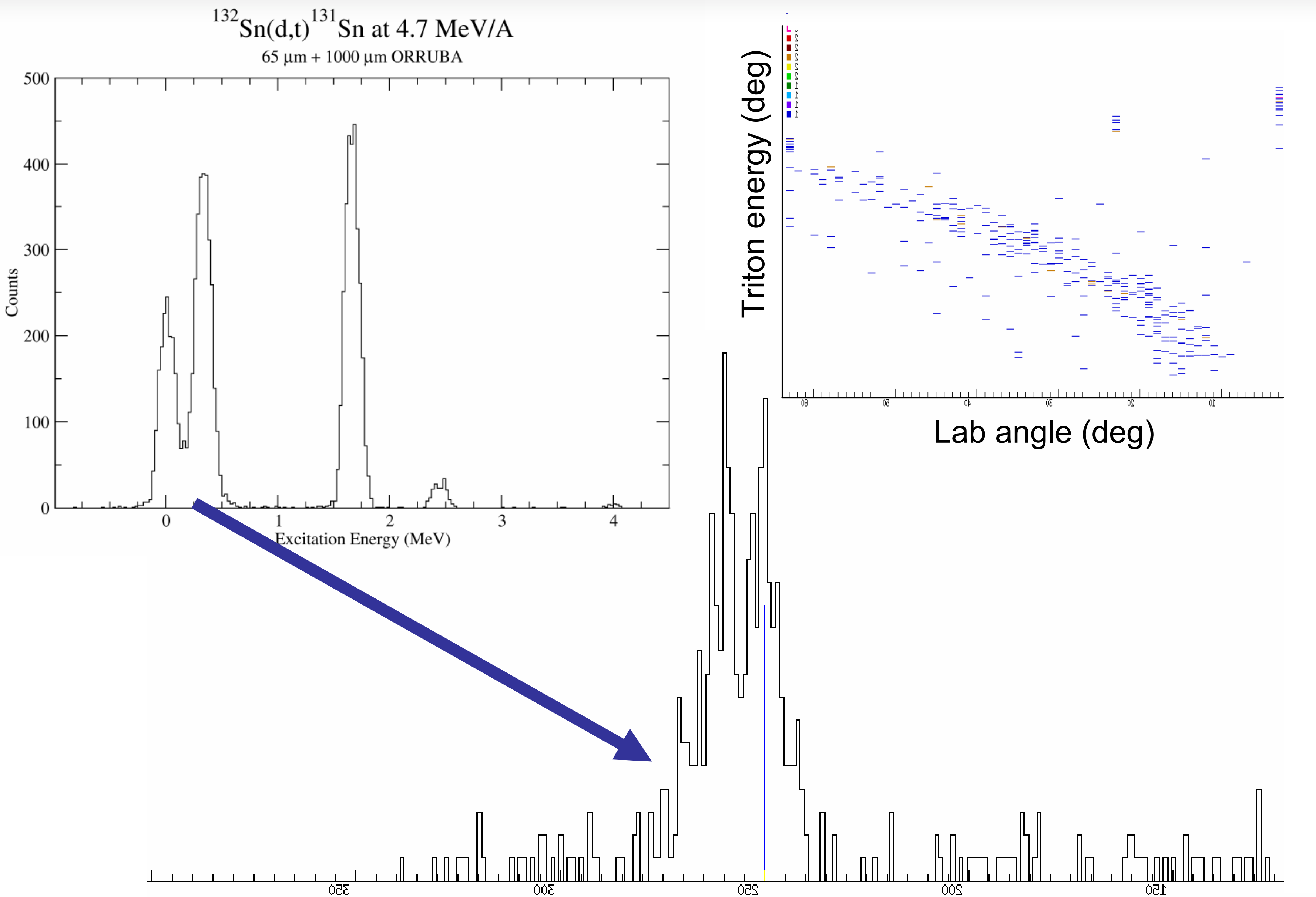

^{26}Al background

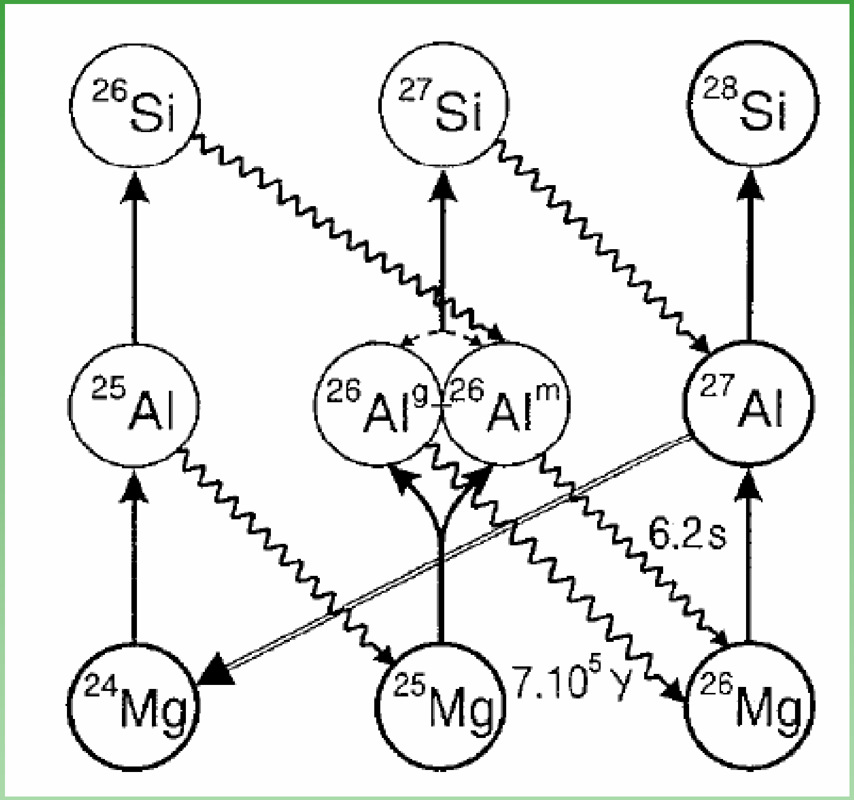

5^+ gs, 0^+ isomeric state at 228 keV

Focus on $^{26}Al^g$ reactions

- ^{26}Al nucleus was the first radioisotope detected in the interstellar medium
- Half life of 7.2×10^5 years
- Observation of γ rays associated with its decay provides evidence of nucleosynthesis
- Temperatures ≥ 0.03 GK, the $^{26g}Al(p,\gamma)^{27}Si$ reaction is expected to govern the destruction of ^{26}Al
- Essential to reduce the uncertainty in order to determine the contribution of heavy stars to the overall Galactic abundance of ^{26}Al

^{26}Al background

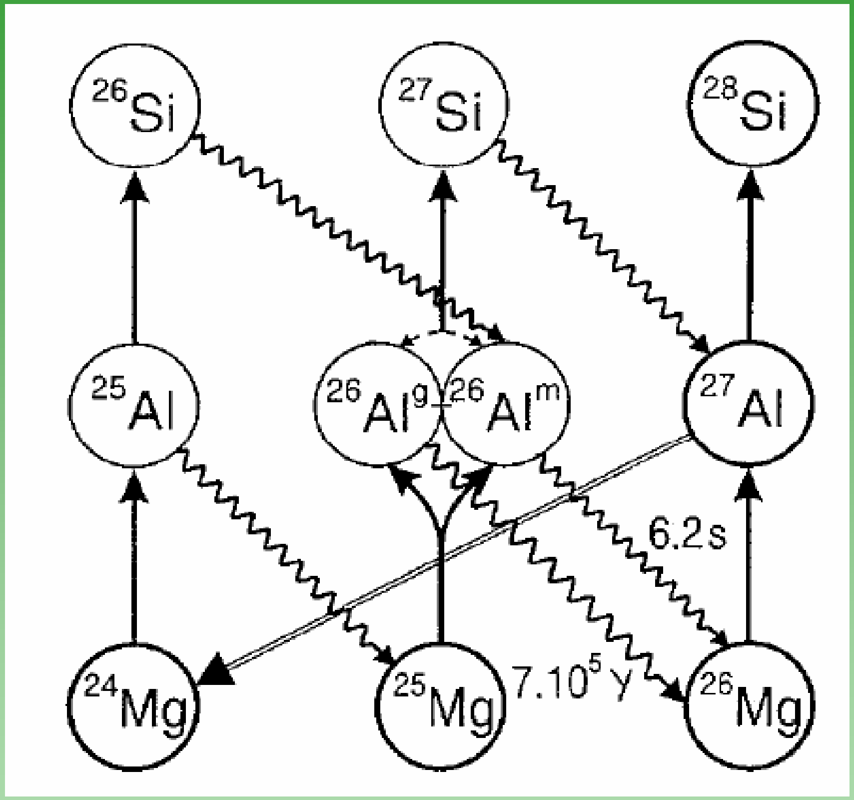

N. Prantzos, R. Diehl. **Physics Reports 267** 1-69 (1996)

- Core-collapse supernovae

  massive star collapses
  T_c ~ 3 GK
  long favored source

- Novae

  accretion onto a white dwarf
  estimated < 0.4 M_O ^{26}Al ejected – depends on uncertain reactions
  T < 0.4 GK

- Wolf-Rayet stars

  >30 M_O stars – develop strong stellar winds blowing material into space
  T < 0.05 GK

need to know ^{26}Al+p rates over large temperature range

^{26}Al – early inference

First inference of ongoing ^{26}Al synthesis

February 8, 1969

Several tons of material deposited

Material dated to predate formation of the Earth

Excess of ^{26}Mg found in calcium and aluminium inclusions of the Allende meteorite

If decay occurred in situ, then 5×10^{-5} 26/27 at time of solar system formation

^{26}Al – observation

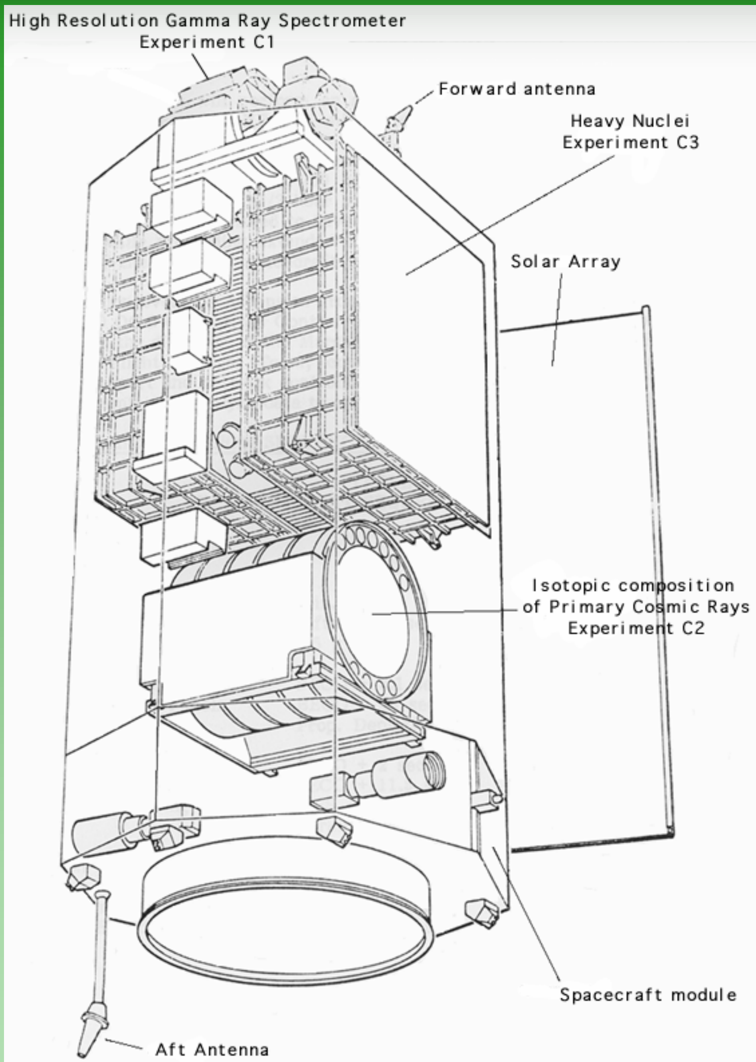

First astronomical observation of ^{26}Al

HEAO (High Energy Astronomy Observatory)

Largest germanium spectrometer placed in orbit at that time

High Resolution Gamma Ray Spectrometer (HRGRS):

50 keV - 10 MeV

3 keV resolution

FOV 30°

1979-1981

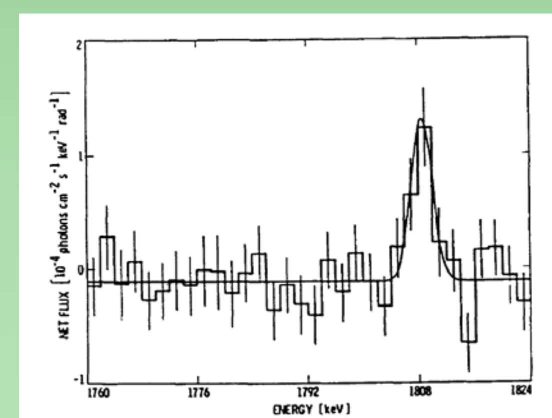

Four p-type Ge detectors

CsI anti-coincidence

^{26}Al – galactic mapping

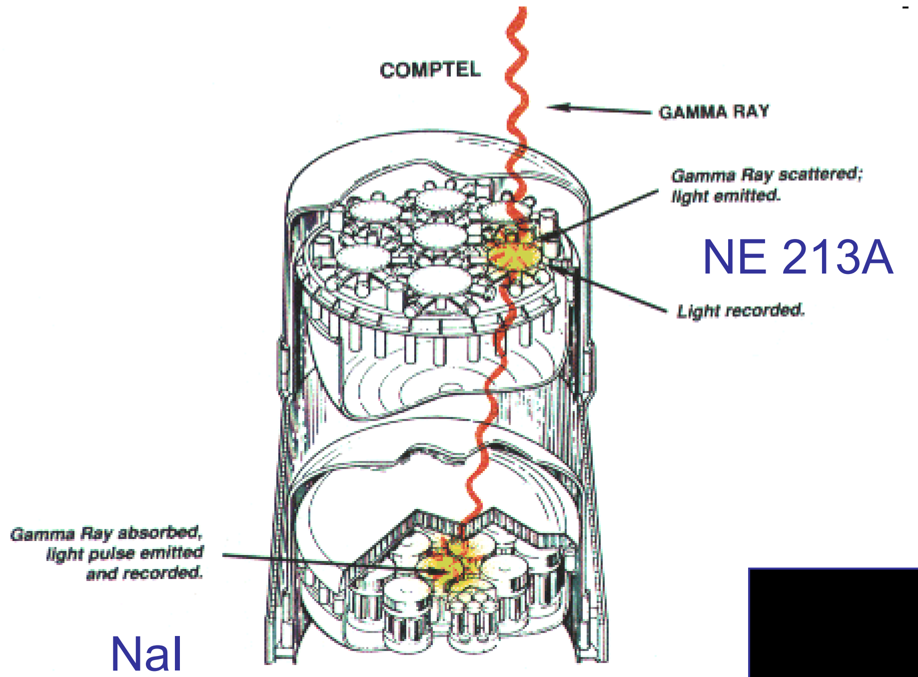

Weight: 1460 kg
Dimensions: 2.61 m x 1.76 m diameter
Power: 206 W

Compton Gamma Ray Observatory - COMPTEL

Energy resolution
5 - 8% (FWHM)

Angular resolution
1.7 - 4.4 degrees (FWHM)

Launched 1991

young giant stars

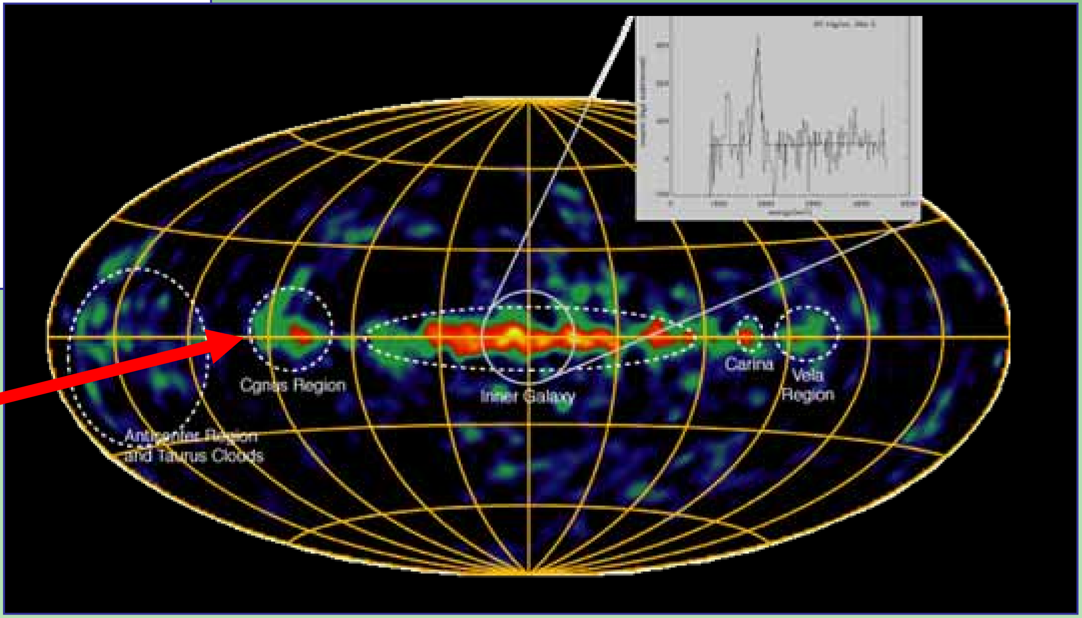

INTEGRAL

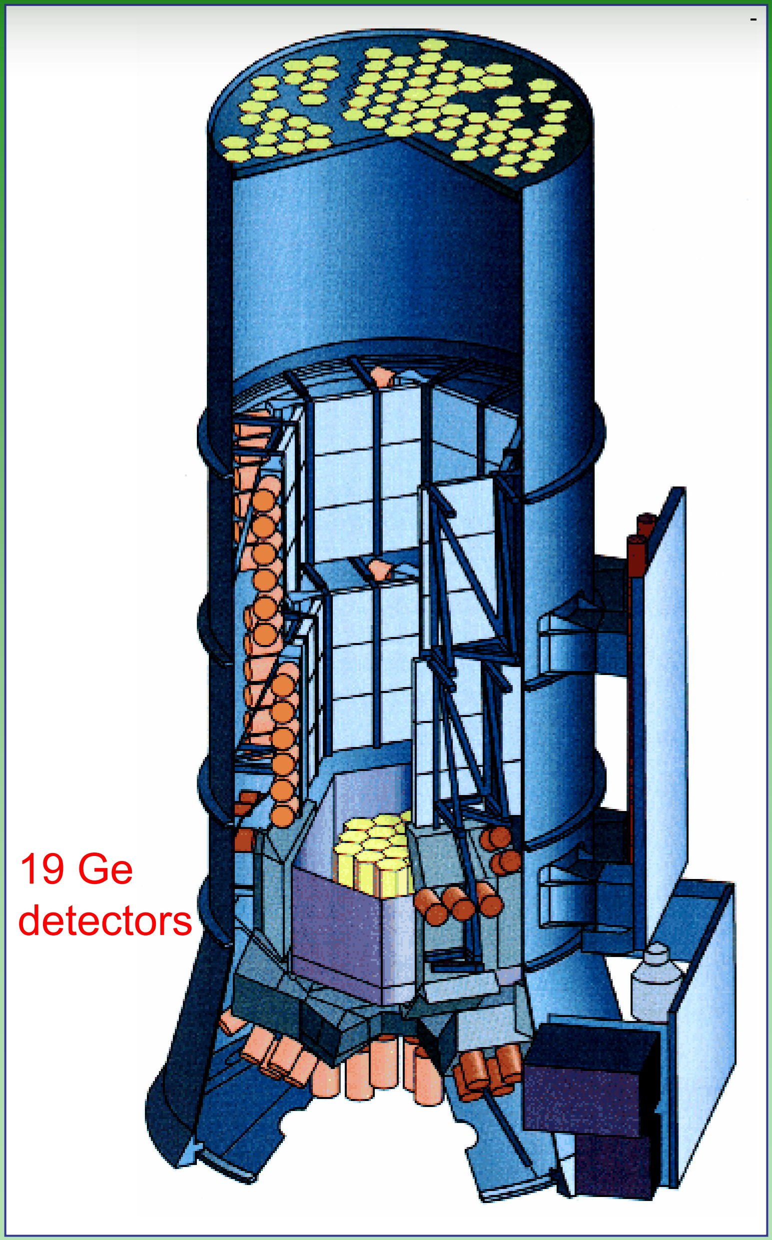

Energy resolution (FWHM):
2.2 keV at 1.33 MeV for each detector
(3 keV for the entire spectrometer)

Angular resolution
2.5° for point sources

Field of View
fully coded: 14° flat to flat,
16° corner to corner

Launched October 2002

^{26}Al – pan-galactic source

Vol 439|5 January 2006|doi:10.1038/nature04364 nature

LETTERS

Radioactive ^{26}Al from massive stars in the Galaxy

Roland Diehl[1], Hubert Halloin[1], Karsten Kretschmer[1], Giselher G. Lichti[1], Volker Schönfelder[1], Andrew W. Strong[1], Andreas von Kienlin[1], Wei Wang[1], Pierre Jean[2], Jürgen Knödlseder[2], Jean-Pierre Roques[2], Georg Weidenspointner[2], Stephane Schanne[3], Dieter H. Hartmann[4], Christoph Winkler[5] & Cornelia Wunderer[6]

SPI (INTEGRAL)

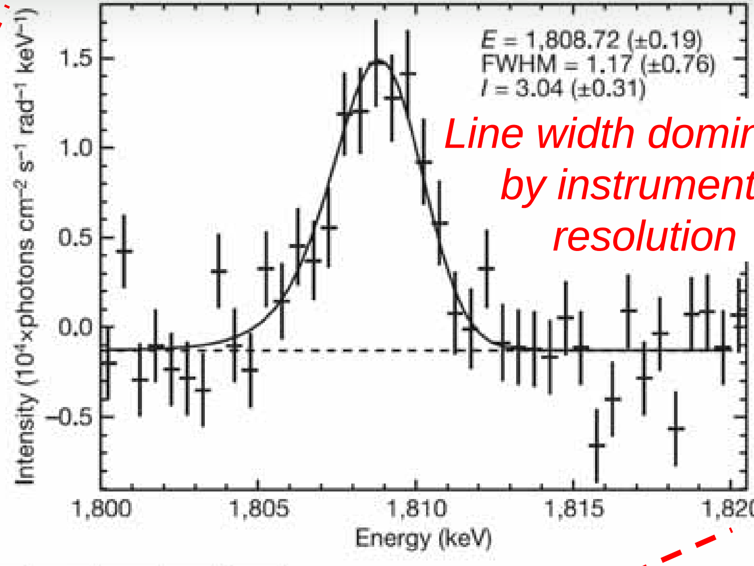

Line width dominated by instrumental resolution

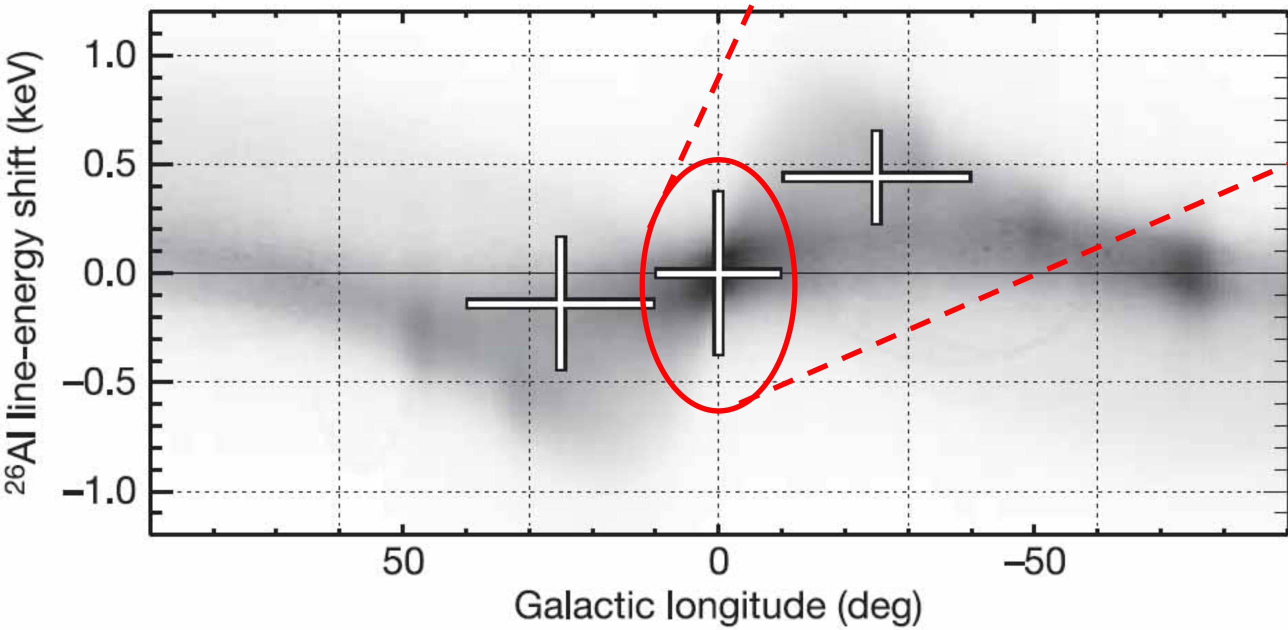

Doppler shifts suggest ^{26}Al is co-rotating with the Galaxy

^{26}Al – astrophysically important states

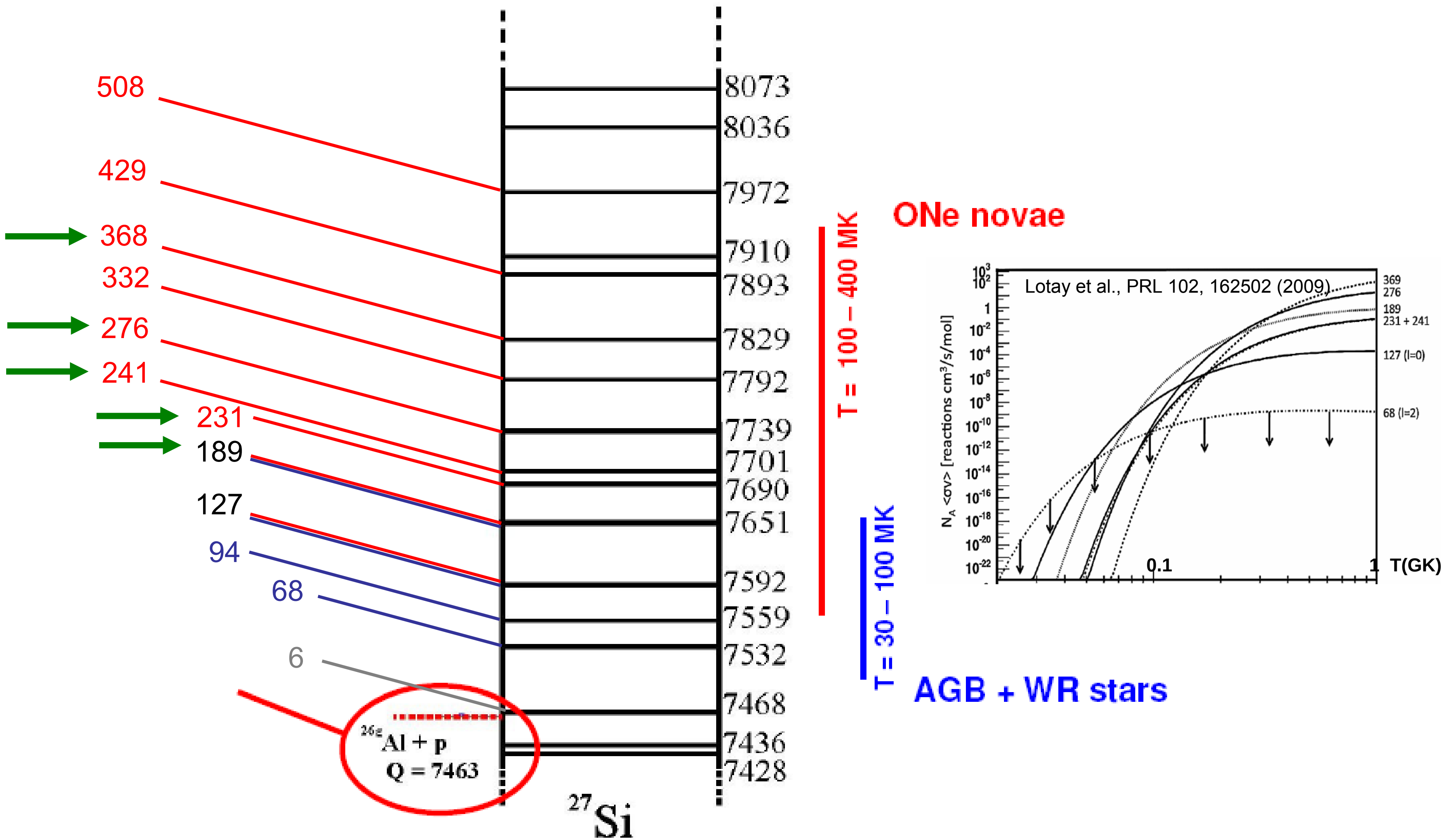

^{26}Al – identification of mirror states

G. Lotay *et al*, **PRL 102** 162502 (2009)

- Fusion-evaporation reaction to populate states and study γ decays with Gammasphere
- 6 pnA, 26 MeV beam of ^{16}O ions on ~150 $\mu g/cm^2$ thick ^{12}C target
- Location of low-lying resonances constrained stellar rate
- SF for these states necessary for further constraint

^{27}Si			^{27}Al
E_{res} (keV)	E_{ex}	J^{π}	E_{ex}
6	7468	$5/2^+$	
68	7532	$5/2^+$	7578
94	7557		7858
127	7592	$9/2^+$	7806
189	7652	$11/2^+$	7948
231	7690	$5/2^+$	
241	7702	$7/2^+$	
276	7740	$9/2^+$	
332	7792	$7/2^+$	
368	7831	$9/2^-$	

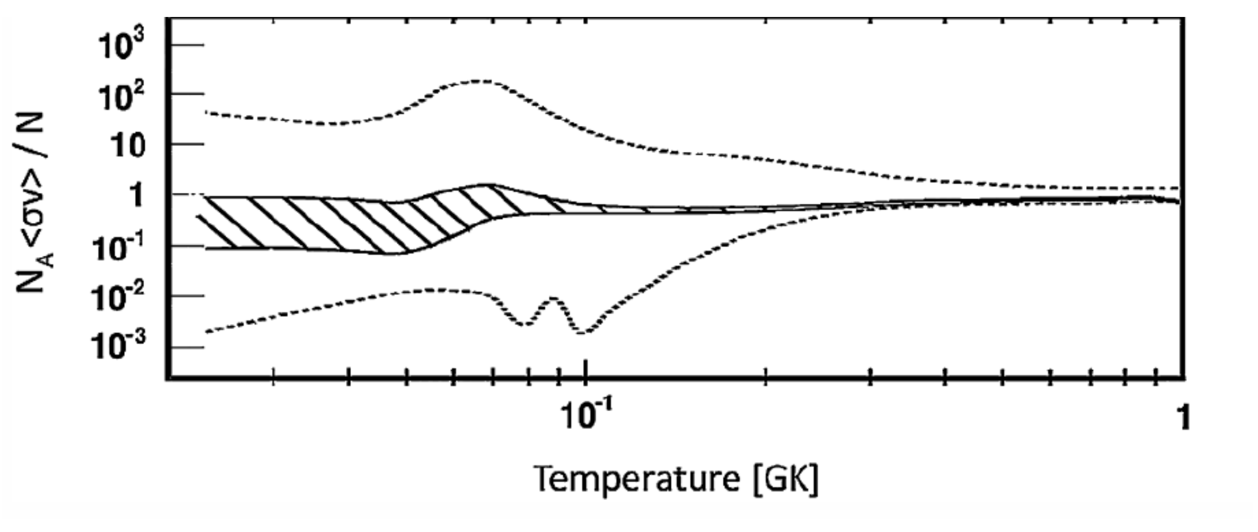

lowest direct (p,γ) measurement

C. Ruiz *et al*., **PRL 96** 252501 (2006)

What about proton transfer?

- (d,n) is tricky because of neutron detection
- Can measure (d,n) by measuring only the recoil, and coincident gamma rays, but no angular distributions, feeding issues, etc
- (^{3}He,d) can be performed with detectors just like for (d,p), but how do you make a localized target?
    - Cell –backgrounds and straggling from windows, bulky (shadowing)
    - Implantation (difficult to make uniform, backgrounds from foils, thickness of foils)
    - *Can measure (d,p) and use mirror symmetry*

$^{26}Al(d,p)^{27}Al$ data – Setup

- 117 MeV ^{26}Al
- 5×10^6 pps
- 150 μg/cm² CD_2

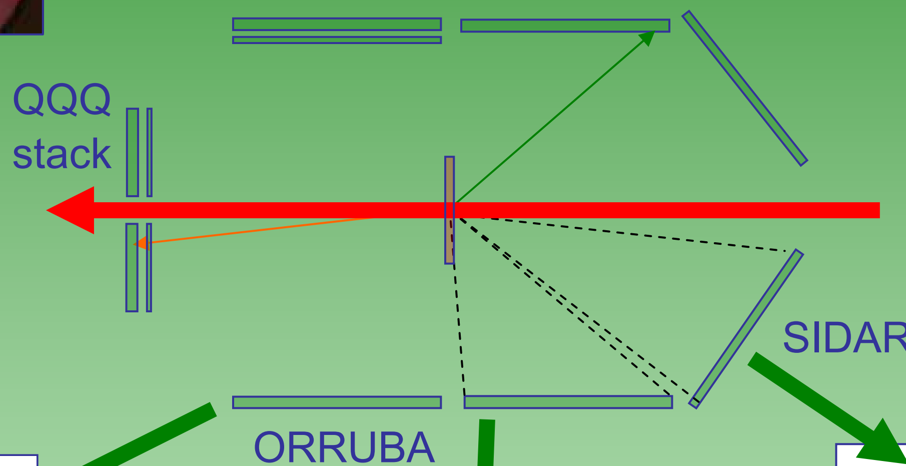

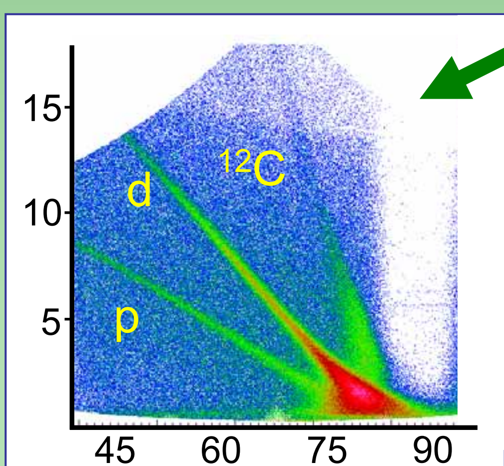

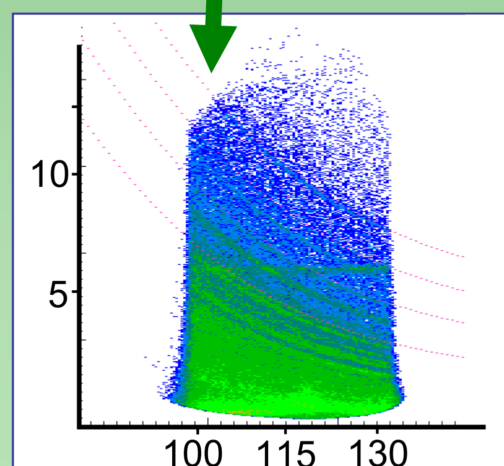

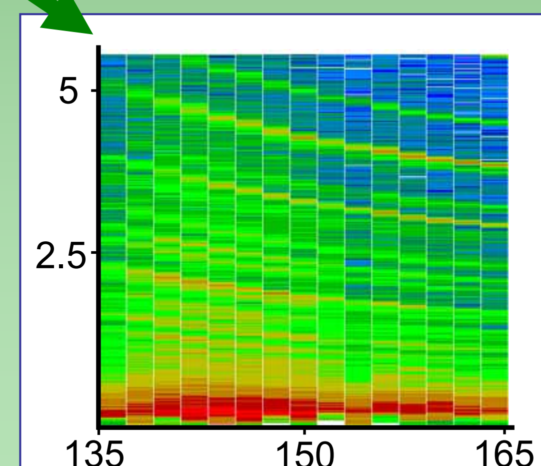

$^{26}Al(d,p)^{27}Al$ – Excitation Energy

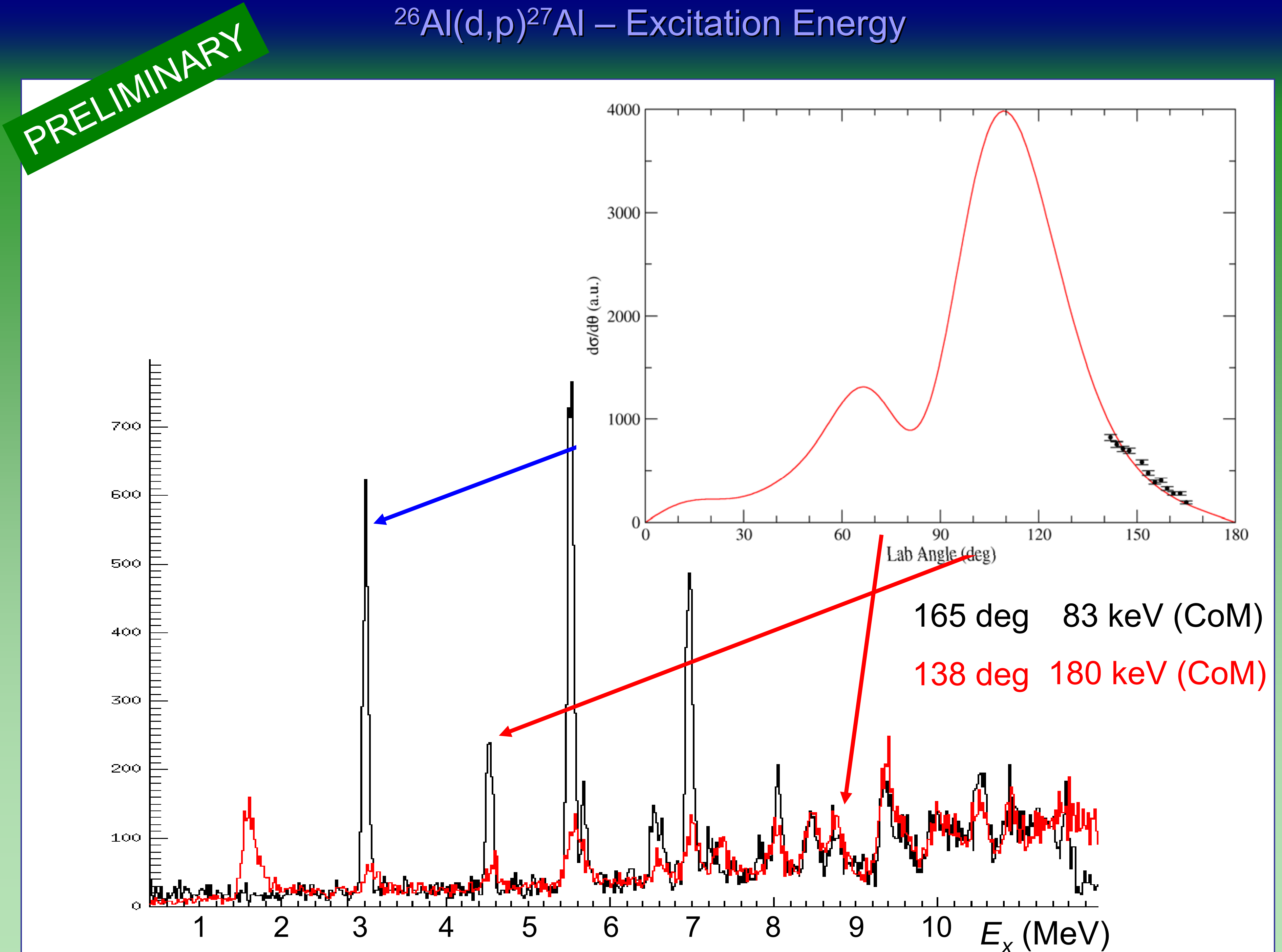

$^{26}Al(d,p)^{27}Al$ data – Excitation energy

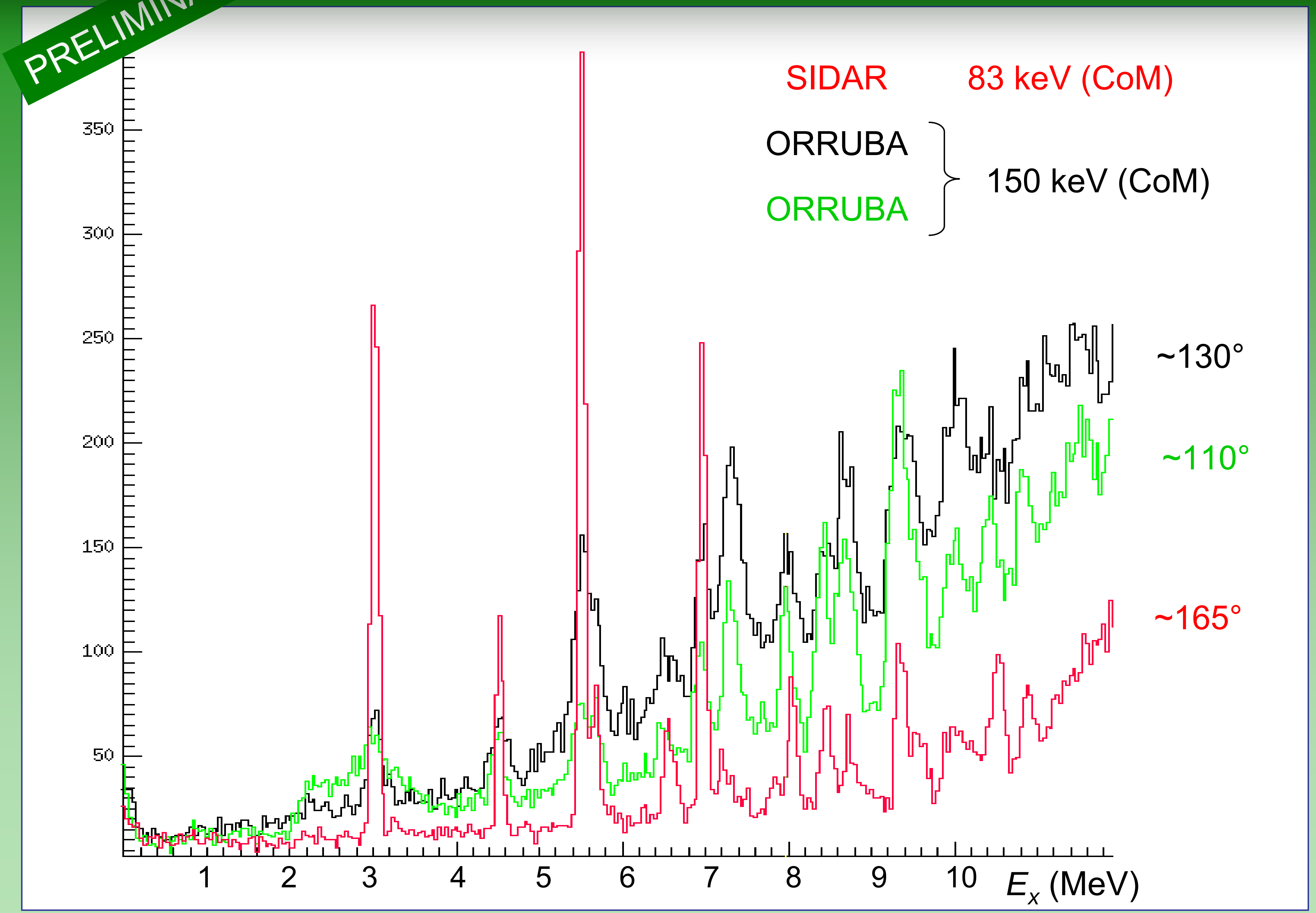

$^{26}Al(d,p)^{27}Al$ data – Excitation energy

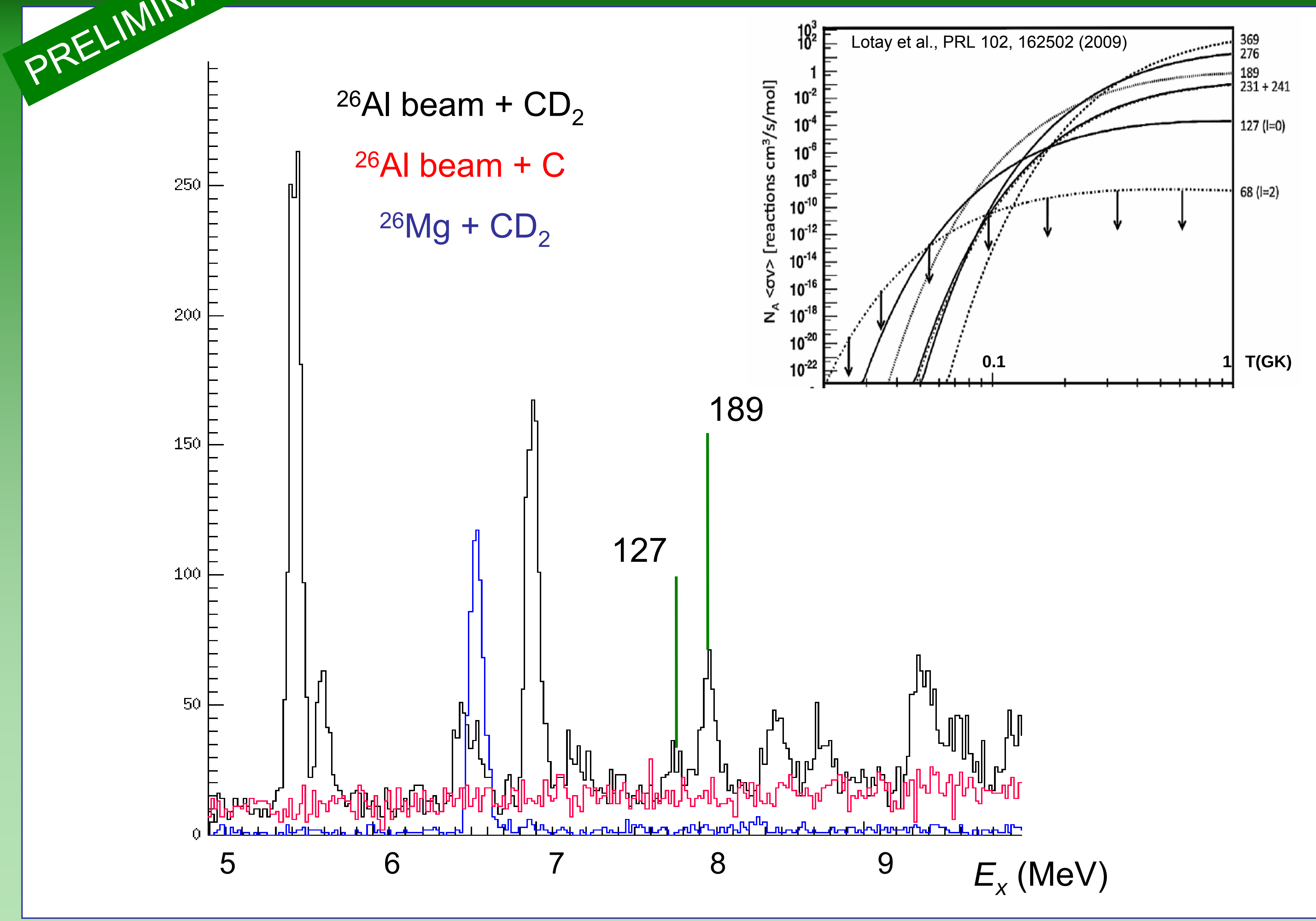

Measurement of (d,pγ) reactions in inverse kinematics

TIARA at GANIL

2×10^5 pps ^{24}Ne

1 mg/cm^2 CD_2 target

2 mm beam spot

PRL **104,** 192501 (2010) PHYSICAL REVIEW LETTERS week ending 14 MAY 2010

Migration of Nuclear Shell Gaps Studied in the $d(^{24}\text{Ne}, p\gamma)^{25}\text{Ne}$ Reaction

W. N. Catford,[1] C. N. Timis,[1] R. C. Lemmon,[2] M. Labiche,[3,2] N. A. Orr,[4] B. Fernández-Domínguez,[5] R. Chapman,[3] M. Freer,[6] M. Chartier,[5] H. Savajols,[7] M. Rejmund,[7] N. L. Achouri,[4] N. Amzal,[3] N. I. Ashwood,[6] T. D. Baldwin,[1] M. Burns,[3] L. Caballero,[8] J. M. Casadjian,[7,9] N. Curtis,[6] G. de France,[7] W. Gelletly,[1] X. Liang,[3] S. D. Pain,[1] V. P. E. Pucknell,[2] B. Rubio,[8] O. Sorlin,[7] K. Spohr,[3] Ch. Theisen,[9] and D. D. Warner[2]

[1]*Department of Physics, University of Surrey, Guildford GU2 5XH, United Kingdom*
[2]*Nuclear Physics Group, STFC Daresbury Laboratory, Daresbury, Warrington WA4 4AD, United Kingdom*
[3]*School of Engineering and Science, University of the West of Scotland, Paisley PA1 2BE, United Kingdom*
[4]*LPC–ENSICAEN, IN2P3/CNRS et Université de Caen, 14050 Caen, France*
[5]*Oliver Lodge Laboratory, University of Liverpool, Liverpool L69 7ZE, United Kingdom*
[6]*School of Physics and Astronomy, University of Birmingham, Birmingham B15 2TT, United Kingdom*
[7]*GANIL, BP 55027, 14076 Caen Cedex 5, France*
[8]*Instituto de Fisica Corpuscular, CSIC-Universidad de Valencia, 46071 Valencia, Spain*
[9]*IRFU, CEA-Saclay, 91191 Gif-sur-Yvette, France*

(Received 22 September 2009; published 10 May 2010)

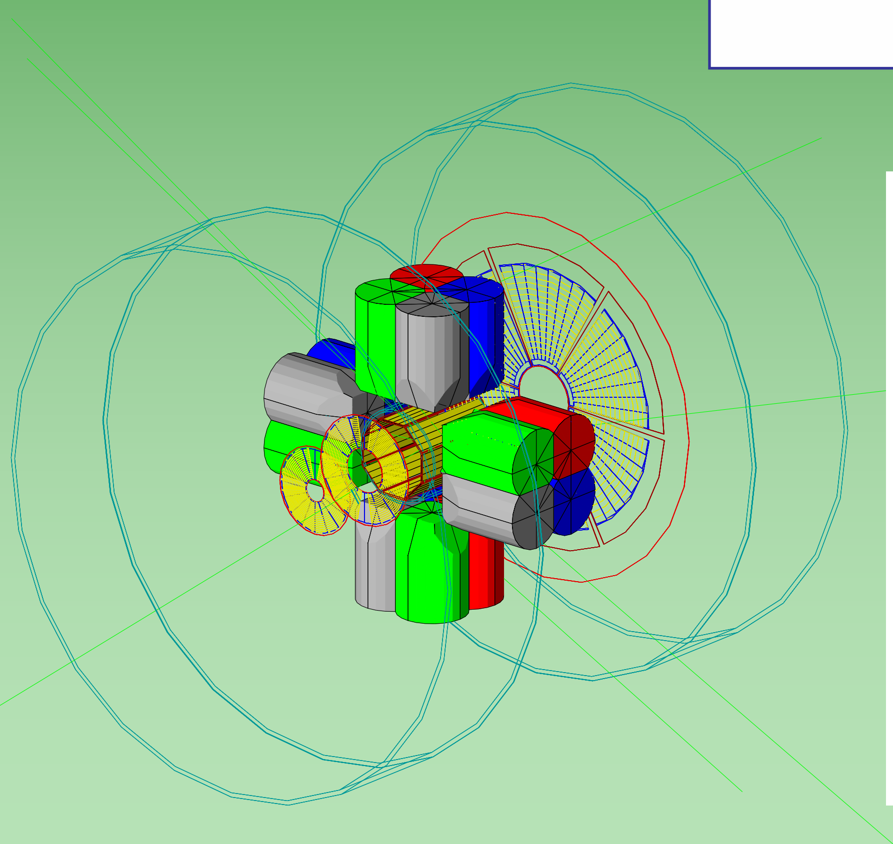

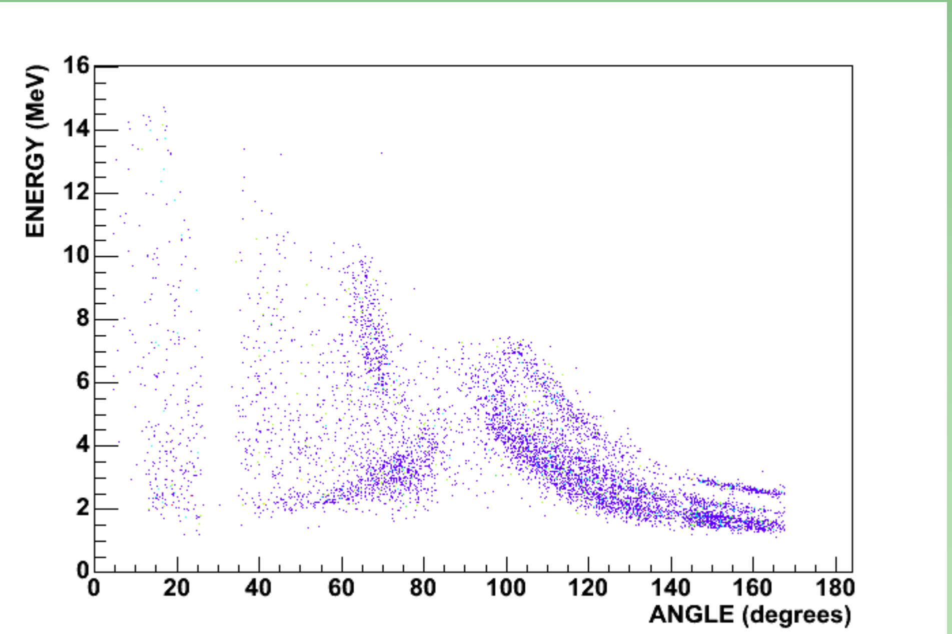

Measurement of (d,pγ) reactions in inverse kinematics

Only core signals from EXOGAM clovers, limiting Doppler correction to 65 keV broadening

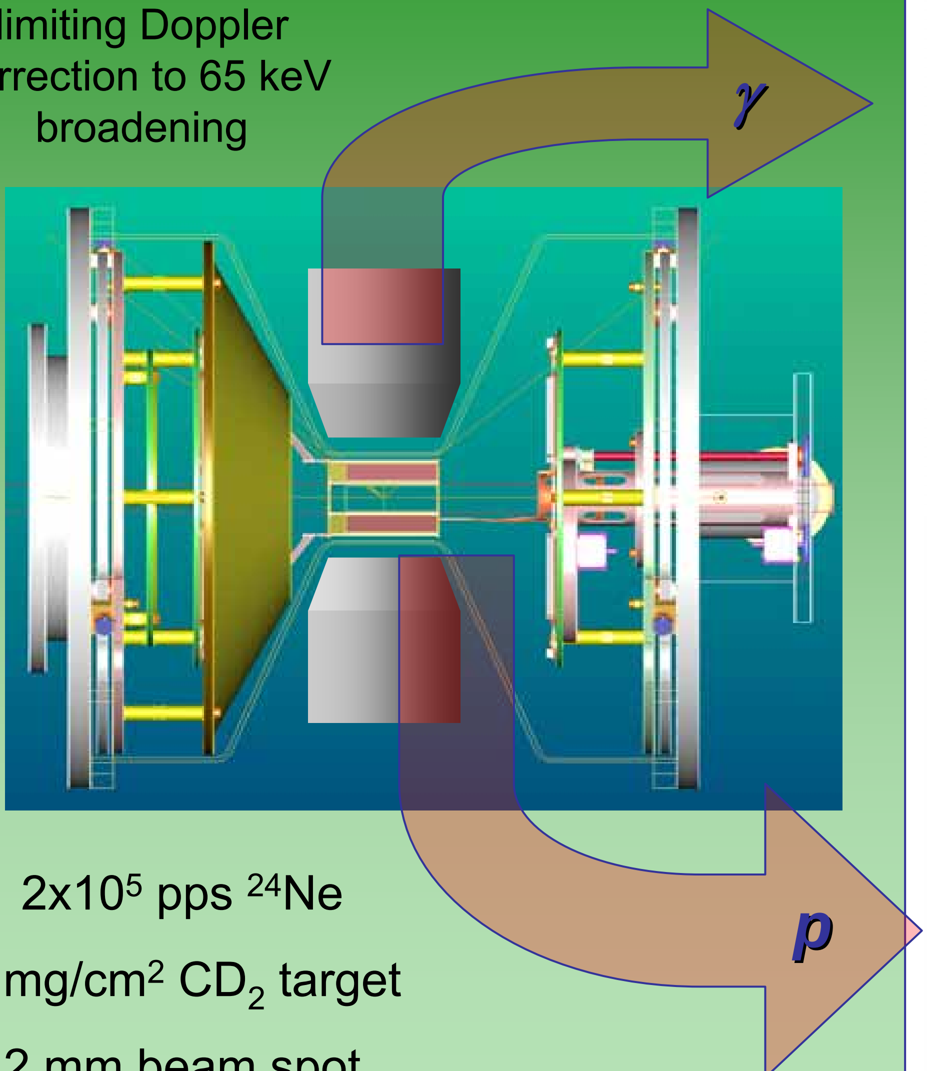

2×10^5 pps ^{24}Ne

1 mg/cm^2 CD_2 target

2 mm beam spot

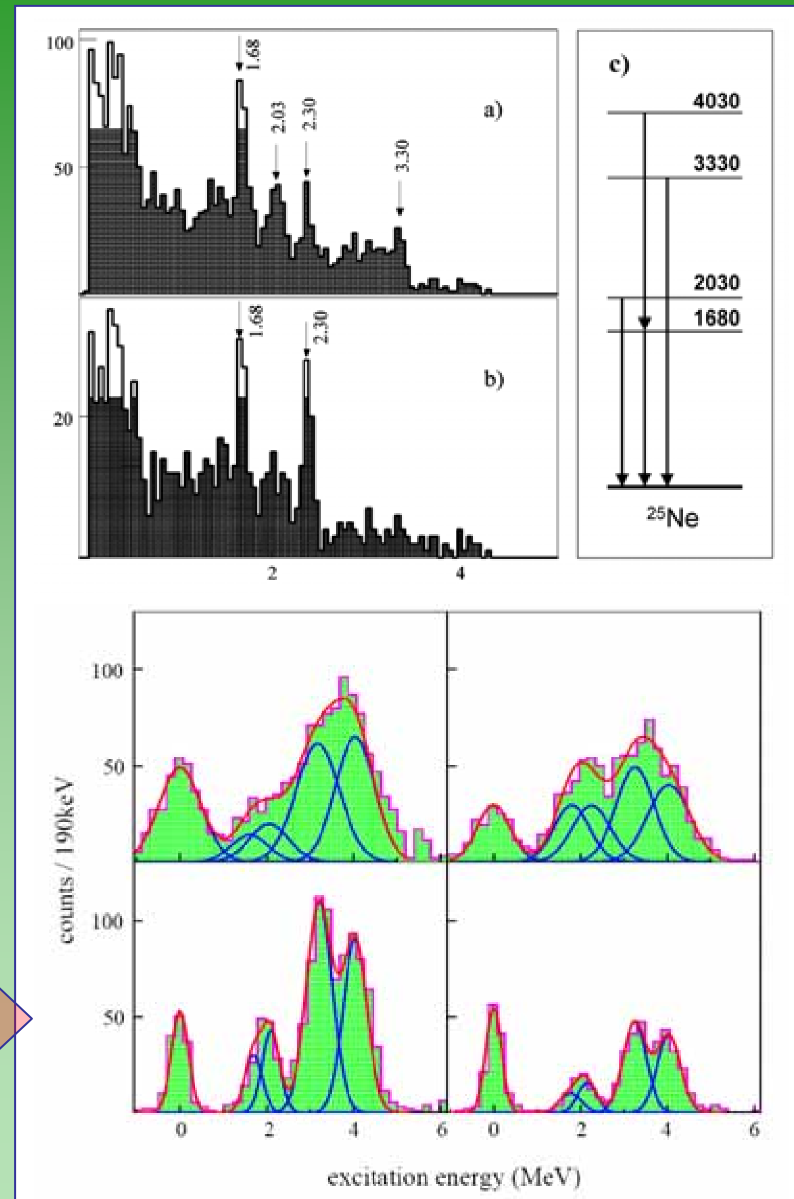

Measurement of (d,pγ) reactions in inverse kinematics

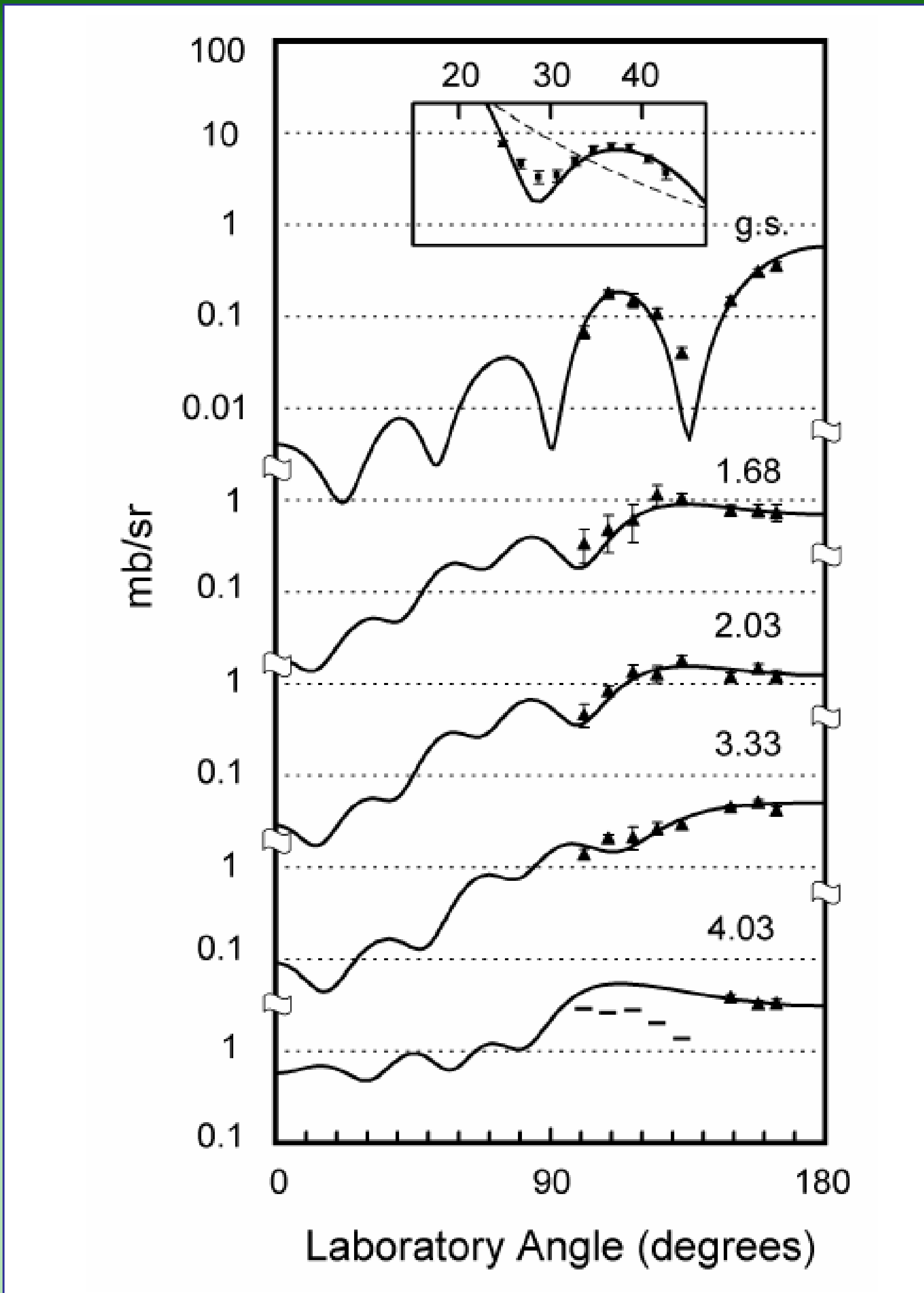

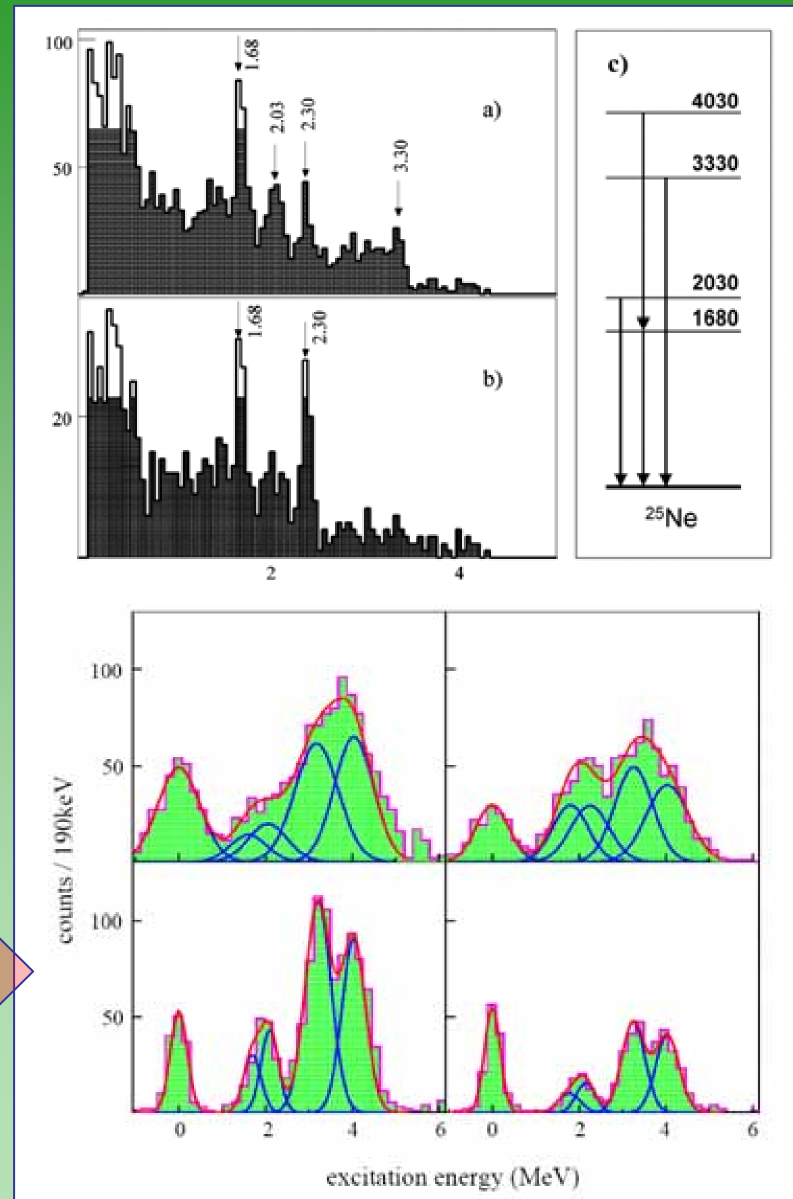

What about proton transfer?

- (d,n) is tricky because of neutron detection
- Can measure (d,n) by measuring only the recoil, and coincident gamma rays, but no angular distributions, feeding issues, etc
- (^{3}He,d) can be performed with detectors just like for (d,p), but how do you make a localized target?
    - Cell –backgrounds and straggling from windows, bulky (shadowing)
    - Implantation (backgrounds from foils, thickness of foils)
    - Gas jet target

$^{17}F(^3He,d)^{18}Ne$

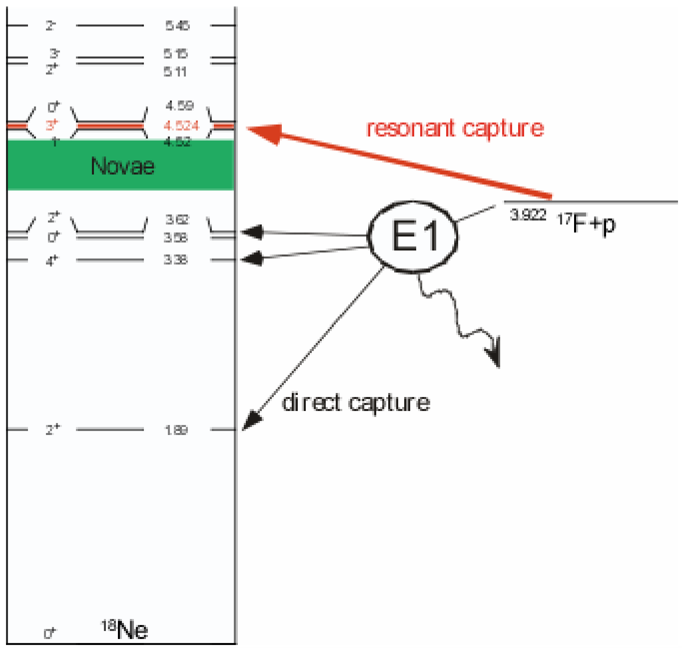

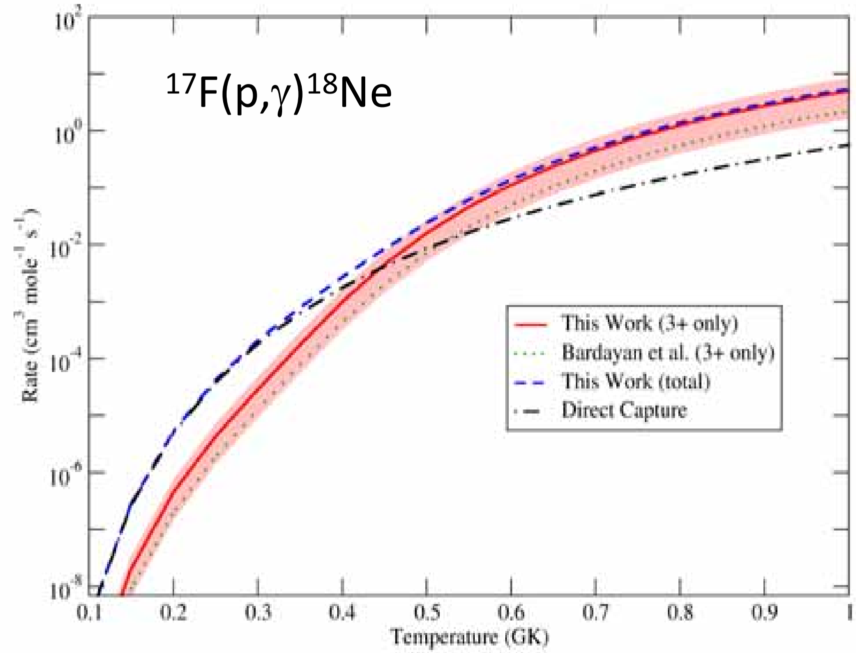

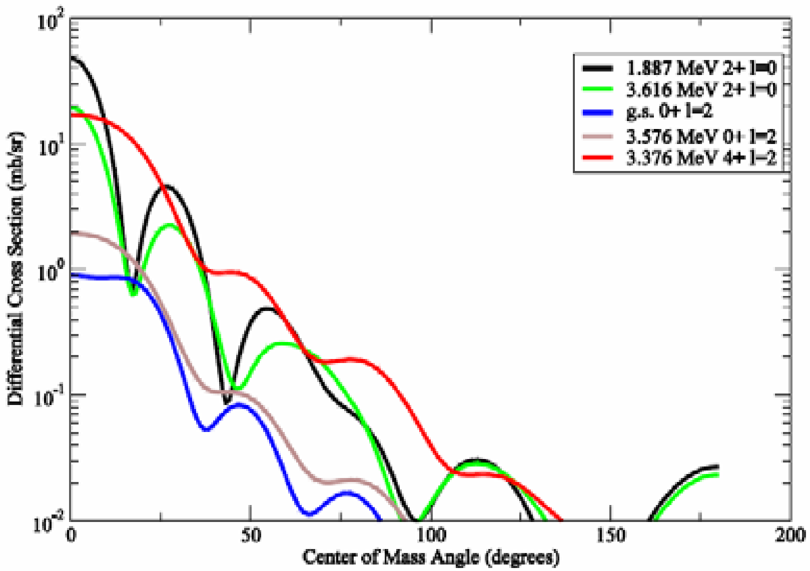

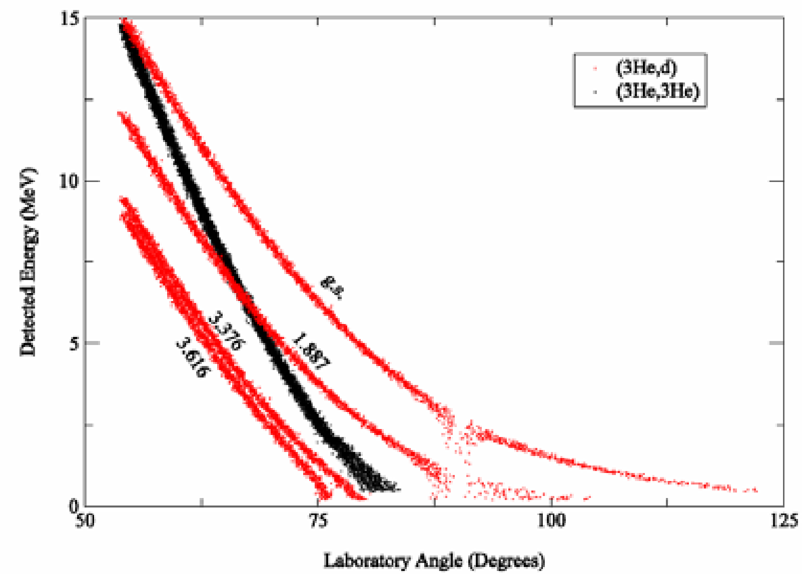

JENSA gas jet target

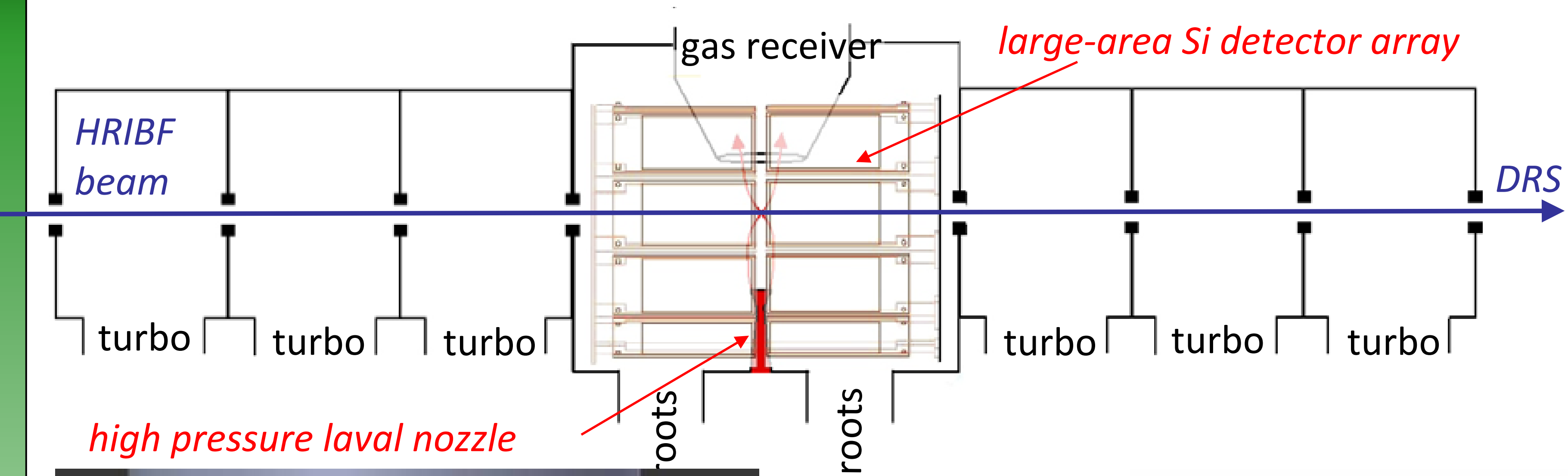

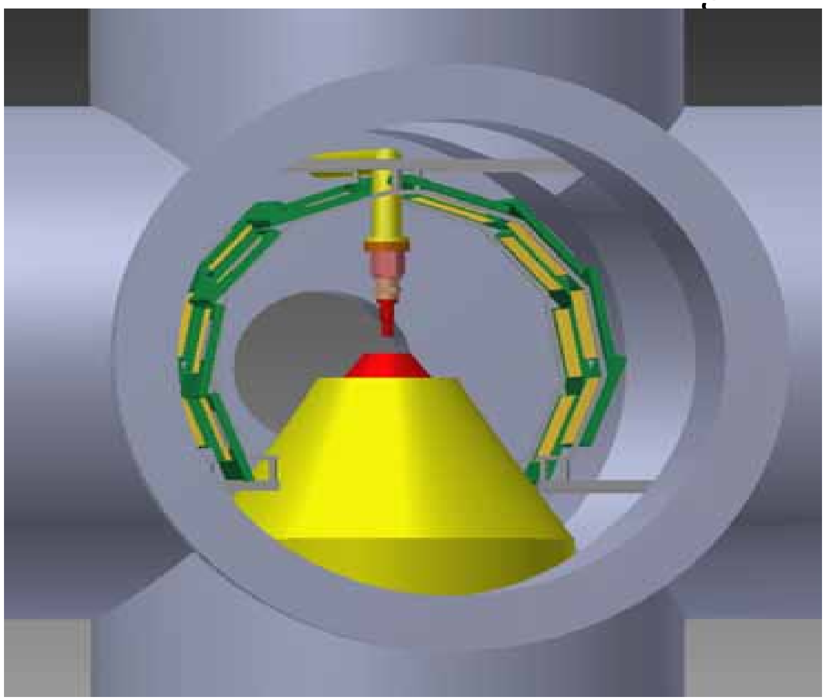

JENSA : Jet Experiments for Nuclear Structure and Astrophysics

(Colorado School of Mines, ORNL, LSU, and NSCL)

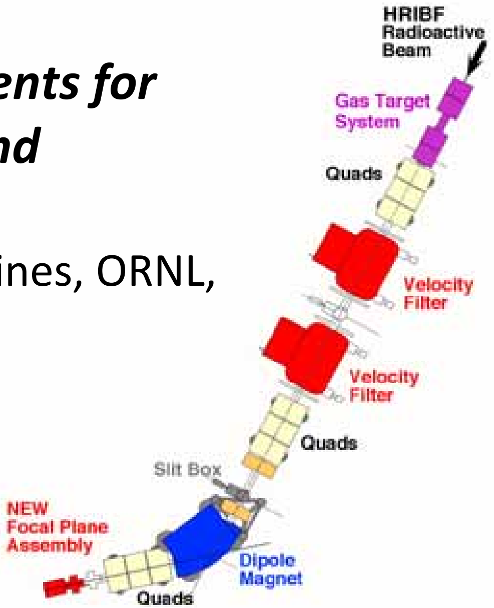

Supersonic gas jet

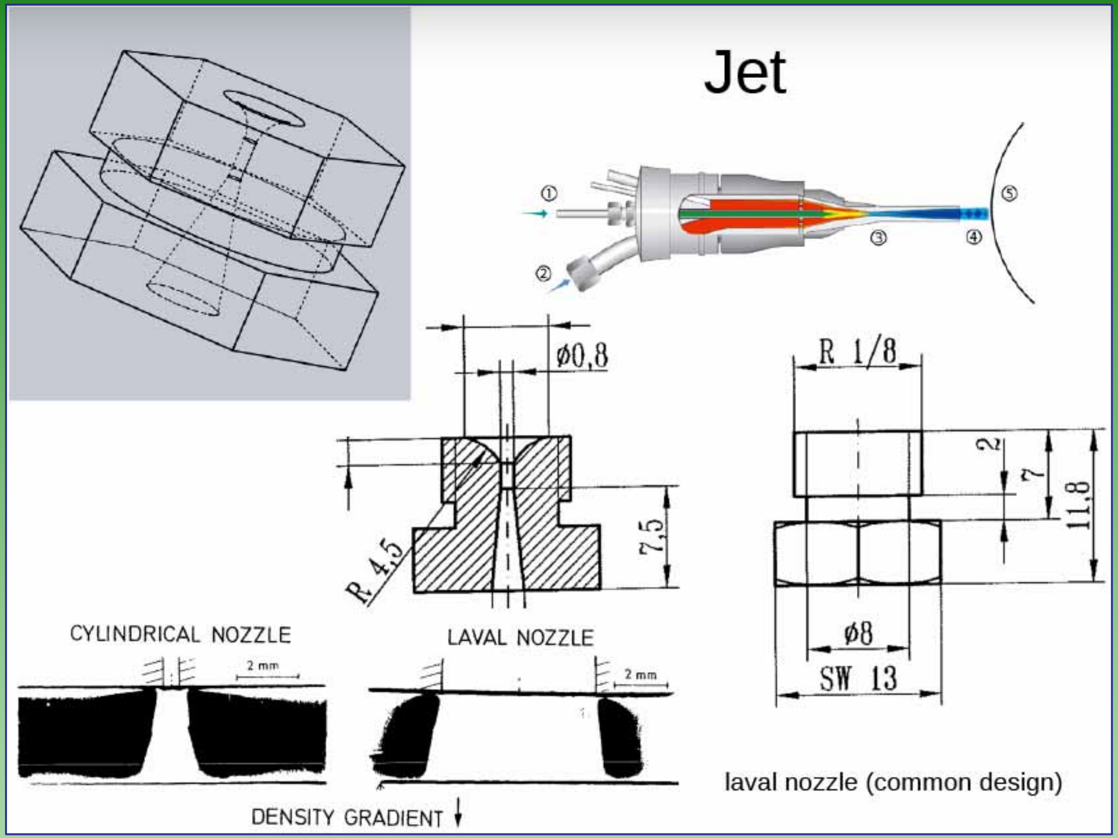

Gustaf de Laval (1865 – 1913)

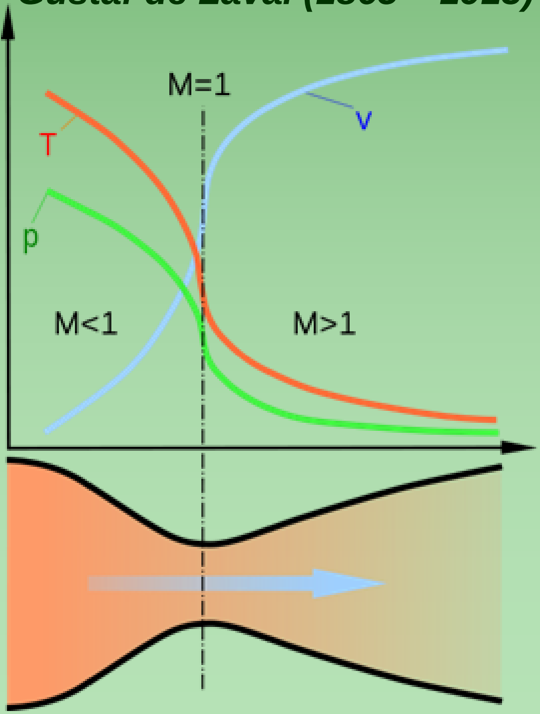

Operates in a choked-flow mode (constant entropy), in which flow is proportional to inlet pressure

JENSA gas jet target

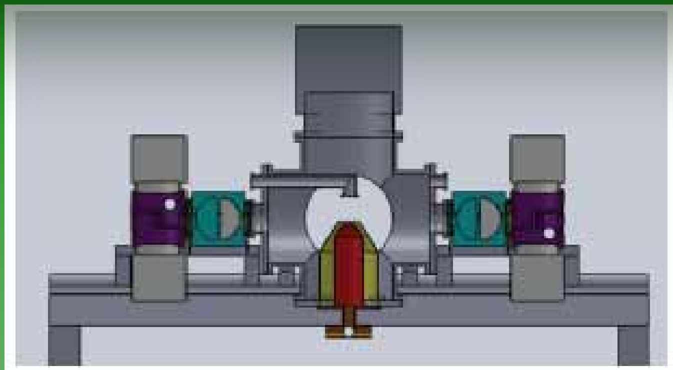

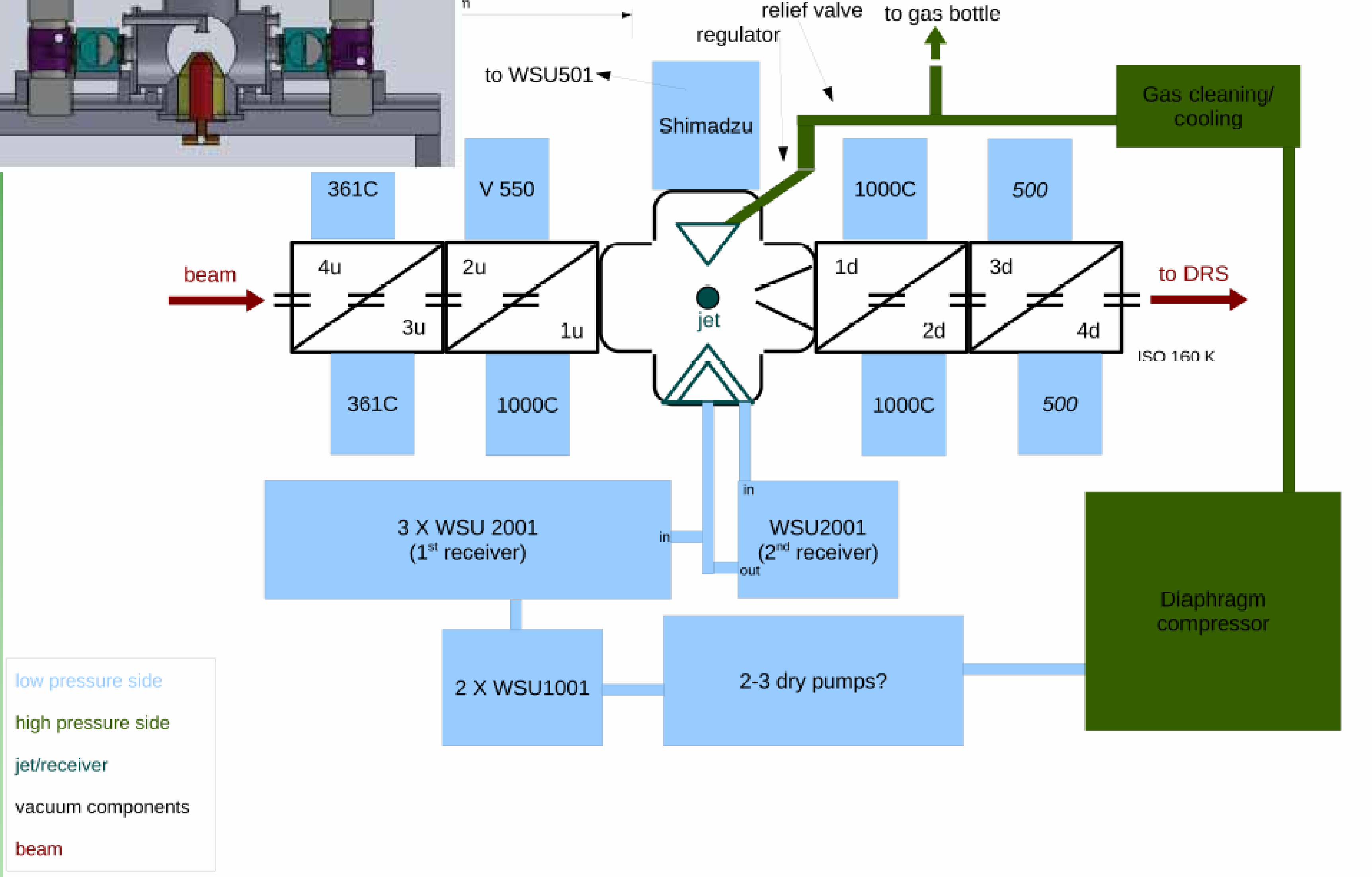

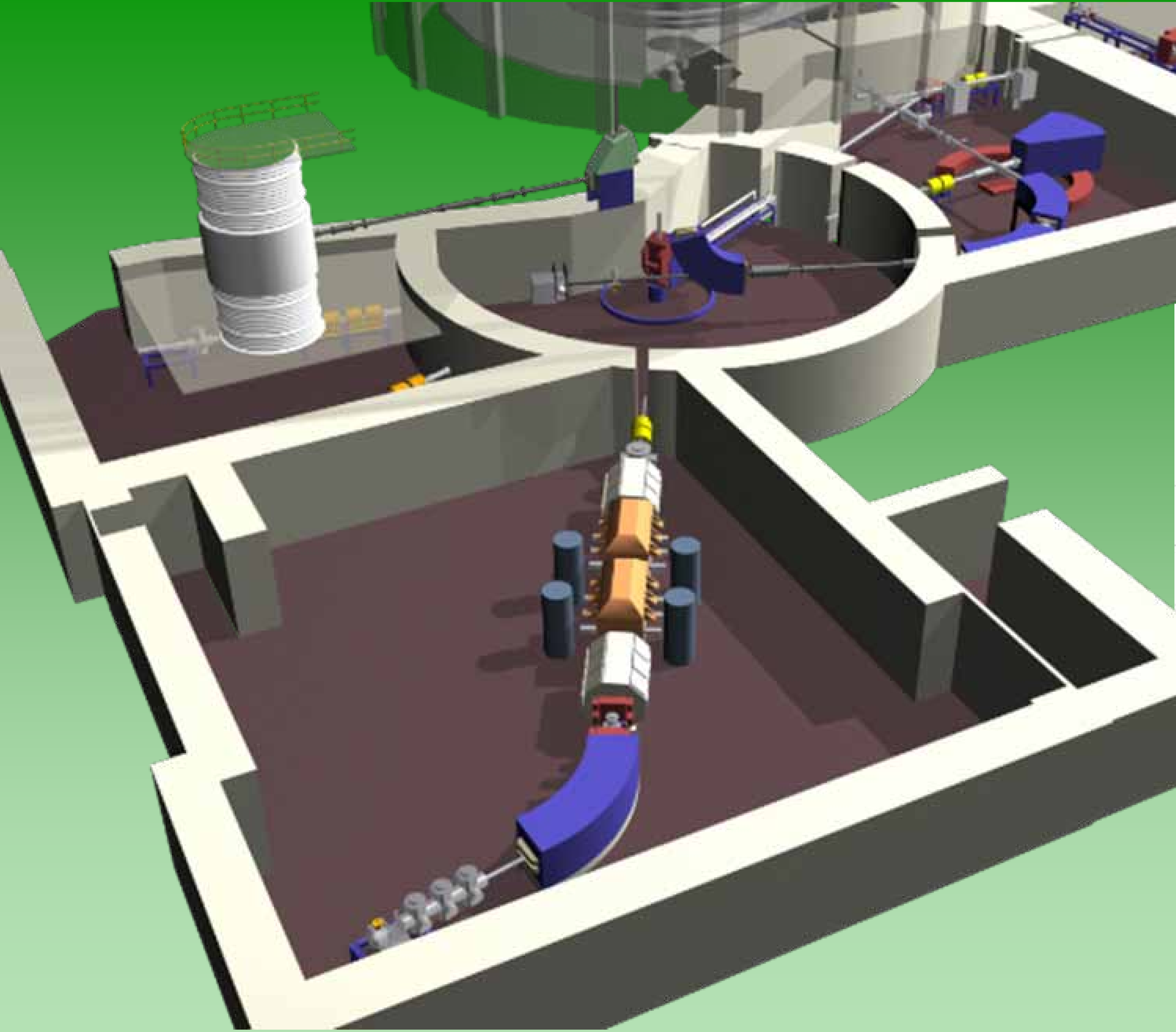



63-7135
T300



284






After construction of JENSA at ORNL, it will be moved to the new reaccelerated beam facility (ReA3) at Michigan State University

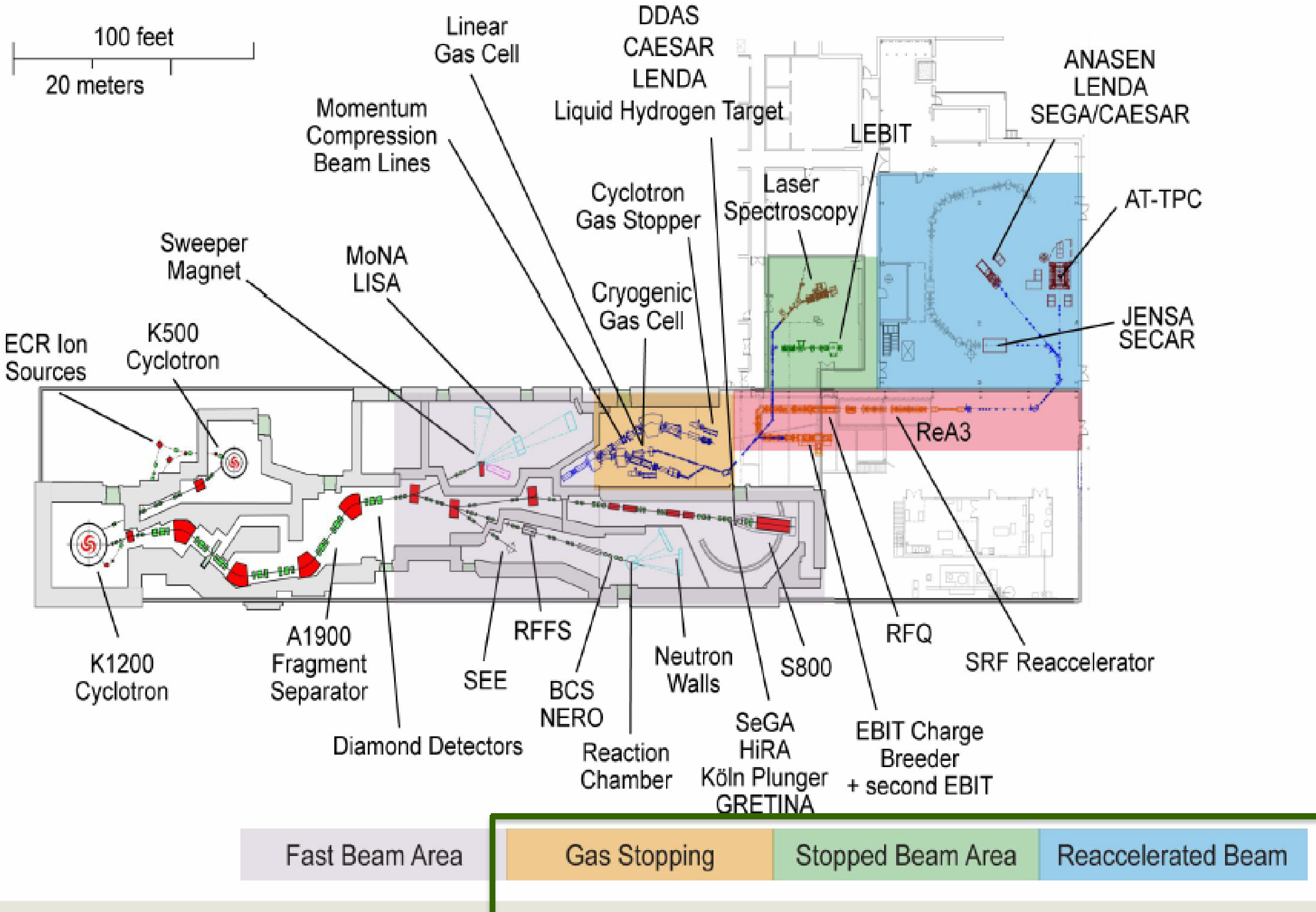

Thank you